UNIVERSITY OF OKLAHOMA

GRADUATE COLLEGE

AUTOMATION AND INVESTIGATION OF INTELLIGENT DRILLING AND ITS IMPLEMENTATION IN EXPERIMENTAL SETUP

A THESIS

SUBMITTED TO THE GRADUATE FACULTY

in partial fulfillment of the requirements for the

Degree of

MASTER OF SCIENCE IN NATURAL GAS ENGINEERING & MANAGEMENT

By

SAURABH AGARWAL

Norman, Oklahoma

2019

AUTOMATION AND INVESTIGATION OF INTELLIGENT DRILLING AND ITS IMPLEMENTATION IN EXPERIMENTAL SETUP

A THESIS APPROVED FOR THE

MEWBOURNE SCHOOL OF PETROLEUM AND GEOLOGICAL ENGINEERING

BY

Dr. Catalin Teodoriu, Chair

Dr. Suresh Sharma

Dr. Mashhad Fahes

Dedication

I feel thankful for all the support, motivation and inspiration that I have received from several people around the globe in my journey so far on different life fronts especially in pursuing and completing master's at the University of Oklahoma, USA. I would like to dedicate this thesis to

- My parents and my brother, for their unconditional love and support, as well as for encouraging me to do my best;
- My advisor, Dr. Catlin, for the insightful and collaborative work environment, and friendship;
- My roommates (Aditya and Ashutosh), for their continuous support and motivation and for being part of my family in the USA;

Acknowledgment

I gratefully acknowledge the guidance and suggestions of Dr. Catalin Teodoriu, who was always very helpful, inspiring and considerate since the beginning of my journey at the University of Oklahoma. I am continued support, guidance and mentoring throughout the length of the project and my studies without him this thesis might not have been written.

I would like to thank my mother Manjana Agarwal for her continuous motivation that was one of the driving forces in completing my thesis research.

To my father Kapil Dev Agarwal for giving all this support and taking care of all the needs which kept my focus on the actual task in hand.

To my brother Gaurav Agarwal who was a constant motivator and a great friend supporting and encouraging me.

To my friends and people who have directly or indirectly have supported me for me to accomplish my goals.

To all, my deepest and sincerest appreciation.

Saurabh Agarwal

Nomenclature

P	Pressure
T	Time
V	Voltage
I	Current
RPM	Rotations Per Minute
BHP	Bottom-Hole Pressure
BHA	Bottom-Hole Assembly
ROP	Rate of Penetration
MSE	Mechanical Specific Energy
WOB	Weight-On-Bit
LOA	Level of Automation
PID	Proportional Integral Derivative
MPC	Model Predictive Control
VI	Virtual Instrument
DAQ	Data Acquisition
SPE	Society of Petroleum Engineers
VFD	Variable Frequency Drive
H&P	Helmerich and Payne
AC	Alternating Current

Table of Contents

List of Figures

List of Tables

Abstract

On January 9, 1845, Robet Beart in Great Britain was granted a patent on the first of a new style of rig, the rotary rig with continuous circulation [21]. Since then, not many advancements have been made in drilling technology as compared to other fields such as aviation, communication technology, etc. Drilling rigs are still dangerous to operate, and many rigs operate with unguarded equipment and hazardous operation. Automotive and aeronautical industry recognized this issue for years; thus, they mechanized and automated the operations to make them safer and efficient. The drilling industry is behind the other industries in the implementation of automation; there is a vast scope of automation implementation in this industry. Only 25% of the active rigs working on land in the US are AC equipped, according to H&P data.

As the natural gas prices are falling and drilling cost is on the rise, there is a pressure on the drilling industry to do things differently. Automation can reduce the time needed to drill a well by around 25% as compared to manual controlled drilling and reduce the cost of the well by 17% [15]. There is a grouping interest for process automation in the drilling community. Many efforts are made by drilling industries towards automation as an overall objective to achieve efficient drilling. Other benefits of automation are making drilling operation environment safer, allowing remote access, and gather more data.

Through this research, the goal is to advance the automation in the field of drilling to make it safer, cost-efficient, faster and conveniently accessible. In this research past work in the area of drilling, automation has also been examined extensively to contribute further to it. This includes past experimental setups, as well as, the automated drilling setups built in Drillbotics competition by different universities. Best practices from these past setups, and current research practices have been implemented into this research.

This research proposes implementing closed-loop control for automation that continually monitors drilling parameters and drilling performance in real time and constantly adjusts the weight on bit (WOB), rotary speed (RPM), and torque on bit (TORQUE) to maximize the instantaneous rate of penetration (ROP). Precise control of these parameters through closed-loop helps reduce vibration during drilling which significantly improves drilling efficiency [22].

To carry out this research, downscaled experimental setup of a drilling rig has been used. This downscaled model was designed and constructed by Antonio & Teodoriu [6], and it is used in this research to create an intelligent control system for this rig. This experimental setup has all the necessary mechanical components such as top drive, a hoisting system, and more but is missing the necessary brain and sensory system for it to operate autonomously. For example, a human body needs a brain and the six senses to perform any action, similarly, an automatic drilling rig system requires sensors and a program that will automate the action it needs to perform, which is the scope of this research.

Experimental setup requires downscaling of the drilling rig, as downscaling helps mitigate some of the problems such as high inertial forces, large weight, and space requirement. Applying certain methods and using advanced technologies such as six-degree precise vibration generator to replicate bit rock interaction used for re-creating drill conditions becomes easier. The experimental

setup provides a safer environment for testing the concept of execution. The closed-loop control system implemented on drilling parameters is thoroughly tested on the setup to analyze the behavior experimental setup and align it with that of a real drilling rig. The downscaling factor used for this setup is 40. Later the results can be upscaled using the same factor to operate in an actual drilling rig.

There is a lot of variability in drilling operation and uncertainty in knowing what is being drilled i.e. the type of formation which is one of the reasons. This intelligent system is using automation and continually monitoring the performance parameters such as weight on bit (WOB) or rotary speed (RPM) and torque which help address this uncertainty and achieve a higher rate of penetration (ROP). This facility is unique in the sense that it is automated completely through hardware in the loop and using an intelligent algorithm. This simulation has been developed in LabVIEW.

The goal of this research is to investigate the behavior of an actual drilling rig and replicate the same behavior in the downscaled experimental setup and automating it with focus on the top-drive drilling parameters (WOB, RPM, TORQUE). Automation of these drilling parameters makes drilling safer, faster, cost-effective, and improves ease of operation and gathering data for better decision making. This is another step in driving the drilling industry towards a technology-oriented approach.

Display panel mimicking drilling simulator is developed with three layers of safety into the system. This experimental system is capable of representing an upscaled drilling rig (factor of 1:40) and able to autonomously control top-drive drilling parameters WOB, RPM and TORQUE. This experimental system has been programmed through LabVIEW. The test result for this experimental setup show that the system can precisely mimic an actual drilling rig after few suggested changes in the sensor has been made.

Chapter 1: Introduction

1.1 Motivation

Drilling is an important part of the exploitation of oil and gas reservoirs. A huge amount of investment is made in drilling a well. Most companies engaged in drilling operations have an exploration and development budget that is significantly influenced by the drilling budget. For some companies, it can be more than $1 billion. Increasing well costs in the absence of parallel increasing revenues will reduce the number of wells that can be drilled in a given time. The cascading effect reduces the chances for a company to supplement reserves and future cash resources. Reducing drilling costs is a major avenue for providing more available funds for more drilling or other ventures.

There are many motivations for automation of rig and its mechanization. Automation of a rig refers to eliminating the need of human interaction from the tasks required to control rig operations and mechanization is introduction of machines for automation. Thus, automation will result in requiring fewer people in the area where heavy moving machinery is operated reduces the risk of human safety. Many companies providing drilling service, operators and regulatory agencies prefer this goal around the world. Rig floor has also seen many accidents in the past, reducing the number of people operating on the rig floor will clearly enhance safety [21]. Many rig operations are in a harsh environment which is another reason for automation. Severe weather conditions such as extreme cold and wind or severe wave conditions reduce the human ability to operate on the rig floor [21]. Machines being able to operate continuously in a severe environment without the requirement of any human intervention will delimit the rig operation from human ability to control the rig [21]. Thus, technological advancement in this area makes the drilling operation much safer. Present drilling operation needs experienced personnel, as well as readily available personnel for emergency or help as the need may arise [21]. For the same reason, workers must work in shifts onsite so that at all times help is available in case of emergency. A robust automated monitoring system can solve this problem. More amount of data is collected by installing more sensors to make better decisions. The current system has an advantage of aiding onsite as needed but automation overshadows when it comes to providing benefits. For example, the amount of data available to the driller may be partial or not fully utilized to decide to result in incompetent performance. Whereas, more sensors can be used to monitor and automate the controller. Controllers can be programmed in such a way that they seek for the optimal solution utilizing maximum data while operating within the safe limits. Less personnel will be required on the rig area, thus, resulting in fewer chances of a human-related accident [21].

Another benefit is efficiency drilling; efficiency in drilling is commonly defined by its rate of penetration or MSE (mechanical specific energy). Failure of drilling facilities or inefficiency will have an inverse effect on the direct and indirect cost of drilling. Optimum rate of penetration can be achieved by reducing the vibrations such that equipment is functional for greater life cycle as well as the formation is drilled in less time [21]. Furthermore, issues such as premature failure of the drill string, the decrease in bit life and performance, noise in sensing data from downhole thus reducing the accuracy of measurement, deterioration of the Well trajectory, and excessive bit and

stabilizer wear can also be addressed at the same time. All these issues incur an additional cost of drilling such as reduced penetration resulting in more drilling time or failure of equipment adding to the investment cost on equipment. Average cost of a drilling an oil rig varies widely from approximately $20 million to $1 billion depending on the drilling conditions, such as depth and formation challenges including kick, vibrations, and formation burden pressure. A major part of the capital expenditure goes towards the cost of a drilling rig and its equipment [24]. Drilling optimization will clearly result in cost saving as a direct benefit to the company without compromising the safety of the process.

Automation of rig will allow a reduction in rig weight allowing smaller size and smaller environmental footprint. It will be easy to mobilize and demobilize a smaller rig and takes less time. An automated rig can be remotely monitored for its performance, operations, and maintenance from anywhere around the world. Furthermore, the data received from these automated control systems can be used to optimize drilling performance in future drilling operations.

Better drilling simulators can be created with automation. Using a software tool, the simulator recreates the same drilling condition (e.g., environment), allowing repeated testing by changing the control parameters. Today, simulators look exactly like a drilling control room and all the operations are mimicked to provide an actual drilling interface. These simulators are widely used in training engineers to become familiar with various drilling situations.

Better remote access to the drilling performance parameters is another great benefit of its automation. Today, the industry is shifting its focus to be able to operate a drilling rig remotely and collecting all the data from drilling operation as much as possible. Remote access to the drilling rig operation provides more flexibility to its operations. Experienced personnel can review the operations of multiple drilling rigs from a different location. Remote access allows secure data storage. More storage space allows one to gather more data that can be used to optimize both current and future operations.

1.1.1 Importance of automation in drilling natural gas wells

About 34% of natural gas consumption is used to make electricity. Of the three fossil fuels used for electric power generation (coal, oil, natural gas), natural gas emits the least carbon dioxide per unit of energy produced. Natural gas contributed to almost 29% in total U.S. energy consumption (as shown in Figure 1). 76% of residential energy consumption, 45% of industrial energy consumption, and 26% of electric power generation comes from natural gas (as shown in Figure 2). Thus, natural gas makes up a large section in all sectors of energy consumption.

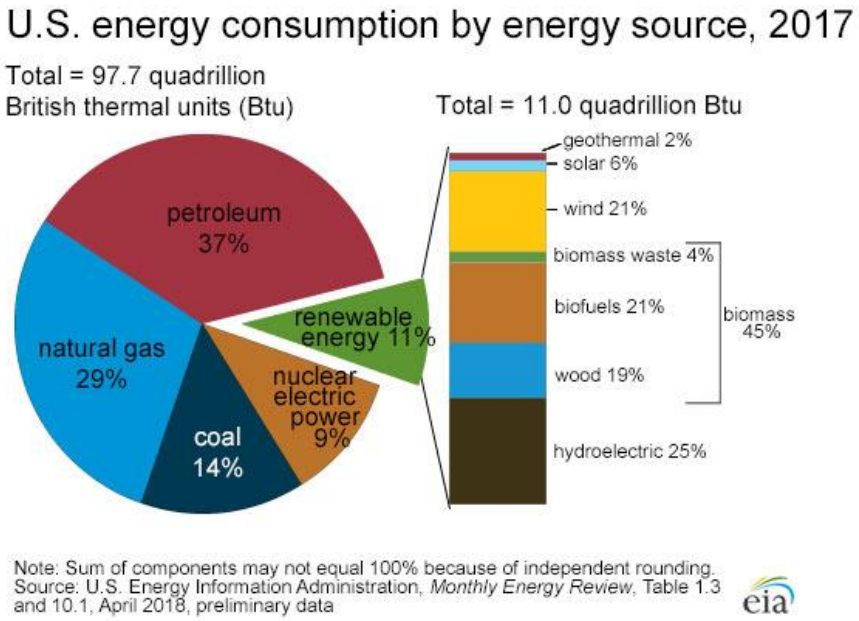

Figure 1. U.S. energy consumption by energy source 2017 [35].

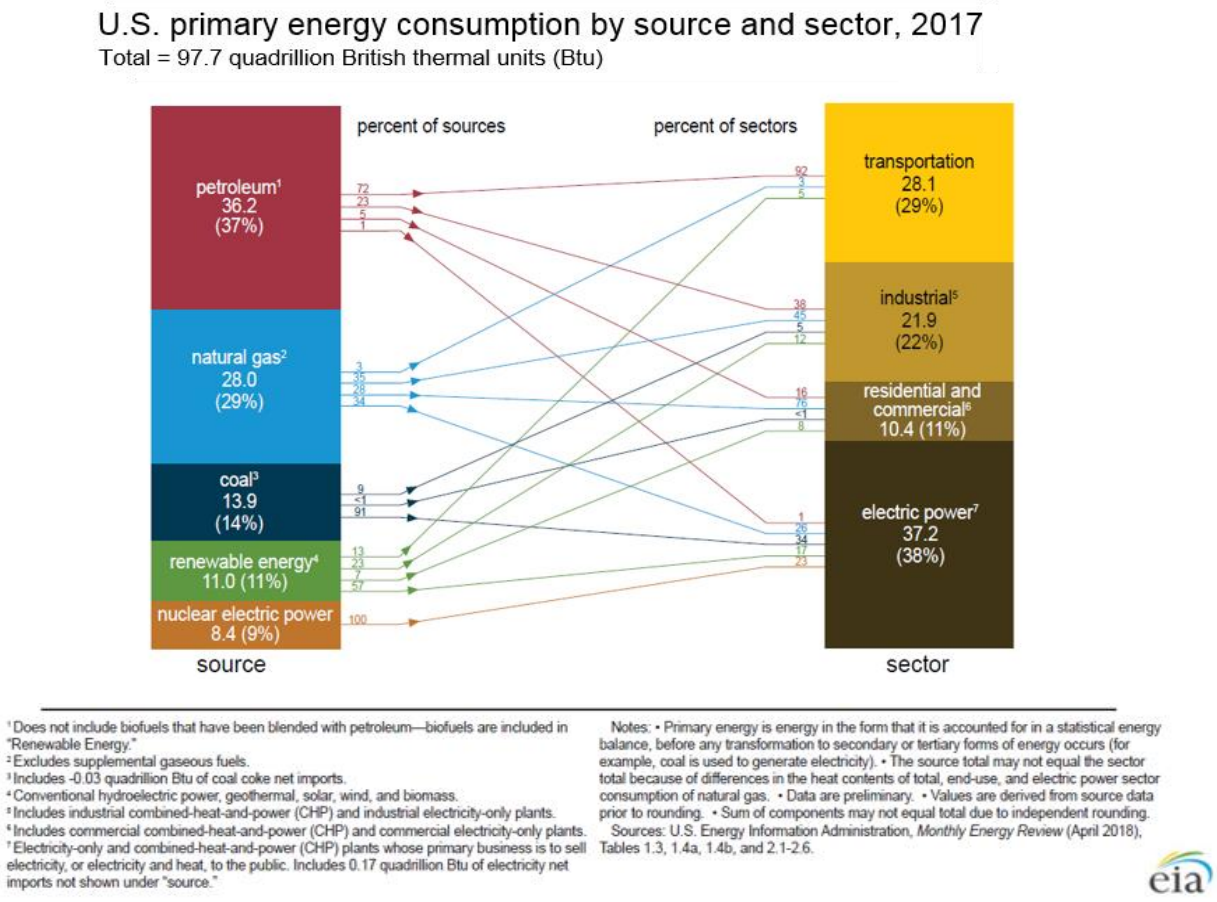

Figure 2. U.S. primary energy consumption by source and sector, 2017 [35].

Natural gas is projected to increase in demand (as shown in Figure 3) making up for energy produced by coal as it generated half carbon dioxide emission compared to coal.

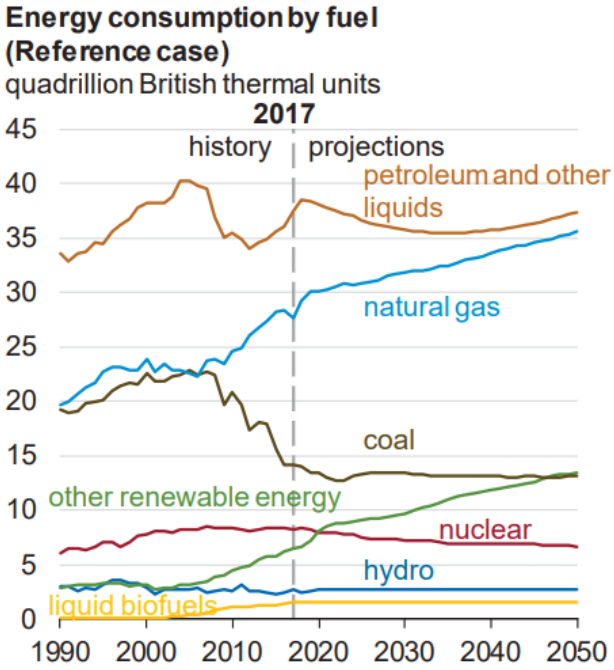

Figure 3. Energy consumption by fuel [35].

Note: The Reference case projection assumes trend improvement in known technologies along with a view of economic and demographic trends reflecting the current views of leading economic forecasters and demographers.

Natural gas is a promising source of energy in the future and must meet some challenges to become the major energy generator in the future market of the energy sector.

As shown in Figure 4 natural gas is found in the deepest level of formation as compared to a heavier source of hydrocarbons such as oil and kerogen. The potential source of dry natural gas is found as deep as 20,000 ft with a temperature higher than 140 degrees Celsius.

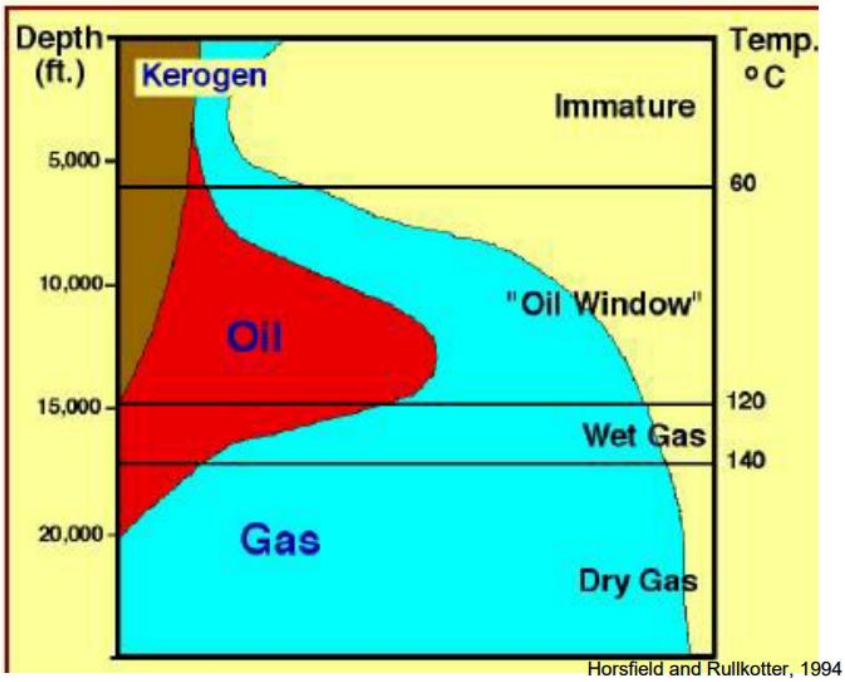

Figure 4. Hydrocarbon cooking zones for different phases [36].

Challenges in such deep wells are plentiful. At extreme depths, very hard rock is encountered slowing down the drilling process. It has been reported that for wells deeper than 15000 ft, 50% of drilling costs are spent in the last 10% of the well because rates of penetration are around 2-3 feet per hour (Schlumberger, 2004). In many of these developments, the ultra-low fracture gradient is encountered placing severe limitations for drilling fluids used in terms of density and circulating pressures. This has pushed the industry to develop new drilling techniques and bringing more automation to it to make existing and new drilling technologies more efficient and safer.

Drilling operation is very complex, especially in ultra-deep wells. And to fully replicate in an experimental setup is another challenge. Simulating the high bottom hole pressure, bit rock interaction, inertial forces acting on the drill string, fluid (mud) interaction with drill string, complex frictional forces acting due to interaction between wellbore and drill string, the depth range of drilling, weight, and size of drilling equipment, etc. cannot be completely recreated through experimental setup. To address these challenges for drilling a natural gas well automation is the key to success. Automation allows less human interference and precise control resulting in both safety and efficiency. Hence, this thesis surfaces the application of automation to the drilling operation by mimicking it in an experimental setup.

1.2 Purpose of the Study

This study serves as the intermediate point for the research on the topic. It is designed to automate the top assembly of the drilling system. Purpose of this study is to develop a downscaled intelligent drilling rig system. Intelligent drilling rig allows control and monitoring of drilling performance without the need for human intervention.

Automate the drilling parameters, such as, WOB, RPM, and TORQUE will result in improved drilling efficiency such as increase in ROP. Identifying and analyzing the effect of these parameters on drilling performance serves the purpose of this research. Top assembly plays a crucial role in controlling these drilling parameters and the performance of drilling. Thee parameters can be controlled through top assembly, WOB is controlled by changing the vertical position of the top-drive and RPM is controlled by simply changing the rotational speed and TORQUE is controlled by changing WOB.

The control system for this experimental setup has been designed, inspired from a drilling simulator, in the form of digital display panel control. The display panel allows controlling drilling parameters in real time such as WOB, RPM and TORQUE and display the current state of different output variables such as ROP, depth, WOB through virtual gauges and display units. This control system has multiple safety layers that ensure the system can be operated safely and under control.

In the future, the experimental setup can be linked to a drilling simulator for inputs.

1.3 Research Summary

Large drilling rigs are expensive to operate and test new implementations such as automation of drilling rig. Experimental setups are smaller and are operated on a safer environment to exercise the new ventures that the drilling industry is looking into. This research project tests and examines the effects implementation of drilling automation in an experimental setup format which can later then be upscaled to implement in a real drilling rig.

The project examines the state-of-the-art in drilling automation to develop an automated hoisting and rotation system (Top assembly) and a friendly human-machine interface (HMI). The state-of-the-art includes both petroleum applications as well as other industries. Areas such as aerospace, manufacturing, and defense research are far more advanced in automation technology applications and hold many valuable insights on how to develop and apply automation. Many downscaled experimental models exist for a drilling process. Adapting these models to the automation and control of the drilling process requires research, in which models will couple with the control system to create a robust system. With the advancement of technology such as high-frequency hexapod to recreate the bit-rock interaction, extremely high precision of repeating movements it is now possible to raise more ambitious experimental models that represent a drilling process more closely than ever.

Automation of experimental setup is achieved through hardware in the loop and using LabVIEW software. A closed-loop control system is developed in LabVIEW software for the rotational and hoisting system. Programming in LabVIEW for automation of top assembly of a drilling rig has been developed and tested on a real environment.

The behavior of hoisting system has been analyzed by varying control parameters for stepper motor such as power supply and other load parameters. Identifying the behavior of the hoisting system in the experimental setup will allow accurate replication of the drilling behavior from an actual drilling rig. An interactive digital panel is implemented for the user to control the top assembly similar to a real drilling simulator.

This research intends to develop complete automation of controlling parameters such as WOB, TORQUE, and RPM mitigating the downhole vibrations that go undetectable by MWD tool. These controlling parameters can be controlled in the top assembly. Hoisting system has different sensor that serves as an input to the controlling algorithm, such as load cell to measure WOB, potentiometer scale to measure vertical position of the drillstring and RPM sensor for the motor. All the controllers are calibrated based on these sensor inputs. It is a closed-loop control where input passed on to controllers is traced by these sensors for the desired output. The digital control panel is built in LabVIEW with control algorithm having the capability to control the system both manually and automatically. Test performed on the experimental setup and it result verify the capability of the system to replicate an actual drilling rig system.

1.4 Scope of the research

Scope of this research is limited to automation of the top assembly section of the laboratory drilling rig experimental setup using LabVIEW that was designed and assembled by Antonio & Teodoriu [6]. Complete automation of top assembly includes closed-loop control and open-loop control for WOB and RPM. Closed-loop and open-loop control allow automatic and manual control respectively.

- Extensive theoretical assessment of past drilling experimental setups is done to implement the best practices for the current experimental setup, identifying technical specifications such as dimensions of drillstring, motor specifications, controllers and sensors used.
- Automation of the hoisting system of the experimental setup using installation and calibration of sensors, controllers and data acquisition card in a hardware loop. Programming of the hoisting and rotational system as needed for the control behavior. Automation of top assembly can be divided into two major sections i.e. automation of the hoisting system and rotational system.
- Designing a simulator inspired control panel for a complete hoisting system. Ability to control/vary the parameters WOB, RPM, and TORQUE so that the nature of vibration can be correlated with these parameters and then vibration can be addressed effectively.
- Conducting experiments to align the behavior of the experimental setup with operation of an actual drilling rig. The behavior of hoisting system is analyzed in detail comparing each of the parameters such as current & voltage supplied to the stepper motor, step size, holding current, running current, acceleration, velocity, drillstring weight, the direction of movement. Identifying the operating range of these parameters within which the top assembly needs to be operated to achieve the desired behavior. The sensors and controllers have been calibrated with the output and input signals respectively for linear behavior to ensure system behaves as expected.

1.5 Importance of drilling parameters WOB, RPM and TORQUE in improving drilling efficiency

WOB, RPM, and TORQUE are the three drilling parameters that are under human control, playing an important role in controlling drilling vibrations [22, 23]. Vibration results in loss of energy, reduction in equipment life cycle, unsafe environment for operators around the machines, reduction in ROP and ultimately drilling efficiency. There are many parameters such as bit-rock interaction, rock type, wellbore hydraulics that play an important role in defining drilling efficiency but are out of human control. WOB, RPM, and TORQUE are the only controllable parameters, achieving autonomous control over these parameters for optimized performance is the goal of this research. TORQUE is critical to the cutting force, TORQUE affects stick-slip, hence, ROP. TORQUE also varies with change in WOB and RPM [23].

Figure 5 shows the correlation of drilling parameter WOB and RPM with different kinds of vibrations encountered during drilling. This graph was plotted by Dunlop [22] highlighting the constraints of the system as shown by red dashed lines. The white region in between the envelopes is safe operating region. Thus, WOB and RPM parameters can be utilized by auto-driller to operate within the safe region.

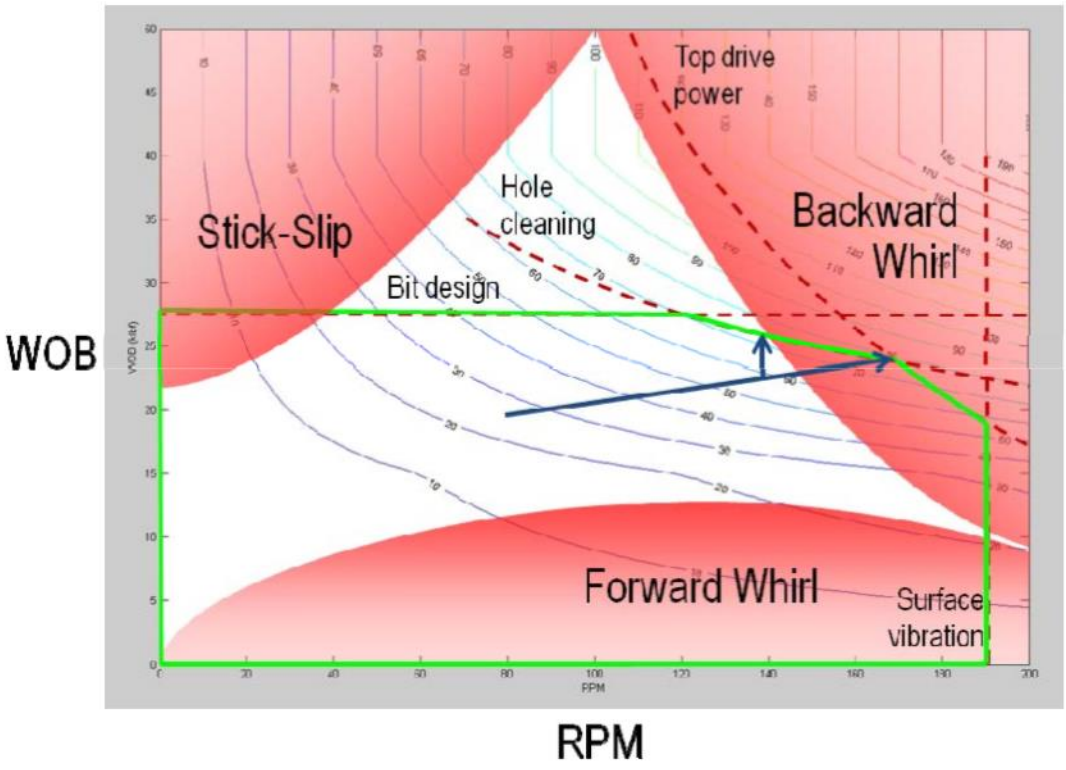

Figure 5: Contours of the ROP plotted in the (ROM, WOB) plane. Constraints to the system are shown with red dashed lines. The safe operating envelope is shown in green. The region where drillstring vibration may occur is shown in red [22].

Founder point is a “sweet spot” at which the ROP drilling efficiency is maximum. At this point, WOB and RPM are such that it results in a maximum increase in ROP [25].

The concept of the founder point is closely related to the drilling efficiency as it correlates ROP and WOB. The concept is that the ROP increased as the WOB increases until a certain point after which the ROP continues to decrease with increase in WOB. The maximum WOB at which the ROP is maximum is called a founder's point. This point shifts with a change in RPM as shown in Figure 6.

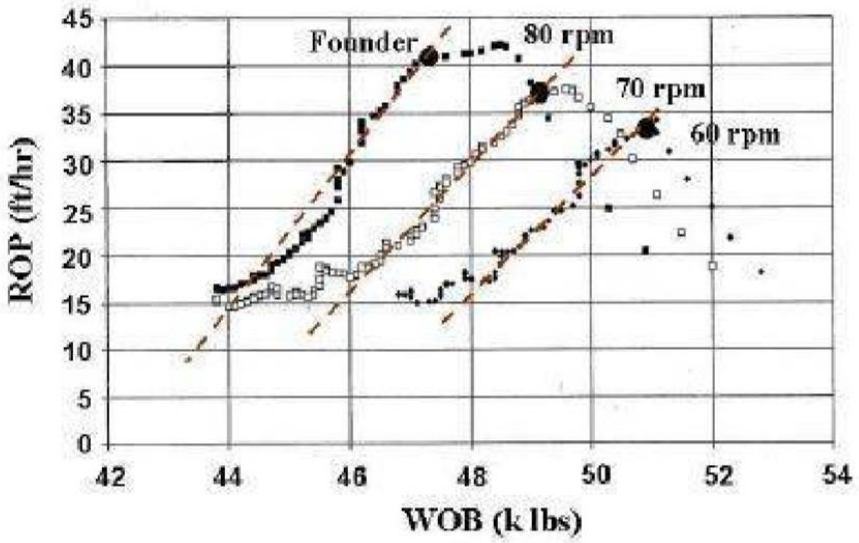

Figure 6: Passive drill of test [16].

1.6 Past experimental research setups

Table 1 displays a summary of the past experimental setup to study drilling automation. Although there has been many advancement and variety of analytical and mathematical models to predict the dynamic behavior of the drillstring, not much effort has been done to simulate and validate the models through an experimental setup.

Table 1: Summarized table of past downscaled drilling rig experimental setup showing key information.

Researcher (Year)	**Investigation and focus**	**Setup details**	**Sensors, controllers and software**
Mihajlovic [20] (Figure 7)	Study of friction-induced limit cycling in a flexible rotor system. Observations made was that the normal force in the friction component can induce higher negative damping for higher normal forces giving rise to stick-slip	Drillstring length 1.47 m, added mass 0.45 kg	DC Motor for rotary drive
Khulief and Al-Sulaiman [33] (Figure 8)	Studied the impact of drillstring with the wellbore. The model accounts torsional bending and axial bending nonlinear coupling. Sophisticated dynamic models need to be developed to investigate coupling modes of vibrations	Drillstring length 2m long, 2-7mm dia., housed in a plexiglass shell (6 to 10 mm inner dia.) RPM: 50- 1000	DC motor for rotary drive, Lateral excitation by 200N shaker, 0-125 Hz Watertight proximity probes for lateral displacement
Lu [34] (Figure 9)	Reproduction of stick-slip vibration in the laboratory for D-OSKILL mechanism. Smaller ROP with D-OSKILL mechanism due to loss of optimal WOB while effectively mitigating stick-slip vibrations	Drillstring stiffness 0.6706 Nm/rad, 190 RPM, Nominal WOB 180 N	
Franca [17] (Figure 10)	To prove the drillstring response model based on literature. The drilling rig has the ability to provide ROP from 0.01-100 mm/s. The rock sample is driven instead of the drilling assembly	10-400 RPM	
Foster [10] (Figure 11)	To reproduce lateral vibrations. Understand and quantify the behavior of AVDT. Inertia wheels used to replicate the top drive and the BHA. Accelerometers used to measure shocks occurring between the drillstring and borehole.	Drillstring length 2 m, dia. 5 mm, WOBs 1, 1.5 and 3.5 Kg, for torsional rig dia. 1 mm, wellbore dia. 8 mm, 400 RPM	

Foster [11] (Figure 12)	Experimental model to Axial excitation as a means of stick-slip mitigation	Drive system: 0-30 V DC motor Speed: 0-1000 rpm shaft dia.; 5mm drillstring dia.: 1mm, length: 1250 mm Upscale ratio 6:1 Data logger rate 40 Hz Flow rate 800-900 GPM	System pressure was recorded using 0-10 bar pressure transducer WOB determined in the data logger Solenoid actuators for axial excitation.
Esmaeili [9] (Figure 13)	Investigation of drillstring dynamics. Increasing WOB and rotary speed increases ROP. Keeping constant WOB and by reducing rotary speed, vibrations and ROP decreases	Drillstring length 0.524 m, dia. 40 mm, 360 RPM, WOB 800 N.	DC Motor for the rotary drive. Vibration sensor sub to record vibration
Patil [13,14] (Figure 14)	Investigation of drillstring dynamics. Recreated the BHA of a drillstring.	Drillstring length 5 m, drillstring OD 6 mm, drillstring ID 4 mm, 0-200 rpm, WOB 0 - 15 Kg, TORQUE 370.3 Nm, stiffness 0.02 Nm/rad DC Motor	Software: MATLAB/SIMULINK DC motor for the rotary drive. Feedback response from the control system to the drillstring actuator
Kovalyshen [8] (Figure 15)	Investigation of drillstring dynamics with drag bits. No drillstring was used, only a small shaft and a drill bit. Rock sample was used in the experiment.	Bit dia. 49 mm, torsional stiffness 0.05-14 Nm/rad, 10400 RPM	Servomotor, Linear actuator Accelerometer Torque sensor Force sensor LVDT
Kapitaniak [7] (Figure 16)	Investigation of drillstring dynamics. Limited in size. Finite Element Model used to calibrate setup. Calculated TORQUE from WOB and RPM.	Drillstring dia. 10 mm, RPM max.: 1370 DC motor WOB 0.85-2.19 kN	LabVIEW Angular velocity measured by two encoders (top and bottom) torque, lateral and axial force: Dynamic for transducer ROP: displacement transducer

Cayeux [18] (Figure 17)	Compares laboratory rig with full scale. Experimental data on WOB and RPM for stick situation.	Drill pipe OD: 9.5 mm, ID: 8.7 mm bit: 28 mm BHA mass: 0.97 kg max. rotational speed: 180 rpm sampling rate: 33 ms max. load: 100 N amplifier: 0 to 3.3 V output digitized microcontroller: 1:4096 resolution	Slip ring for signal transmission through cables. 12 electrical cables to the sensor placed in BHA WOB: four load cells elevation control: Leadscrew with a pitch of 8mm/rev, stepper motor with 2000 step/rev
Ren [19] (Figure 18)	To investigate dynamic buckling in horizontal drilling	WOB: max applied 30 kgf RPM: max applied 300	Servo motor Tension-compression sensor Eddy current displacement sensor

Below discussion aimed to highlight key takeaways from the analysis of past drilling rig setups developed for analyzing different drilling behaviors, as mentioned in Table 1.

Discussion

- None of the past experimental setups has been designed to reproduce to replicate as many aspects of a drilling rig as compared to the experimental design setup used in this research. All the developed setups have limited drilling depth capability, replicate only certain kind of vibration behavior, buckling of the drillstring and other. There has never been a focus on creating a more complex form of drilling setup that can generate complex behavior closer to an actual drilling rig.
- Most of the setup use LabVIEW as their programming interface. LabVIEW offers an interactive user interface for drilling automation.
- Sensors used in most of the setup are unique with the purpose of measuring specific parameters such as a tension-compression sensor to measure buckling, eddy current displacement sensor, vibration sensor, accelerometer, force, LVDT and other. In our experimental setup, we have used WOB, displacement and torque sensor.
- Most of the experimental setup used DC motors for rotary motion. For hoisting system, diverse options have been used but the most common factor among them was screw based hoisting system.

- Most of the RPM generator has a maximum RPM limit greater than 150 rpm and goes up to 400 rpm.

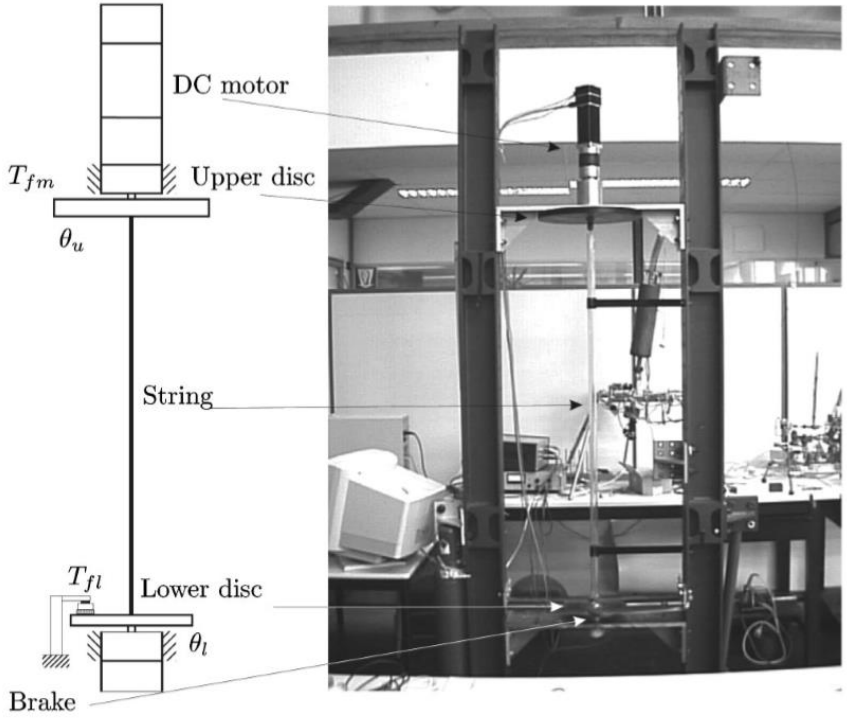

Figure 7: Experimental setup used by Mihajlovic [20].

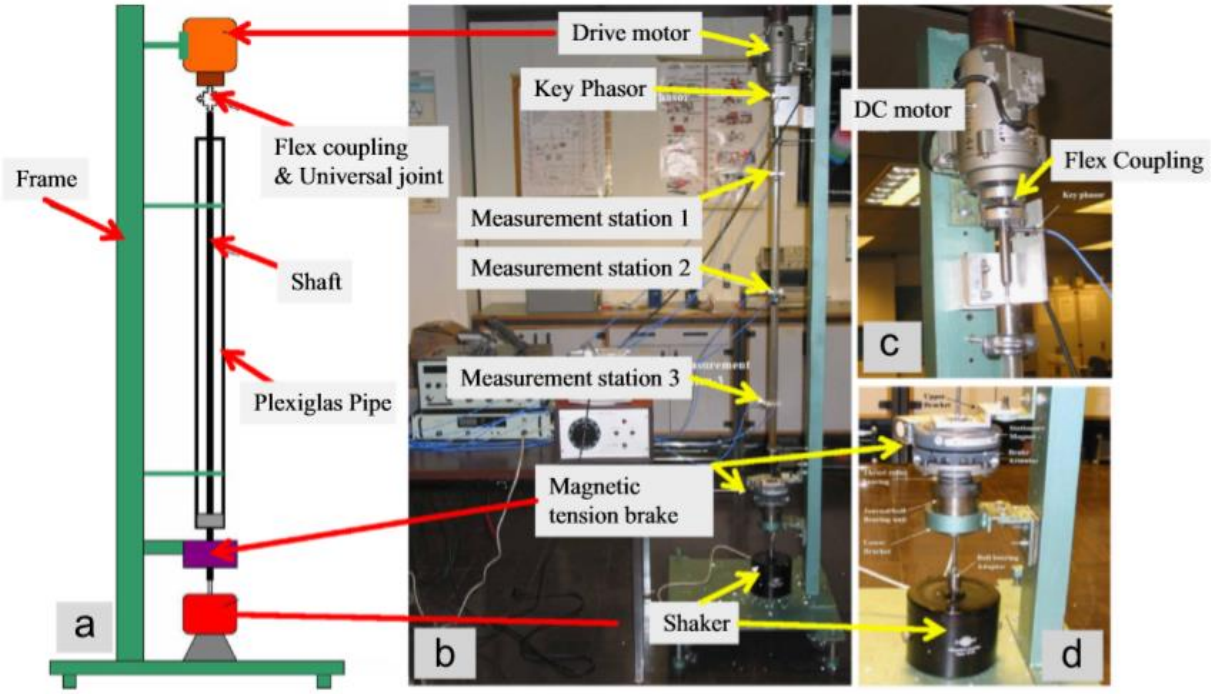

Figure 8: Laboratory investigation of drillstring vibration [33].

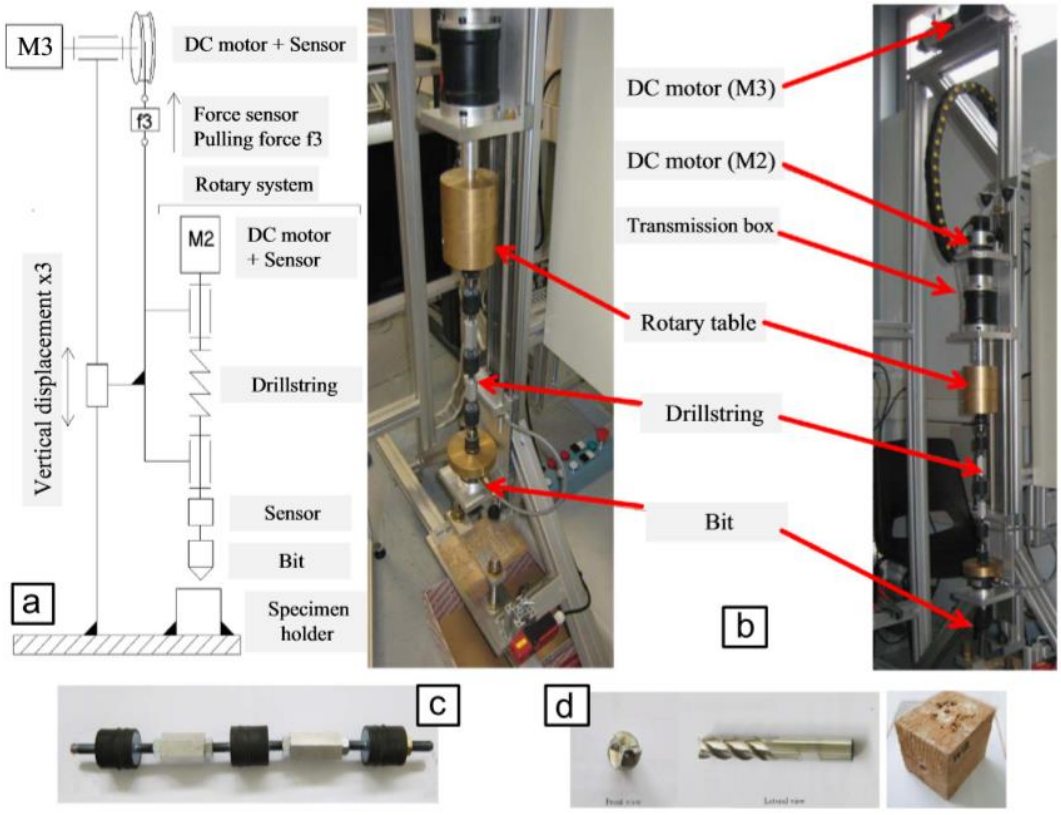

Figure 9: Schematic and experimental setup of the rotary system [34].

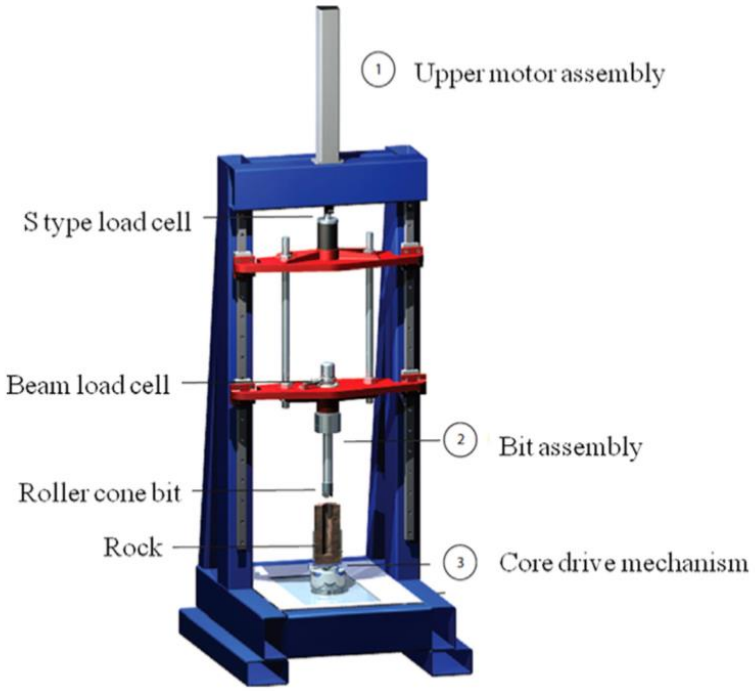

Figure 10: Experimental drilling rig used by Franca [17].

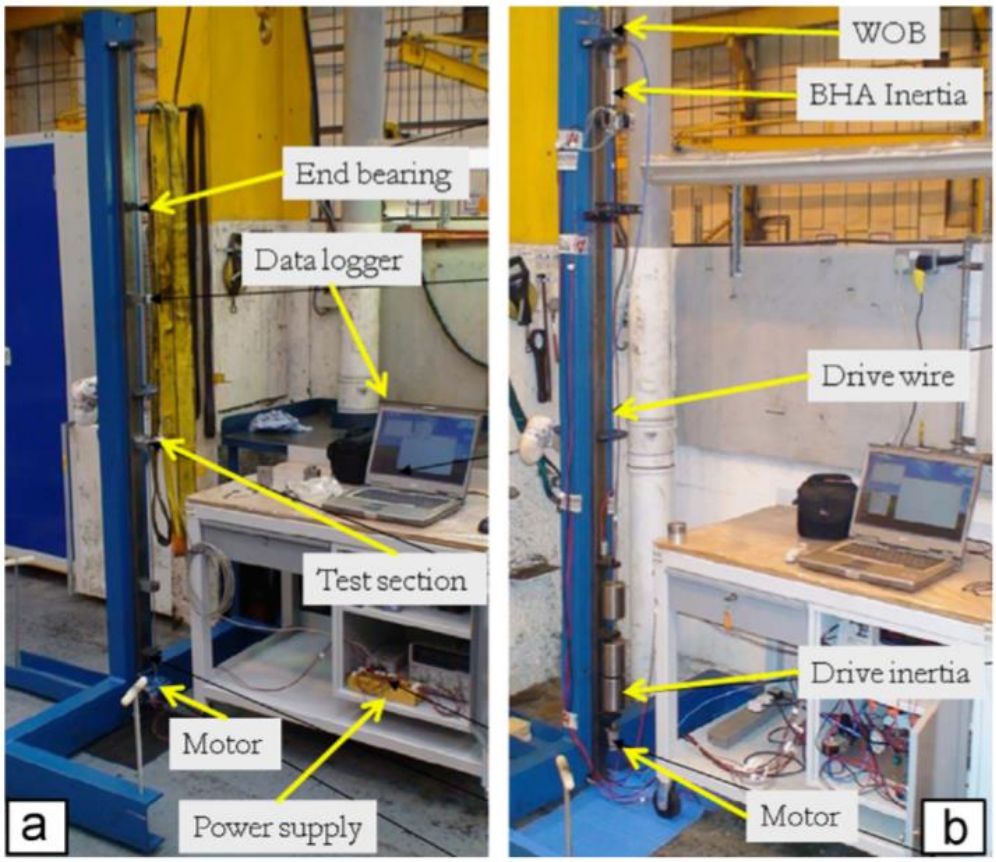

Figure 11. Experimental setup used by Foster [10].

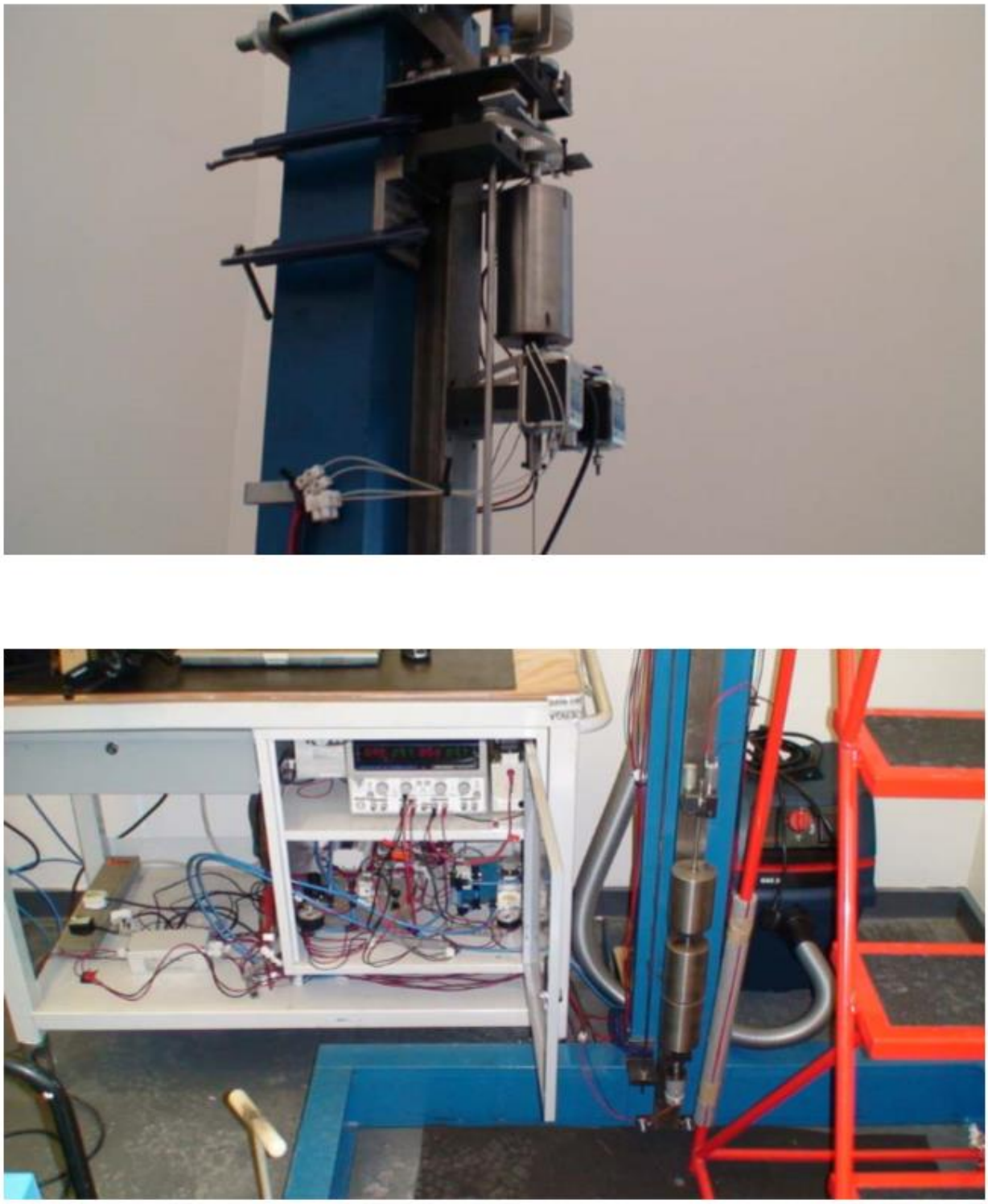

Figure 12: Experimental setup used by Foster [11].

Figure 13. Experimental setup used by Esmaeili [9].

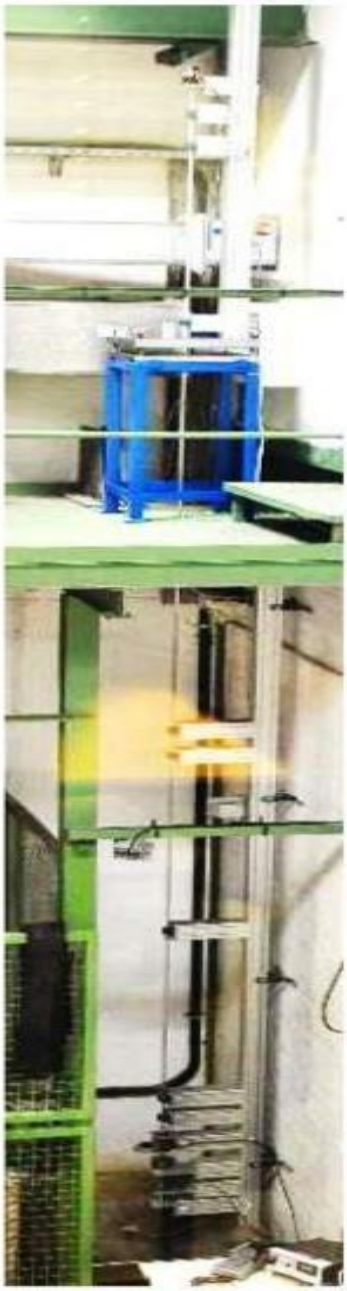

Figure 14. Experimental setup used by Patil [14].

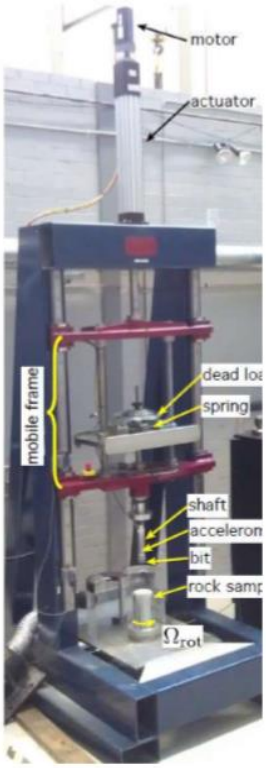

Figure 15. Apparatus used by Kovalyshen [8].

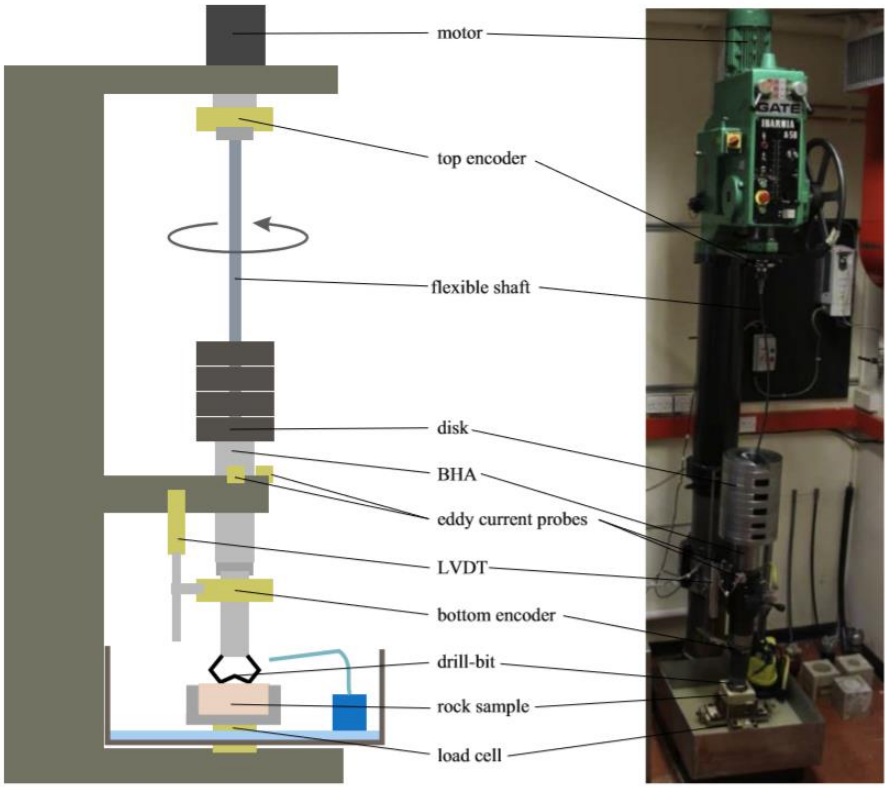

Figure 16. Experimental setup used by Kapitaniak [7].

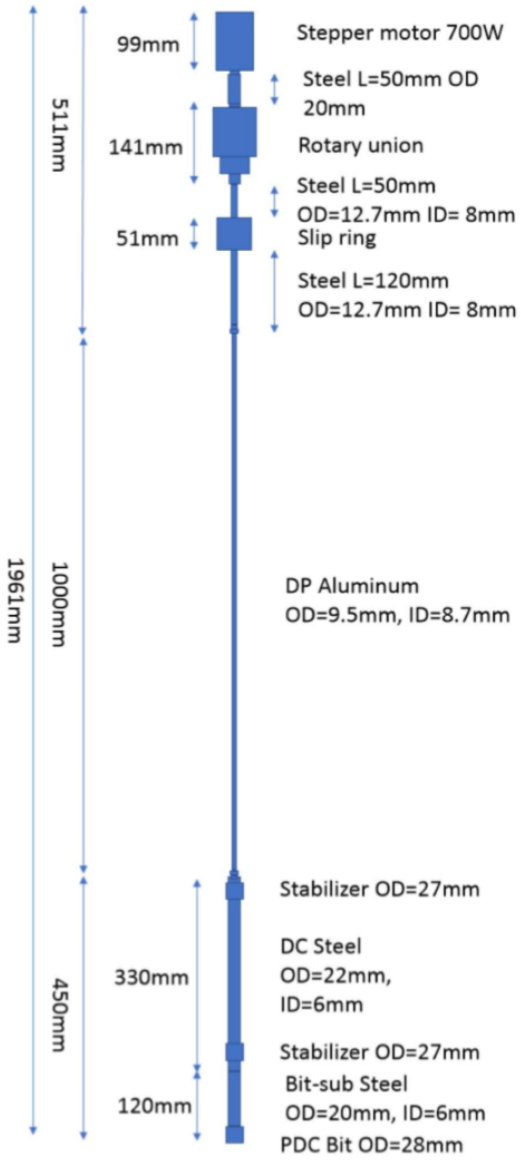

Figure 17: Experimental setup used by Ceyux [18].

Figure 18: Experimental setup used by Ren [19].

1.7 Past Drillbotics® drilling setups

Drillbotics® is an international competition where teams from all around the world take part. It requires teams to design and build a miniature version of automatic drilling rig loaded with sensors using control algorithm to autonomously perform drilling into the rock sample provided by SPE's Drilling Systems Automation Technical Section (DSATS).

The goal of this competition is to the promote development of innovative techniques in drilling automation areas such as drilling machines and downhole tools, allowing participating teams to develop a deeper understanding of the drilling process.

Purpose of including it in my thesis is to compare and discuss the standing of the proposed automated drilling setup in this thesis with the progress made in drilling automation by other groups and organizations.

Table 2, is a technical data sheet of the miniature drilling rig setup built by the winning teams. It provides useful insight into the operational range of different drilling parameters, type of controllers and sensors used, and software and data acquisition (DAQ) system used in their development.

Table 3, based on the key performance indicators listed below, is a summarized form for the work done by different university teams which identify the contribution by them in form of automation in miniature drilling experimental rig setup. This summary is focused on the teams that came at first place in the competition in respective years and compare/discuss their work with the proposed experimental setup.

Key performance indicators:

- Intelligent control system
- Rig mobility
- WOB control
- Hoisting system
- Sensors installed
- Optimization parameter

Table 2: Technical data sheet for miniature drilling rigs developed by winning teams

Setup name	Technical Data			Controllers and Actuators			
	RPM	WOB and TORQUE	Circulation	Top Drive	Hoisting	Sensors	Software, DAQ
2015: University of Oklahoma [26]	Max speed 1170 rpm with 1HP top-drive motor	Maximum torque handled by pipe: 174.77 in-lbf max. WOB: 77.72 lbf	Maximum pressure of 300 psig with 1.5 HP pump 3-phase motor		Pneumatic	- Displacement sensor: Laser - RPM: Optical sensor - Torque sensor: Omega TQ513 - Vibration: Dwyer VBT-1 - WOB: Load cell - Flow: Flow Meter (OMEGA FLR6315D) - BHA: Strain gauge	Visual basic DAQ: Omega
2016: West Virginia University [27]	Max RPM 720, 1/8 HP		maximum flow rate of 7 gpm and a maximum output pressure of 125 psi	Control DC motor Class NEMA 34	Electromechanical Chain to motor operated	- RPM Sensor: Encoders - Torque: strain gauges - Drillstring fluid pressure: Pressure transducer -Bit temperature: temperature probe - Displacement sensor: Stepper lift motor	LabVIEW DAQ: Intel Edison system

						- Hook Load: Load cell - Buckling: Two proximity sensor - Vibration sensor: Accelerometer	
2017: Texas A&M University [28]	maximum rpm of 1200	WOB: 80 lbf max.	Closed loop circulation	2.5 HP DC motor	Drawworks	- Weight-on-bit: S-Beam load cell - RPM: Tachometer Torque: Hall effect current sensor - ROP: LVDT - Vibrations: accelerometer	LabVIEW DAQ: NI CompactDAQ (Model number: NI (DAQ-9174)
2018: Norwegian University of Science and Technology [29]	400 and 1400 RPM	WOB maximum load of 2.5 kN (250 kg) TORQUE limited to 7.1 Nm	7.4 bar from outlets	24 V DC-engine	Linear roller guides. Ball screw mechanism.	- WOB: Cylindrical Load cell - Pressure: Pressure gauge - Downhole sensor: gyroscope and accelerometer - hole inclination and azimuth: Gyroscope - Vibration - accelerometer	Simulink

Table 3: Summary of Drillbotics winning teams to study drilling automation

Setup name	Pros	Cons	Discussion
2015: University of Oklahoma (Figure 19) [26]	- Wheels for rig mobility - Precise WOB control allow mitigation of stick-slip phenomenon - hybrid (hydraulic-pneumatic) - Sensors used are speed, torque, pressure, displacement, flow rate - Optimization parameters used are high ROP and low MSE	- Hardcoded WOB control parameter - Electrical connections limit mobility	Precision control of Drilling parameter WOB allows significant control over vibrations.
2016: West Virginia University (Figure 20) [27]	- AI technique used: simulated annealing - attachable fluid circulation and movable instruments or ease of mobility - lifting mechanism uses a chain with a counterweight to ensure drillstring does not crash - Wireless connectivity over Wi-Fi and Bluetooth capability - Sensors used are speed, torque.	- Limited rig mobility	Advance algorithm used to optimize drilling performance with wireless connection capability. Wireless connectivity improves data monitoring and ease in setup mobility.
2017: Texas A&M University (Figure 21) [28]	- Wheels for rig mobility - Downhole sensor to measure accelerations, vibrations, pressure, etc. connected to the mobile app. - Optimization parameters used are high ROP and low MSE	- Basic optimization algorithm - Hoisting system is draw-works - Whirl causes uneven wellbore quality.	Easy mobility of the rig and extensive safety features. Downhole sensor connected through a mobile app is a useful feature.
2018: Norwegian University of Science and Technology (Figure 22) [29]	- Wheels for rig mobility - Downhole sensor for vibration and azimuth angle - Ball screw hoisting system provides stable and precise hoisting	- Experimental result-based optimization of ROP using WOB and RPM - Wired downhole sensor	Ball screw based hoisting system provides precise and stable control over WOB.

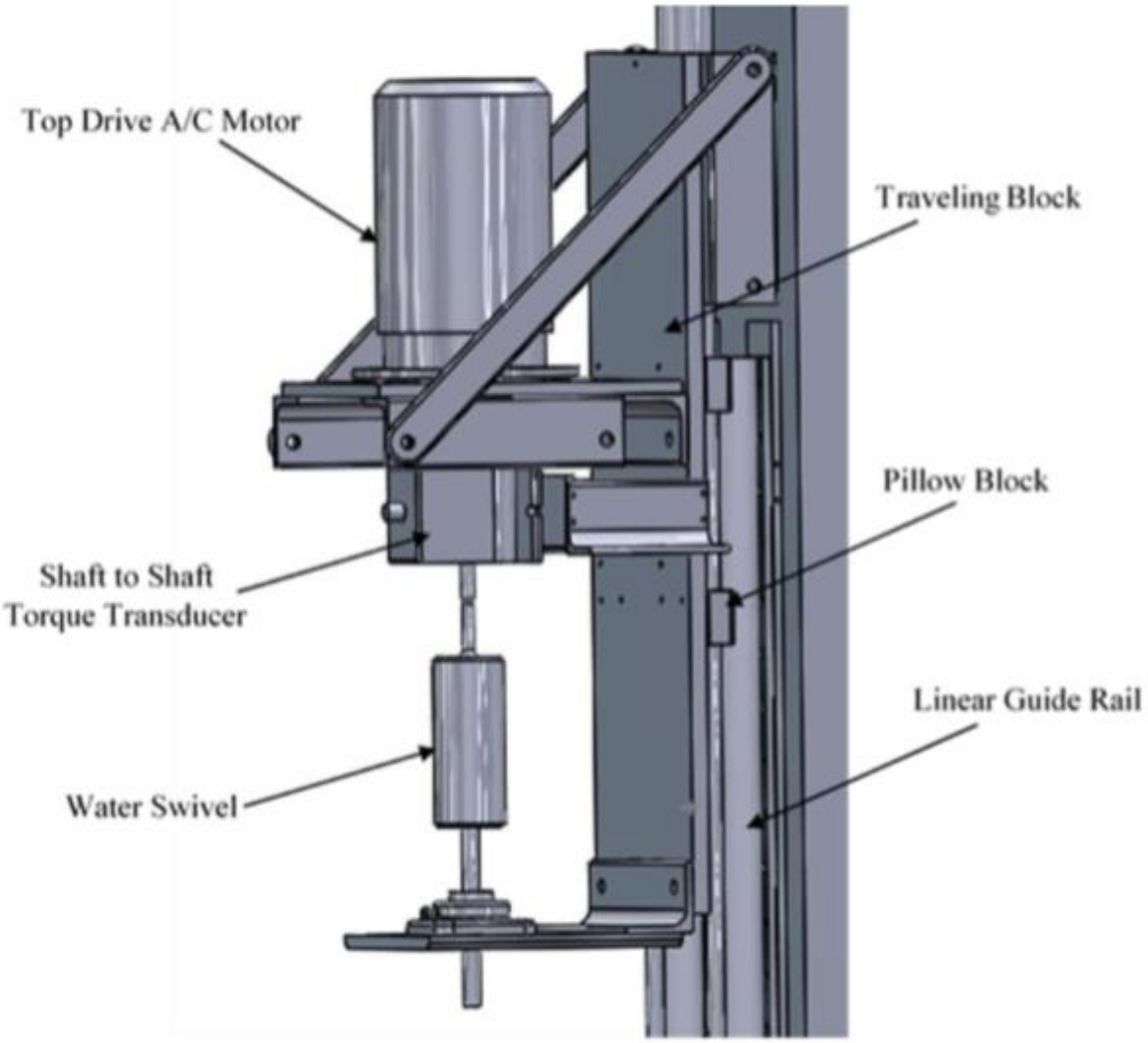

Figure 19: University of Oklahoma drilling rig traveling block [26].

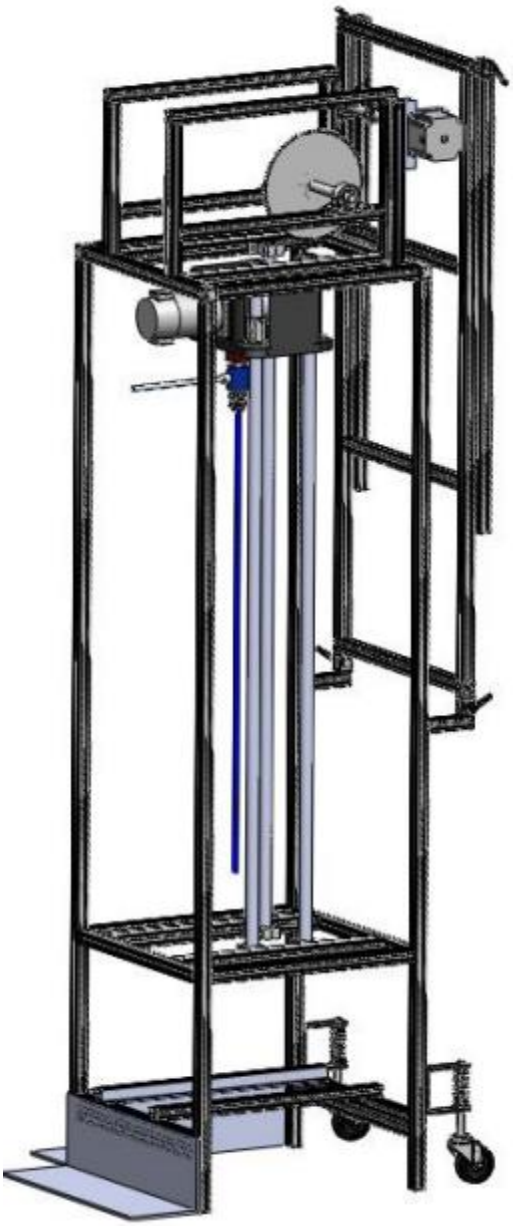

Figure 20: West Virginia University drilling rig setup [27].

Figure 21: Texas A&M University drilling rig setup [28].

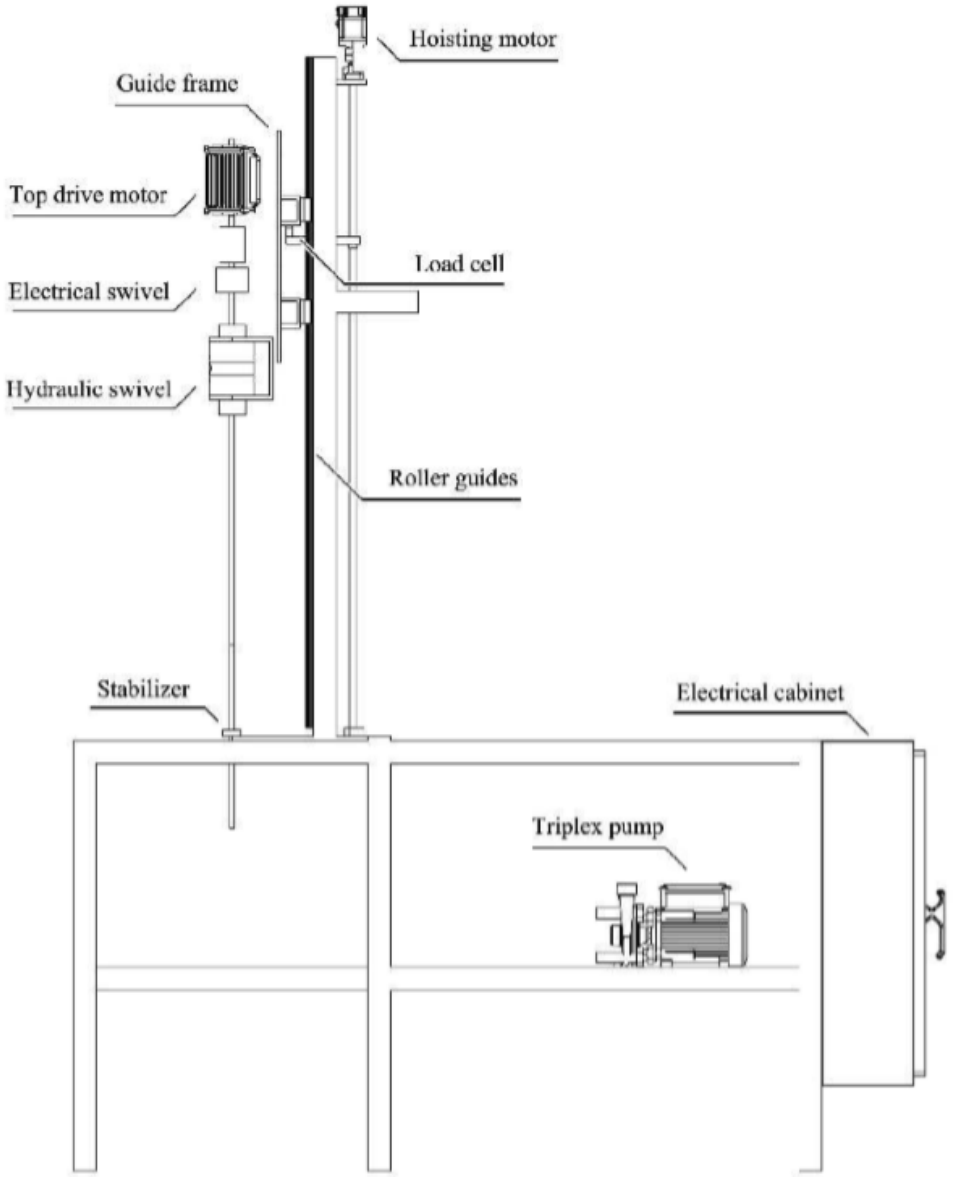

Figure 22: Norwegian University of Science and Technology drilling rig setup [29].

Below discussion aimed to highlight key takeaways from the analysis of automated miniature drilling rig setups developed by different teams, as mentioned in Table 2 and Table 3.

Discussion

- All the developed setups have limited drilling depth capability. Which is understandable, since, their purpose was not to replicate deep drilling well.

- Only a few setups such as University of Oklahoma and Norwegian University of Science and Technology have precise WOB control of 50 grams. Precise WOB control benefits in minimizing vibrations.
- Most of the University setup use LabVIEW as their programming interface. Even the universities that earlier used other platforms switched to LabVIEW in later stages of the competition or included it in the future suggestions.
- Most of the setups have used more than five sensors, which were WOB, displacement, torque, vibration, flow rate, on the rig. Using a greater number of sensors provide more data about different aspects of drilling and helps make a robust decision. It is also important the sensors provide precise data allowing accurate evaluation of the measured parameter.
- Controllers used in most of the setup are DC motors which do not have very high precision. To counter that PID controllers are used by the teams.
- Screw-slider based hoisting system proved to be most robust and precise for moving the top-drive in the vertical direction.

1.8 Current experimental research setup

This setup is targeted to mimic stick-slip situation by generating the conditions based on the value of input parameters. The overall design accounts not only for torsional vibrations but also allows the string to move axially while RPM, WOB, and flow rates are directly linked to the simulator, and, due to the simulator's advanced layout, resembling drillstring with a medium to small radius of curvature, the stick-slip process will be captured and highlighted for a wide range of directional well situations.

In the new designed experimental setup, by Antonio & Teodoriu [6], at the University of Oklahoma some of the above-mentioned issues are addressed. The first is the dimensional limitation of the experimental setup in comparison to the actual model. To properly represent what it is observed in the field, it is necessary to downscale the dimensions and parameters to lab size dimensions. However, as it has been mentioned before, this is a difficult task considering the kilometers usually drilled in comparison to the meters of laboratory space available. That is why the largest experimental setup so far has been 6 meters tall. The new downscaled model being built at the University of Oklahoma, is being designed to have a downscaled factor of 1:40 to recreate 580 m (1920 ft) of the drillstring. This is the largest downscaled model existing in the current research on drilling. The dimensions of the vertical section are shown in Table 4.

Table 4. Dimensions of the new experimental setup [6].

Variables	Real	Model	Units
Length	*580*	14.5 (1:40)	m
OD	**5**	**1/8**	**in**

The second limitation seen in the models, as seen in the past, is that only vertical drilling rig model has been re-created but currently most of the wells being drilled are horizontal wells. Thus, to investigate the combined effect of vertical, curved and horizontal sections of the well the experimental setup for this study has been designed with a vertical, curved and horizontal section. This will allow all three sections to be investigated separately as well as the combined effect of all these on the drillstring dynamics.

The third limitation is replication of complex drillstring vibrations happening downhole for an actual drilling operation. Past experimental setups do not have the capability to replicate the rock bit interaction. The experimental setup that uses an actual rock in drilling operation, introduces further errors, due to that fact that confining pressure in the reservoir rock, rock material is potentially very different from actual drilling conditions. To overcome this limitation, high-frequency hexapod and an electromagnetic brake system is used in the experimental setup, which will allow recreating a wide spectrum of bit-rock interaction behavior. The advantage of a hexapod over a normal vibratory table is that of extremely high precision of repeating movements, the hexapod used in this setup have a strut resolution of 50 nanometers. With up to a 4g acceleration and 250 mm/s speed, the hexapod can reproduce the most severe bit-rock interaction processes.

The fourth limitation, not many of the past experimental setups can replicate the drillstring vibrations accurately and that are visually clear. This experimental setup has transparent casing and wellbore allowing a visual investigation of drillstring behavior.

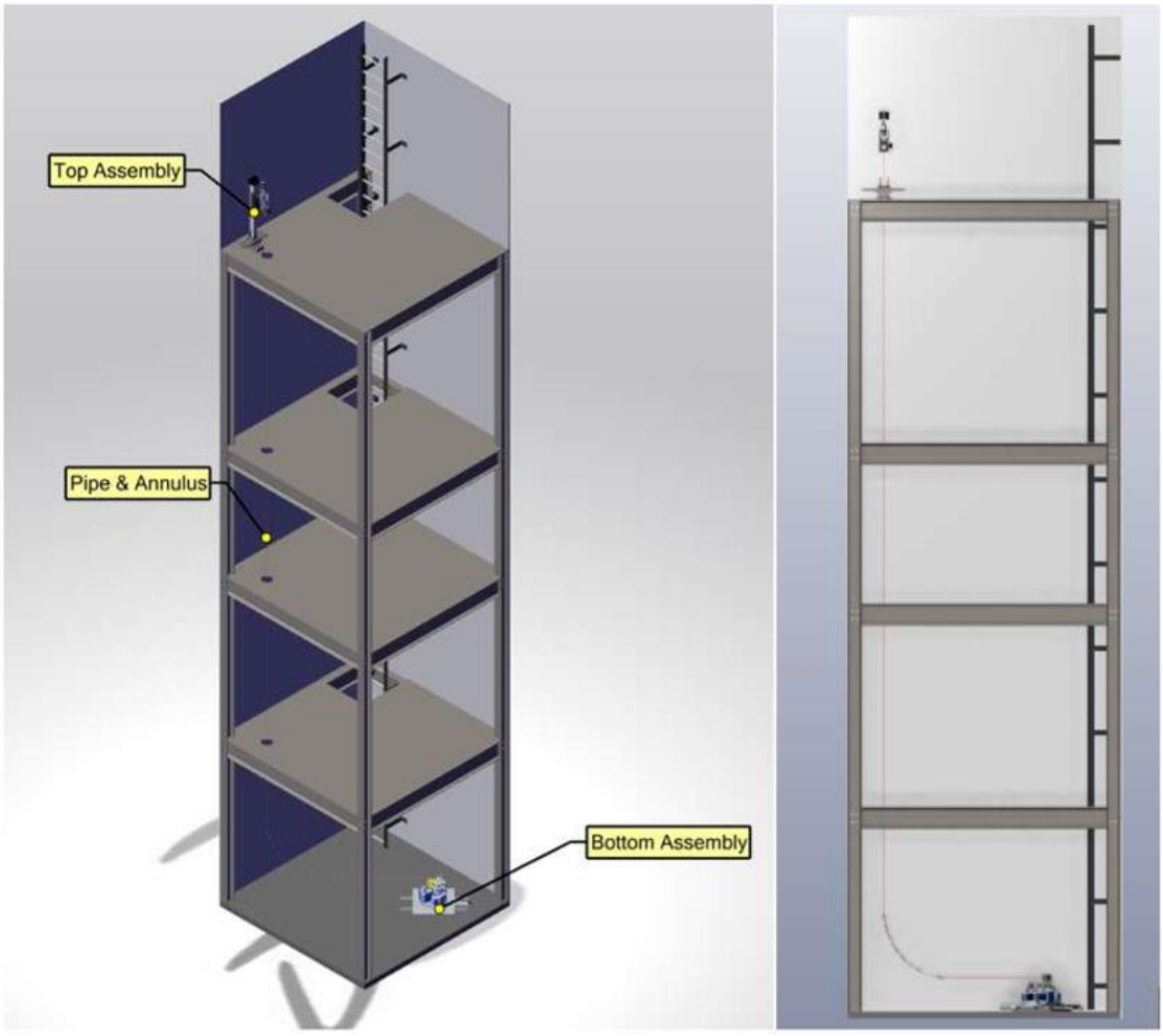

Figure 23. Model of the new downscale experimental setup [6]

The structure of the new setup, shown in Figure 23, is shown with an isometric view and a side view. Drillstring passes through the holes on the levels. Mounted on the top is the top assembly and on the lowest floor is the bottom assembly. In Figure 24, the top drive configuration can be seen in more detail with each component. Finally, the bottom assembly (shown in Figure 25) features the Dynamic Hexapod. Bottom assembly will also have electromagnetic braking to act downhole torque against the bit rotation. All these components together will make a functional downscaled experimental setup of a drilling rig capable of reproducing drilling vibrations.

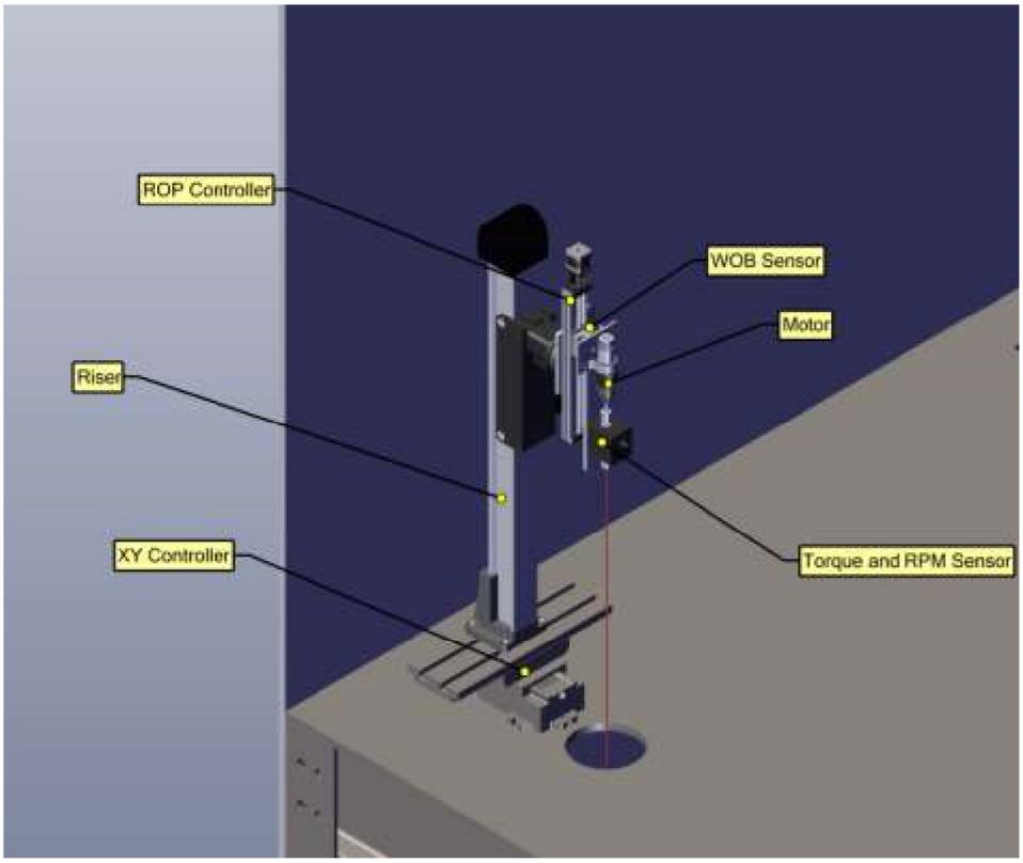

Figure 24: Top assembly setup details [6]

This setup will also allow changing between medium and small curvature in the transition from vertical to completely horizontal, see Figure 23 side view. This range of curvatures allows the study and simulation of stick-slip effects on a wide set of directional drilling situations. This has yet to be seen on any other experimental setup. To simulate long horizontal wells the setup has an additional exit that allows simulating wells with a horizontal to vertical ratio higher than 2.

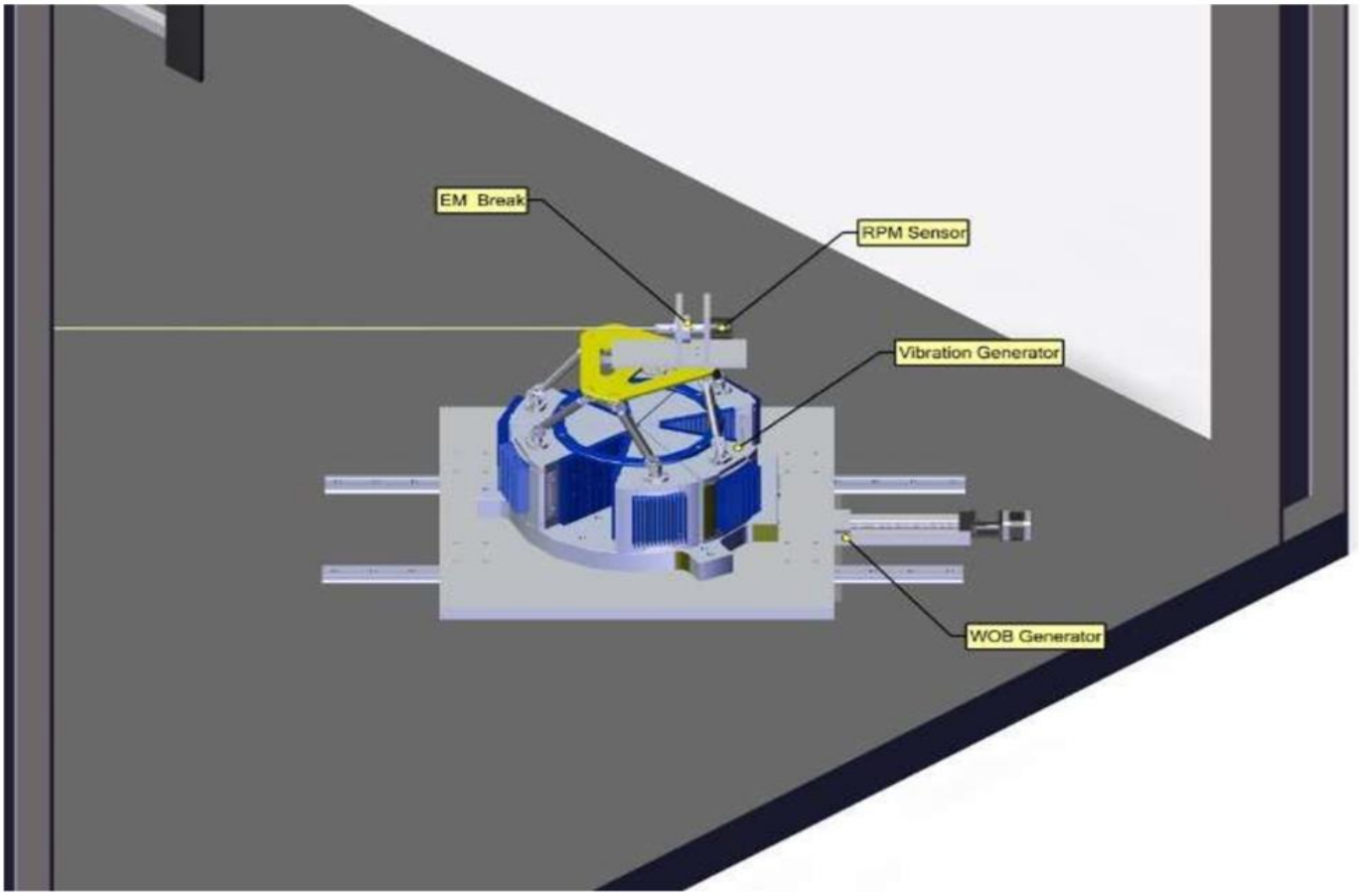

Figure 25. Bottom assembly setup details [6].

1.9 Introduction to LabVIEW

1.9.1 What Is LabVIEW?

LabVIEW stands for Laboratory Virtual Instrument Engineering Workbench. It is a platform that offers a graphical programming environment. In this platform, user can create different application having a sophisticated user interface. It can be used quickly and efficiently to develop a professional measurement, test, and control system application. LabVIEW has many integration tools with both hardware and software. It has many available built-in libraries for advanced usage and analysis. It is most widely used as instrumentation software for its quick and easy to use nature and it provides a virtual visual appearance through which a user can control/operate a physical system of instruments such a stepper motor. LabVIEW is, therefore, also known as virtual instrument language, many VIs are built-in the software to perform complex tasks. Customized VIs can also be built by the user which allow repetitive usage of the same.

1.9.2 Why LabVIEW?

Interactive GUI – LabVIEW has very easy to use, interactive interface on the front panel. This platform does not require writing several lines of code, instead, user can drag and drop the

graphical icons on the screen. This allows very intuitive programming with little or no knowledge of conventional programming knowledge.

Hardware Integration – LabVIEW has built-in tools which can acquire data from different types of data acquisition hardware such as NI, Omega. LabVIEW includes extensive support to interfacing devices such as cameras, instruments, and others. The block diagram in LabVIEW program is in the form of an electrical circuit with wires connecting different VIs, thus, its real-world hardware implementation is easy. This deploys ability to feature in LabVIEW i.e. the deployment of Virtual Instrument (VI) directly into the field allowing HIL/SIL applications as one of the main advantages of building a simulator in LabVIEW.

Advanced Control – There are many built-in toolkits that are very useful in simulating the drilling automation such as MPC controller, PID autotuning in the control design, software, and simulation toolkit. LabVIEW has the capability to execute the program in parallel threads and loops as it treats each independent loop as hardware with voltage applied across them, current flows through them independently.

Multithreading – LabVIEW is very easy to program multiple tasks that are performed in parallel through multithreading. Multithreading allows parallel execution of different parts of the program. This results in faster execution of the algorithm with the compiler, it automatically identifies the part of the code that can be executed in parallel and executes it without the user exclusively specifying it. LabVIEW has a feature of event-driven programming that extends the dataflow environment and allow direct interaction of the users with the program with no need for polling.

1.10 Programming

There are many tutorials that are available for programming in LabVIEW. The programming methodology in LabVIEW is designed such that it is user-friendly and easy to follow.

1.10.1 Programming structure

VIs in LabVIEW program has mainly three components to it, firstly, the Block diagram, secondly icon and, thirdly, Front panel. Figure 26 display example of front panel VI. At front panel user can control various virtual instruments such as knobs, switch. The front panel displays the control system, the output graphs and values to be measured.

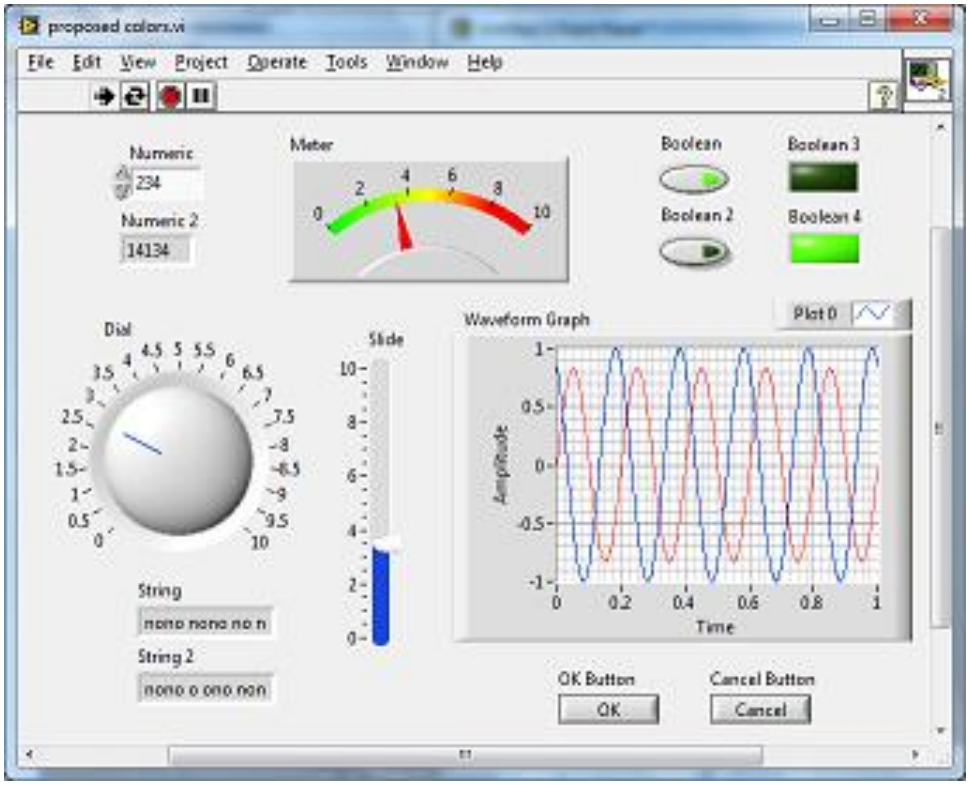

Figure 26. LabVIEW Front Panel [37].

The Block Diagram (shown in Figure 27) is a section where programming (using G-code) is done and it runs in the background.

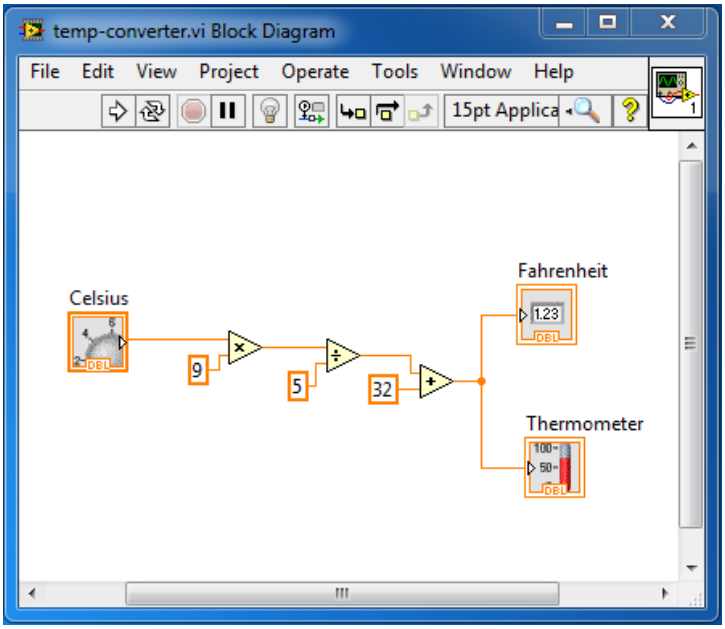

Figure 27. Example of LabVIEW Block Diagram [37].

Note: Above figures are only used as an example to represent the visual aspect of the actual program which is explained in the later section of this study.

In the block diagram, the displayed icons and the connectors represent the node and wire respectively. Where operations happen in the icons (nodes) and the signal is transmitted through the connectors (wires). These icons are available built-in or can be custom built as sub-VI. This block diagram is this analogous to the text-based programming language.

1.10.2 Programming Tools

The programming tools compose of Indicators and Controllers used on the front panel. These are available on the Indicator and Controls Palettes respectively (shown in Figure 28). The controller VIs serves as an interface for the user to provide controlling input to the actuator and indicator VIs are for output display purposes. The controller VI consists of dials, pushbutton, sliders, knobs, switch and other input devices. The indicator VI consists of LEDs, graphs, numerical display, and other displays. The controller VIs generates an output signal that is supplied to the actuators through the hardware device interface. Indicator VIs receives input from sensors or processed output signal from other VIs and are displayed on the screen.

The front panel only displays the Controls and Indicators, to add the code to these graphical object's functions are available on the Function Palette in the block diagram panel. The block diagram displays the graphical source code that is dragged and dropped on the front panel called terminals. In the block diagram, these terminals are connected to the operation VI such as addition, multiplication, or included in case structure and other available options. These operations VI are connected to each of these terminals through wires. These wires decide the order in which the operations will be performed and basically forms the fabric of the program.

In addition, there is a Tools Palette to create, modify and debug VIs. Debugging can be done using toolbar options, for example, single-stepping, probing, creating breakpoints, execution highlighting, etc.

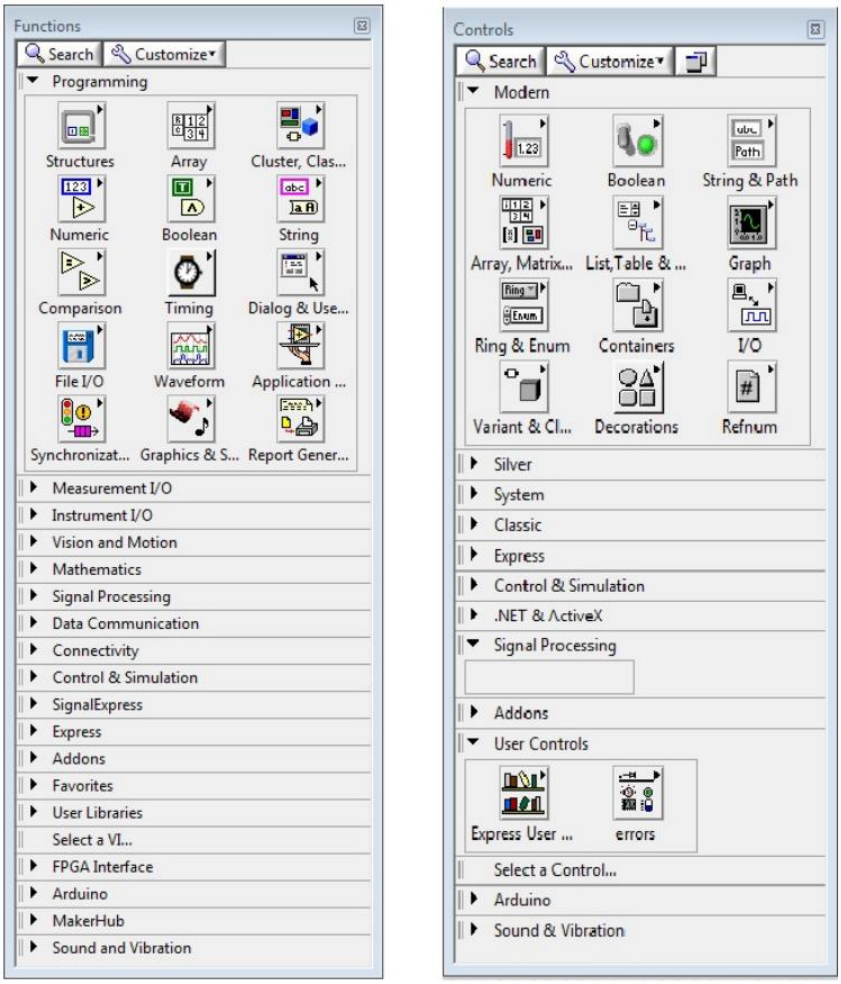

Figure 28. Function palette (on the left) & controls palette (on the right) [37].

1.10.3 Programming Techniques

Times the block diagram becomes very complicated to visualize and understand the logic. There are certain programming techniques to help with that like cleaning the program by segmenting or using cleaning tool to arrange all the VIs and works so that it is easy to visualize, using sub-VI to group a task in the program making the main program compact and building the program effectively using schemas as discussed below. This programming is very useful for drilling automation to prepare simulator like display.

There are a few programming schemas and design pattern which has helped greatly in building an effective program as explained.

1.10.3.1 Event-Driven Programming

Event-driven programming is a parallel way of communicating between user interface or external input/output and the block diagram. The event structure in this programming method includes a certain set of operations that are only executed until the event for that structure of the operations is executed. User can manually interface through mouse keys for execution of the programs. The

benefit of the event structure is that the execution of event and all operation included in that event gets executed when the user provides certain input, triggering the operation.

By using events to respond to specific user actions, you eliminate the need to poll the front panel to determine which actions the user performed. A sample program using Events is provided in Figure 29.

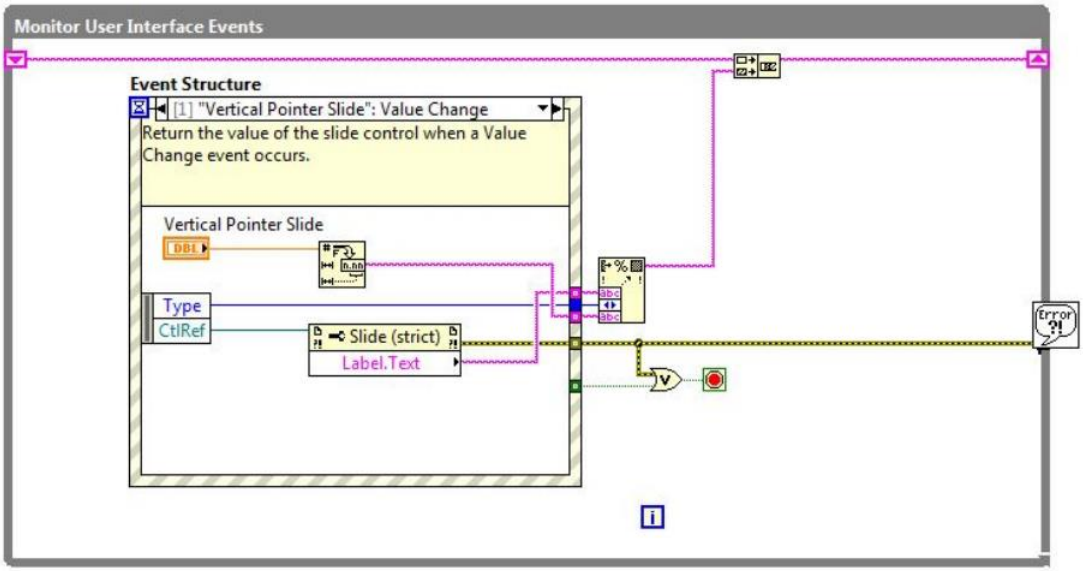

Figure 29. Example of a program using events [37].

1.10.3.2 Multiple-loop Design Patterns

This form of design pattern follows two basic design patterns i.e. Master/Slave and Producer/Consumer design that allow sharing of data among multiple loops running at different rates. The parallel loops sharing data has one as a producer and other as a consumer. In master and slave pattern the outside loop acts as master and the one inside of it as a slave. The slave loop only executes when the master loop gets triggered for execution.

The data queues communicate the data produced by different sections of the loop to other loops i.e. buffer the data from producer to consumer. In this pattern, the producer loop continually queues the additional data while the consumer loop processes the data at its own pace. A sample program using Events is shown in Figure 30.

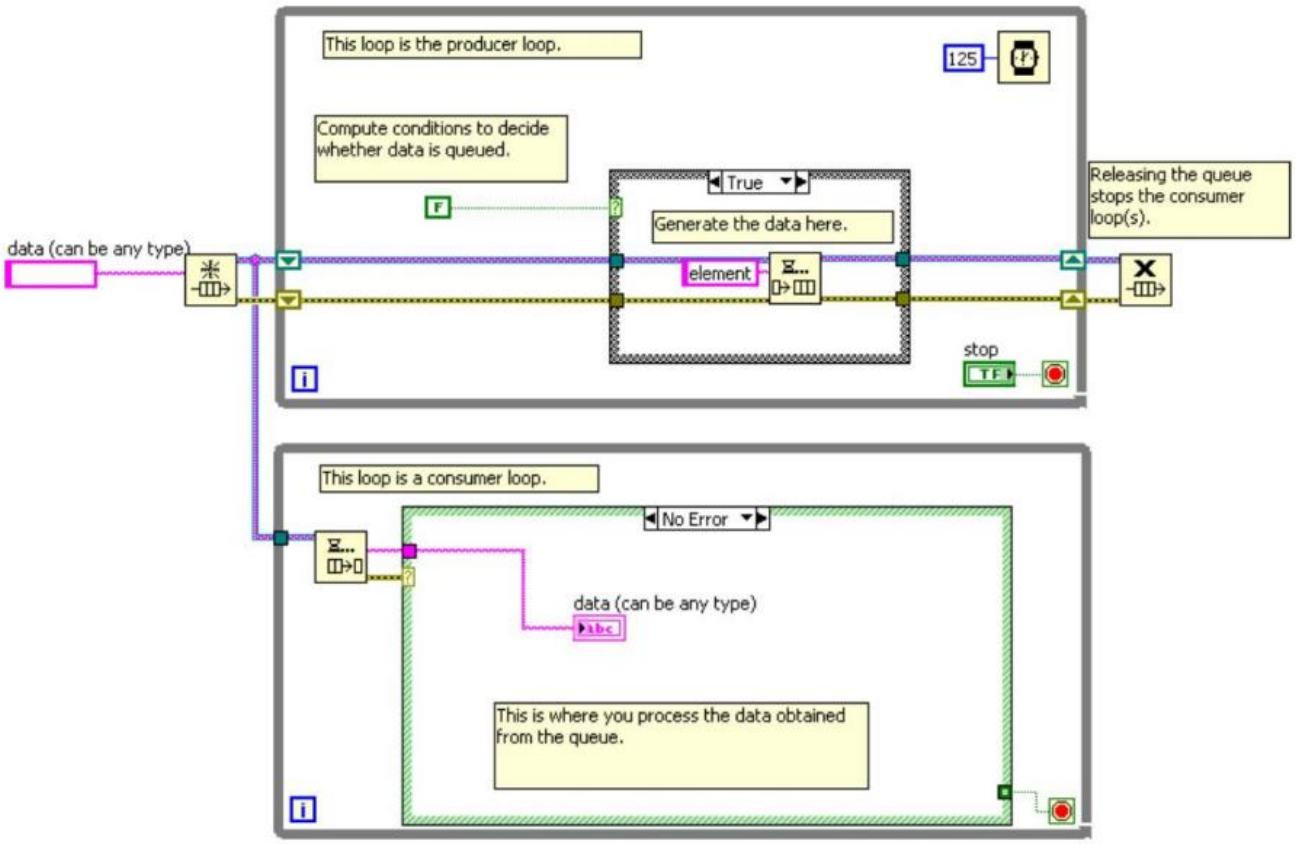

Figure 30. Producer/Consumer design pattern [37].

1.11 Data Acquisition

As the name suggests the data acquisition tool acquired data from different sources using a DAQ card in the form of signal. The sources can be sensors, controllers, or other forms of hardware. Signals can be electrical or physical in the form of temperature, current, voltage, or sound. Data acquisition is one of the most useful aspects of LabVIEW with this ability to acquire data from other applications. A basic structure of the DAQ system is shown in Figure 31.

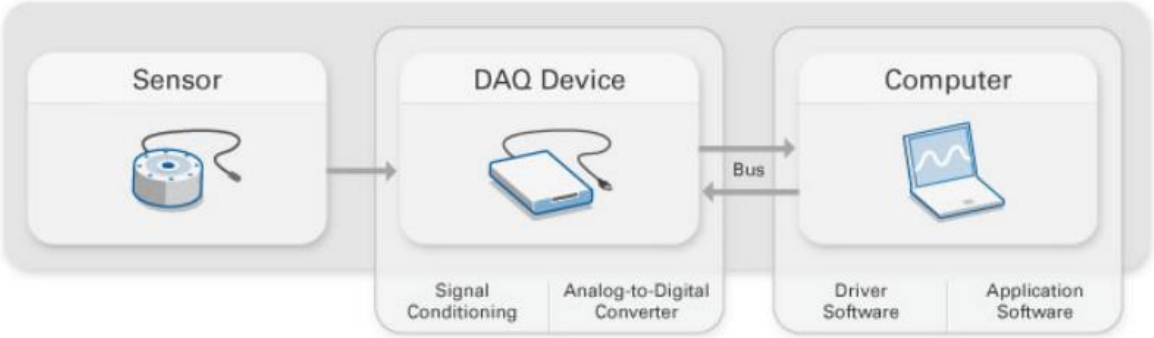

Figure 31. A simple DAQ system [37].

In this research study, the DAQ card receives input from three different channels i.e. torque sensor, displacement sensor, WOB sensor and sends the output signal to the top drive rotary motor for rpm and stepper motor for vertical displacement.

1.11.1 Sensors

Sensors measure the physical phenomenon, such as displacement, acceleration, temperature, flow rate, etc. It converts these measurements in the form of electrical signals generated by the underlying transducers (sensors). The signals received from the sensors can be in the form of current, voltage, temperature, resistance or other attributes. These signals based on their amplitude can be amplified or reduced. These signals are acquired by the DAQ device to be read and then processed through an algorithm. Some of the transducers that are used in a specific type of sensors are listed in Table 5 [37].

Table 5. Phenomenon and the transducers to measure

Sensor	Phenomenon
RTD, Thermocouple	Temperature
Photo Sensor	Light
Microphone	Sound
Strain gauge, Piezoelectric transducer	Force and Pressure
LVDT, Potentiometer	Position and Displacement
Accelerometer	Acceleration
pH electrode	pH

1.11.2 Actuators

An actuator based on the received input sends an actuating signal to the device, which activated the device to perform its specific function. Along with actuator device also needs a source of energy to generate enough energy for the action. Generally, an actuator is tasked to convert the electrical signal to a mechanical form of energy.

1.11.3 Signal Conditioning

Sometimes signals received through sensors are not accurate or clean to be directly used as an input signal for other application. These signals may contain some noise or carry very high variance. To deal with these issues signal conditioning circuitry manipulated these signals to generate the desired form of signal suitable for input into the device. These conditioning circuitries can include filtering, amplification, noise reduction, attenuation or isolation.

1.11.3.1 Analog-to-Digital Converter (ADC)

Conversion of analog to digital signal is required where the signal needs to be further received by digital equipment. Digital signal is provided by an ADC chip that converts an analog signal into a digital, instantly. Analog signal is a continuous form of signal whereas digital is a step form of function. The samples get transferred through a computer bus where the original signal is reconstructed in software, from the samples received.

1.11.3.2 Computer Bus

A computer bus is a communication device such as Ethernet, Wi-Fi, USB and PCI Express. It communicates between the DAQ device and the computer for transferring signals as the measured data. This device connects to the computer through a hardware slot. The data received from the DAQ device through the computer bus into the computer is processed, stored and visualized as needed through software control. For reading the received signal through the DAQ appropriate drivers needs to be installed and after checking the compatibility of the computer system with the driver version.

1.11.3.3 Signal Filtering

LabVIEW has few VIs that can remove the noise from the signal and make it smoother. Appropriate values of the constants given as an input to the VIs is important, it can be done by varying them in a certain range and checking the generated output signal (as shown in Figure 32).

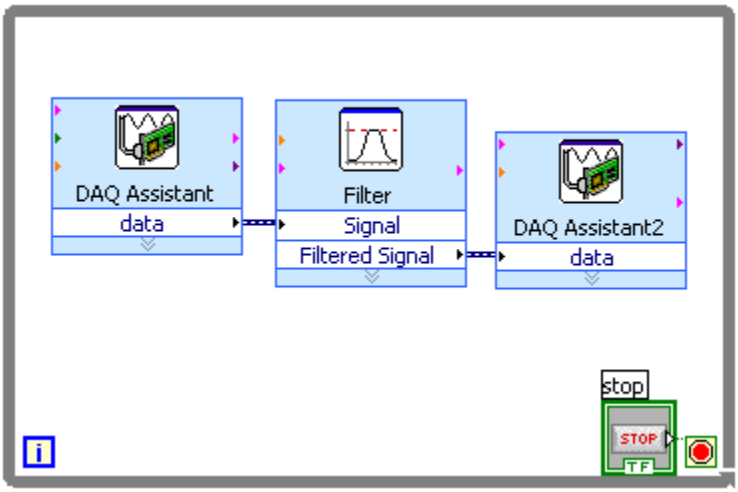

Figure 32: LabVIEW filter VI sample program structure [37].

1.11.4 DAQ Hardware

Data acquisition (DAQ) hardware is a device that communicates between the signal generators such as sensors with the computer. It acts as the interface which receives the signals and pass to the computer as input. DAQ hardware processes these input signals so that it can be read by the computer for interpretation.

There are a bunch of companies that manufacture and sell DAQ hardware. Some of the most commonly available DAQ hardware is from National Instruments (NI), Omega, MComputing and other.

1.11.5 Choosing DAQ Hardware

There are certain parameters that need to be considered before evaluating a Data Acquisition system or before choosing DAQ hardware for your measurement system. Some of these important parameters are discussed here in brief.

1.11.5.1 Type of Signal

DAQ device functions are broadly categorized into the following types:

- Digital Input/Output
- Analog Input/Output
- Counter/ Timer

There are devices that have all the functions listed above or may have a combination of them or even just one. The devices have a fixed number of channels for the functions. Thus, the device needs to be selected most importantly based on the number of channels needed for the specific function type.

1.11.5.2 Sampling Rate

The DAQ receives a continuous input signal from the outside world, this signal is sampled at a rate by the DAQ and sent to the computer. The typical sampling rate for either software- or hardware-timed goes up to 2 MS/s. The sampling rate for your application depends on the maximum frequency component of the signal that you are trying to measure or generate.

1.11.5.3 Resolution

Resolution defines the quality of the signal. Higher resolution means more data is generated per sample. It is the smallest detectable change in the signal that is required of your DAQ device. Resolution refers to the number of binary levels an ADC can use to represent a signal.

Information provided in the above chapter, it is now possible to design and modify the virtual drilling panel or drilling simulator using LabVIEW. Appropriate hardware needs to be selected such as actuators, controllers, sensors and DAQ device to interface with the experimental setup and the LabVIEW program.

Chapter 2: Downscaled system

It is costly and risky to test and verify the performance of drilling control functions on full-scale rigs as to how does it respond to changes in drilling parameters. Therefore, it is smart to test the response on a smaller scale (downscaled) drilling rig and implement to full-scale rig when the response is verified.

System downscaling has been done by using the law of similitude. Downscaling of both mechanical and geometrical parameters are considered. In this section, we further discuss the basis of selection for downscaling parameter and the method.

2.1 Application of the law of similitude

Similitude stands for similarity, law of similitude is used in different applications such as designing downscaled or upscaled model of the existing model, to identify various similarities between two models such as geometric similarity which depends on models shape and size, kinematic similarity depending on dynamic parameters such as fluid flow (changes with time), and dynamic similarity depending on the forces acting on the surfaces. This technique is widely used in the dimensional analysis where the relationship is identified between different physical quantities such as height, width, length and other.

To design and develop an experimental mini drilling rig setup, law of similitude is used. One of the most challenging parts of the job is to identify the critical parameters that have the same nature as that of an actual drilling vibration. The geometrical parameters that a drillstring has are length, diameter, inertia, and stiffness. Drilling vibration is very complicated to replicate as there are many dynamic forces acts on the drillstring which are very complex in nature, thus, in order to replicate the dynamic nature, the parameters that should be selected need to be critical for such behavior.

Three critical parameters were identified, as an objective, that satisfies both dynamic and geometrical downscaling property. Following three critical parameters were considered for scaling of the model [6]:

1. Critical buckling force
2. Angular deflection
3. Power and torque required

Above identified critical parameter play an important role in finding the downscaled parameters for finding dimensional similarity for designing the downscaled model.

2.2 Downscaling Factor

The measured depth of the drillstring can be used as the scaling factor given the good geometry. The measured depth in the laboratory resulting in the downscaling factor ‘n’ can be measured by the following formula.

$$n = \frac{MD_{lab}}{MD_{ac}} \quad (1)$$

Where,

MD_{lab} = Laboratory measure length (ft)

MD_{ac} = Measured depth in the actual drilling rig (ft)

Above formula can be represented using total vertical depth (TVD) as shown:

$$n = \frac{TVD_{lab}}{TVD_{ac}} \quad (2)$$

Where,

TVD_{lab} = Laboratory vertical depth (ft)

TVD_{ac} = Vertical depth in the actual drilling rig (ft)

Above scaling factor reduces to low values that are impractical for the experimental setup. This is because the scaling factor is as low as 100 times calculated from vertical depth result in low diameters of the drill-string pipes. In general, the outer diameter (OD) of a drill-string is somewhere around 5". Scaling of OD result in hair like drill-string which is impractical for experimental purposes. Therefore, downscaling on OD would result in a more realistic and practical geometrical design.

The expression for downscaling based on OD of the drill-string is as follows,

$$n = \frac{OD_{lab}}{OD_{ac}} \quad (3)$$

Where,

OD_{lab} = Smallest acceptable outside diameter for drill-pipe of any material (in)

OD_{ac} = Typical outside diameter of a drill-pipe (in)

Downscaling factor 'n' obtained from OD expression can now be used to determine the vertical depth that would be needed to design the experimental setup.

2.3 Calculating shear modulus and maximum torque

To re-create different states of torsional vibrations in the experimental model, to study the vibration, such as stick-slip require estimation of torque for the downscaled model. To derive the expression for calculating torque for the downscaled model, we use, below expression,

$$Torque = \frac{\tau J}{R} \quad (4)$$

Where,

τ: Shear Stress (psi)

J: Polar moment of inertia of an area (in^4)

R: Distance from the center to stressed surface in the given position (in)

Next, knowing that the polar moment of inertia is expressed as,

$$J = \frac{\pi}{4}(OD^4 - ID^4) \quad (5)$$

Where,

OD: Outer diameter of the cylinder or pipe (in)

ID: Inner diameter of the cylinder or pipe (in)

Then, solving for the shear rate and equating both the real and downscaled expression,

$$T_{lab} = \frac{T_{ac}G_{lab}}{n}\left(\frac{od^4 - id^4}{OD^4 - ID^4}\right) \quad (6)$$

Where,

T_{lab}: Torque needed in the model (lbf ft)

T_{ac}: Torque applied in the real case scenario (lbf ft)

G_{lab}: Shear modulus of the model's material (psi)

G_{ac}: Shear modulus of the real case material (steel) (psi)

2.4 Weight on Bit

Weight on bit (WOB) is a critical parameter to analyze the vibration caused in drill-string during drilling. Using force balance from Newton's 2nd law, assuming acceleration is the same in both the lab and actual model, calculating the downscaled WOB for the experimental model. Assuming fixed WOB of 5 tons, below is the expression derived for downscaled WOB,

$$F_{real} = M_{real}a = M_{ds}a = F_{ds} \quad (7)$$

$$F_{ds} = 2000 * WOB * n\left(\frac{od^4 - id^4}{OD^4 - ID^4}\right)\frac{\rho_{ds}}{\rho_r} \quad (8)$$

Where,

WOB = Weight on bit (tons)

n = Downscaling factor

od = Downscaled outside diameter (in)

id = Downscaled inside diameter (in)

OD = Outside diameter (in)

ID = Inside diameter (in)

ρ_{ds} = Density of the selected material ($lb/in3$)

ρ_r = Density of steel ($lb/in3$)

$$F_{cr} = 2\left(\frac{EIWsin\theta}{r}\right)^{\frac{1}{2}} \quad (9)$$

Where,

E = Young modulus (psi)

I = Axial moment of inertia (in^4)

W = Weight per unit length (lb/in)

θ = Inclination

r = Radial clearance (in)

Chapter 3: Intelligent drilling system

3.1 Automation

Drilling Automation is an area with unbounded technological development. Automation has strengthened its root in drilling industry within the last few decades (2). Traditionally machines have been built to replace manual labor, these machines are controlled by a human, needing skilled labor and effective control to prevent any errors. With fast-paced development in the robotics and automation industry process became safer, accurate, controllable and reliable.

Automation of process reduces the chance of error by performing repetitive tasks with higher accuracy as compared to humans. There have been many incidents when workers have lost their lives on the rig floor. Rig floor is a dangerous place to work on, handling such heavy equipment's leaves a little room to recover from any mistake. Automation increase human safety by eliminating such physical interaction with their drilling environment. Furthermore, Oil and gas industry continuously challenge the drilling service companies to reduce the time of drilling, since, cost of drilling is directly proportional to the drilling time. Automation significantly accelerates the action; process operation becomes more economical due to faster drilling.

Drilling operation requires highly skilled crew who spent most of their time on the drill floor. Automation gives a competitive edge by increasing productivity, reduced man power, improved hole quality (3). Increase control and monitoring through predictive maintenance using sensors, low installation, maintenance and operation costs.

Much of the advancement in the field of automation made is attributed to the explosion in electronics technologies such as sensors, controllers, VFD and computer technology over the past few decades. For automation electronic system is the core for building the open and closed-loop system. Electronics allow sending, processing and receiving signals in the control loop. The function of an electronic system is to automatically regulate the output and keep it within the systems desired input value or "set point". If the systems input changes for whatever reason, the output of the system must respond accordingly and change itself to reflect the new input value.

Likewise, if something happens to disturb the system's output without any change to the input value, the output must respond by returning to its previous set value. In the past, electrical control systems were basically manual or what is called an open-loop system with very few automatic control or feedback features built in to regulate the process variable and to maintain the desired output value.

Automation can be achieved in the form of closed control. Automation requires calibrating input to achieve the desired output.

3.2 Top assembly setup

The top assembly of the experimental setup needed to recreate the same functions as a drilling rig. That is, it needed to have a top drive that generates the RPM and provides rotational torque to the drillstring and a hoisting system that can control the weight-on-bit. The top drive assembly of the

setup is shown in Figure 33. The RPM generator is the motor of an 18 V hand drill that functions with DC current. Its voltage is controlled via a digital power supply. Then, the WOB representing the hoisting capabilities of the system is made by the combination of a translocator and a stepper motor which control tripping motion of the drillstring. The top drive rests on top of an 'XY controller' which moves the string in any coordinate within a certain range in the perpendicular plane. The setup includes three sensors WOB, Torque, and RPM, as shown in Figure 33.

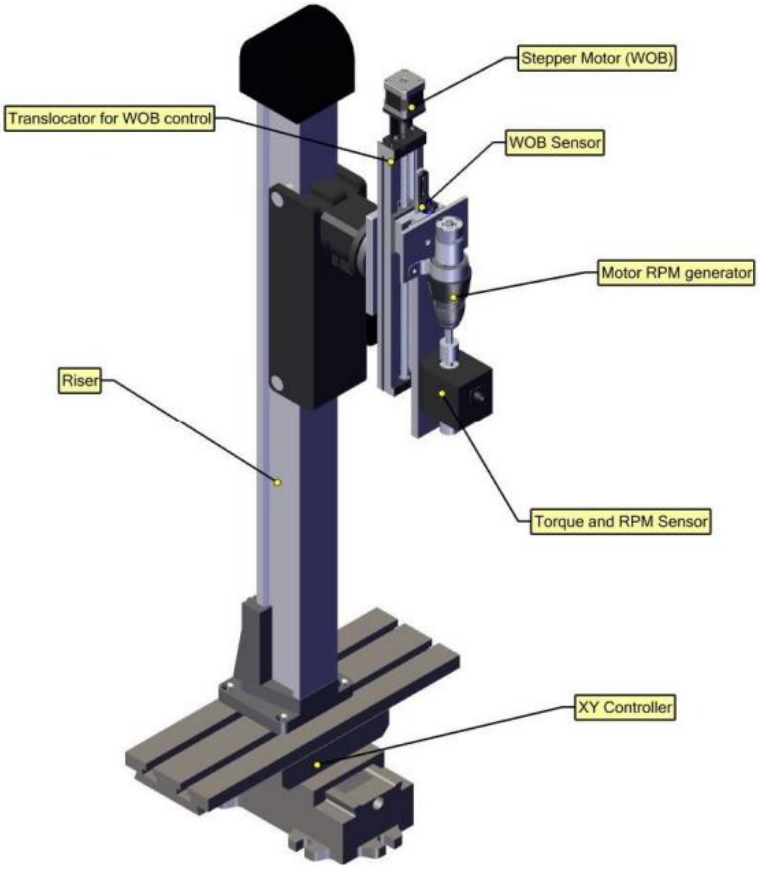

Figure 33. Top assembly CAD model and breakdown [6]

This setup has seven main components, first, riser device that allows the entire structure to be raised and secured at a vertical location. Second, the XY displacer to allow motion in along X and Y axis perpendicular to the vertical motion of drillstring. Third, stepper motor allows precision movement of the top drive in the vertical direction (z-axis) allowing adjustment of WOB. Fourth, the sliding screw controlled by the stepper motor (3) on which the top drive assembly slides vertically. Fifth, the WOB sensor, placed in the connection between the vertical displacer and the motor of a manual drill, senses the weight acting on the connection where it is placed. Sixth, rpm motor rotates the drill-string to generate bit rotation and torque. Seventh, it is the torque sensor monitors the torque experienced by the string is attached to the motor via a metal link.

3.2.1 Sensors

Sensors and actuators having high accuracy serve a better purpose in providing drilling data by increasing the accuracy better data-driven insight can be extracted, with ability to respond quickly in a drilling environment, thus, increasing the drilling efficiency. Accurate data also ensure better safety in drilling operations.

3.2.1.1 Weight-On-Bit (WOB)

This is an indirect measurement. WOB is calculated by having a cylindrical load cell measure tension in the drill line of hoisting system and relate it to the weight applied on the bit. The weight of the Transducer is based on principle force is directly proportional to the electrical signal generated. Corresponding tension to weight conversions is done in the program. The sensor measures the Hook Load, WOB is calculated with the below equation, where, Drillstring Weight is constant.

$$WOB = Drillstring\ weight - Hook\ load \quad (10)$$

Sensor Type: Cylindrical load cell

Name of the Sensor used: Omega, LC201-25

Specification: 25 lb Tension & Compression Load cell

3.2.1.2 Rotational Speed (RPM)

An optical tachometer as shown in Fig. 5.4, using infrared (IR) sensing technology to measure the rotational speed of the top drive motor.

Sensor Type: Reflective Optical IR Sensor

Name of the Sensor used: TCRT5000L TCRT5000

Specification: Transistor Output Infrared 950mm 5V 3A

3.2.1.3 Torque

This sensor measures the torque acting on the drillstring. It is located on the top drive. This sensor converts torsional mechanical input into an electrical proportional output signal through the transducer. Figure 35 shows the concept design of applying torque on the cable. Figure 36 shows the breakdown of the torque application and measurement system. Torque is applied by simply rotating the wheel whose angle of rotation directly proportional to the load applied and to the applied torque. Wheel measurement, as shown in Figure 37, are required to calculate the torque acting on the cable.

Company: Omega Engineering Inc.

Name of the Sensor used: Current Sensor Module; Model: TQ513-012, S/N: 194940

Specifications: 66 to 185 mV/A output sensitivity, Range: 200 IN OZ

Figure 34: Figure showing the TQ513 series torque sensor [38].

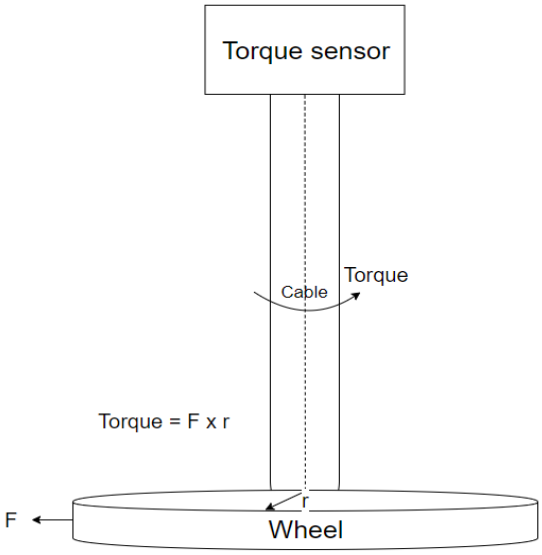

Figure 35. Block diagram of torque on the cable by the wheel

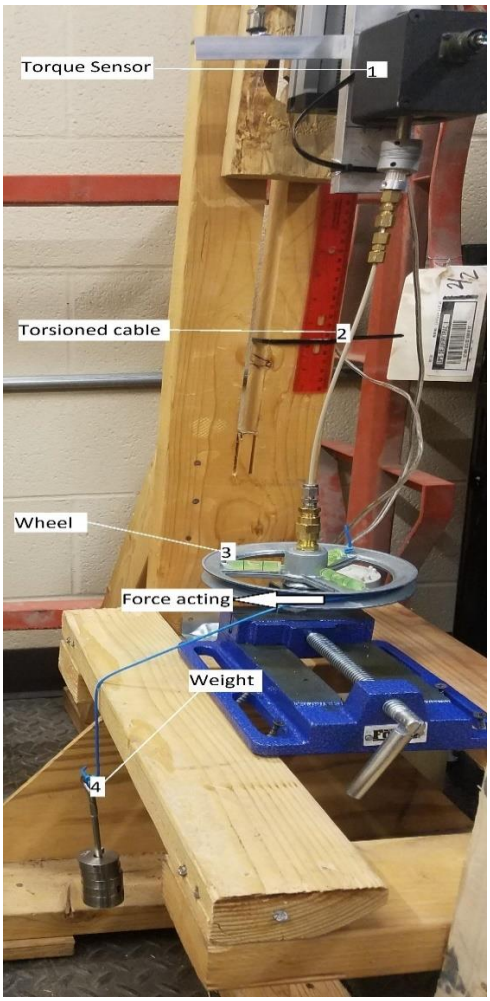

Figure 36. Breakdown of the torque application and measurement system

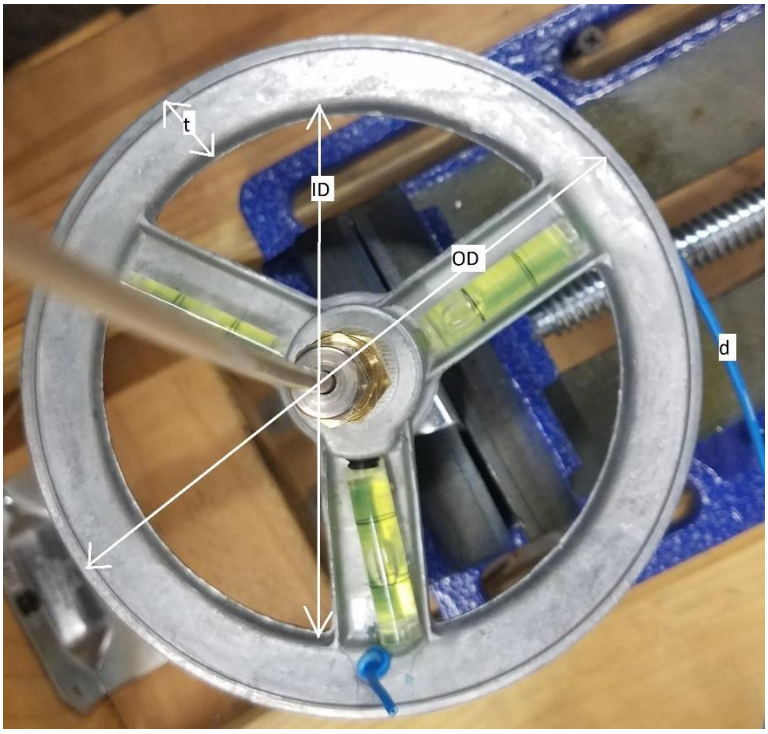

Figure 37. Dimensions of the torque applying system

Where,

ID: Inner diameter of wheel in mm

OD: Outer diameter of wheel in mm

t: thickness or concentric ring

d: diameter of blue wire

r: radius of the inner wheel

F: Downward force applied by the weight

T: Torque applied by force F at the wheel

g: Gravitational constant

ID	OD	t	d	r
120.1 mm	152.1 mm	16 mm	2.15 mm	60.05 mm

$$r = \frac{ID}{2} = \frac{OD}{2} - t + \frac{d}{2} \quad (11)$$

$$T = F * r = mg * r \quad (12)$$

3.2.1.4 *Rate of Penetration (ROP)*

This sensor accurately gives the position of the top drive with an accuracy of up to 1 mm. This sensor is incorporated in a hard wire loop and act as feedback control for positioning the top drive. It works on the principle of potentiometer, such that, change in resistance is directly proportional to distance traveled.

Sensor Type: Resistance measuring Potentiometer

Specification: 30 mm in length

3.2.2 Actuators

3.2.2.1 RPM control

Rotation of the drillstring is controlled by a DC motor which is powered by variable power supply source (KORAD). This source is then controlled by the algorithm by varying the input voltage. The voltage supplied to the motor, through KORAD, is changed by sliding button on LabVIEW virtual pane. This varying voltage input, in turn, changes the rpm at which the drill-string motor rotates. RPM, thus, can be controlled manually or automatically through the panel.

3.2.2.2 Hoisting control

Vertical motion of the top drive is controlled by a stepper motor that act as the hoisting controller. Hoisting is controlled both manually and automatically. Manual control is performed by a Boolean switch which moves the top drive up or down with a constant speed. Automatic control of the top drive depends on the desired WOB at the bottom of the assemble. For example, if the WOB at the bottom need to be increased the top drive move down and vice versa with speed proportional to the difference, allowing control system to respond quickly to the change in WOB. Figure 38 shows the hoisting actuator connection loop.

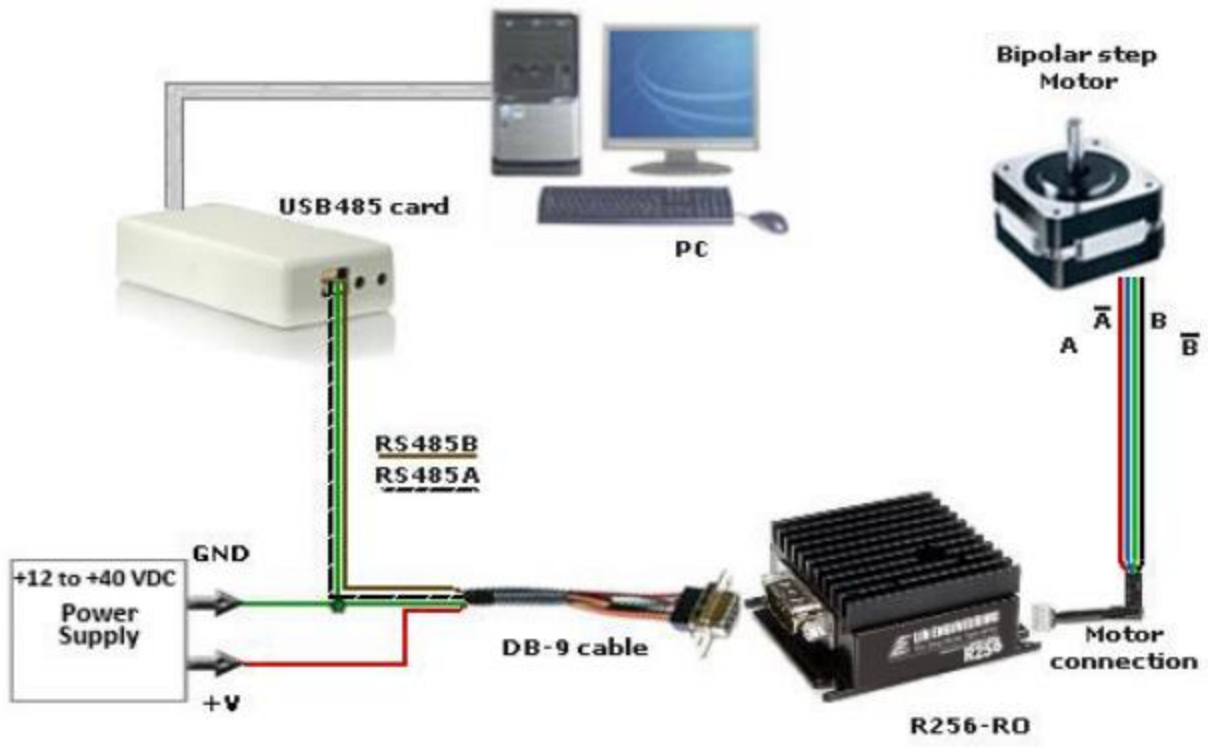

Figure 38. Hoisting actuator connection loop [38].

Controller Specifications

High Torque Stepper Motor: This motor mimics the rotary of the top drive whose function is to provide rotating torque to the drillstring. This motor allows accurate controlling of top drive movement.

Actuator type: R256-RO controller

Company: LIN ENGINEERING

Holding torque = 0.59 N-m

3.2.2.3 Variable power supply

KORAD hardware allows precision control of Voltage and current output. Through KORAD aH user can manually vary the voltage and current output as well as it can be synced with software such as LabVIEW to control its output signal. In this experiment, this is used to generate an output signal for controlling the rotational motor for the top drive.

3.2.3 Data Acquisition

The next important part of the control system is the Data Acquisition hardware. DAQ devices as shown in Figure 39 serve as an interface between hardware that is sensors and actuators and software that is LabVIEW runs on a PC.

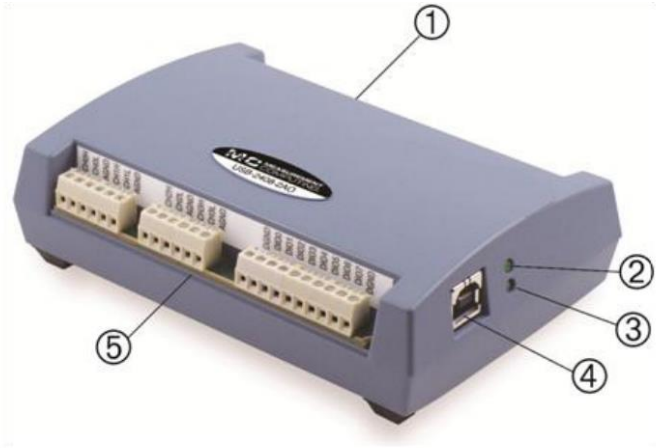

1	Screw terminal pins 23 to 44	4	USB Connector
2	Status LED	5	Screw terminal pins 1 to 22
3	Activity LED		

Figure 39. Measurement computing USB-2048 DAQ [41].

The USB-2408 Series of USB data acquisition (DAQ) devices have a 24-bit resolution for highly accurate measurements. Features include thermocouple or voltage configuration per channel along with digital and counter functions. Up to two analog outputs are available.

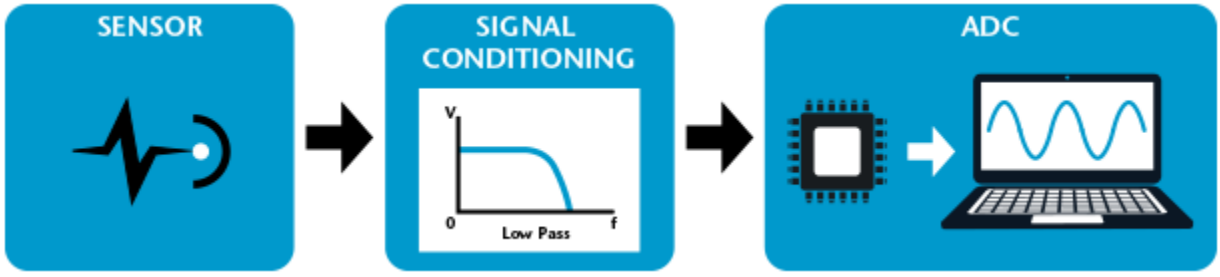

Figure 40. Components of data acquisition system [41].

All data acquisition systems consist of three essential elements – Sensor, Signal Conditioning, an Analog-to-Digital Converter (ADC).

This DAQ device is only connected to the sensors and a separate hardware system is installed for connecting actuators with the PC.

3.2.4 Hardware in loop

3.2.4.1 Open-loop control

Then an Open-loop system also referred to as a non-feedback system, is a type of continuous control system in which the output has no influence or effect on the control action of the input signal. In other words, in an open-loop control system, the output is neither measured nor feedback is sent for comparison with the input. Therefore, an open-loop system is expected to faithfully follow its input command or set point regardless of the result.

Also, an open-loop system has no knowledge of the output condition so cannot self-correct any errors it could make when the preset value drifts, even if this results in large deviations from the preset value.

Open-loop can manipulate output simply by varying input. It is in this experiment is desired in controlling RPM of the drillstring, as shown in Figure 41.

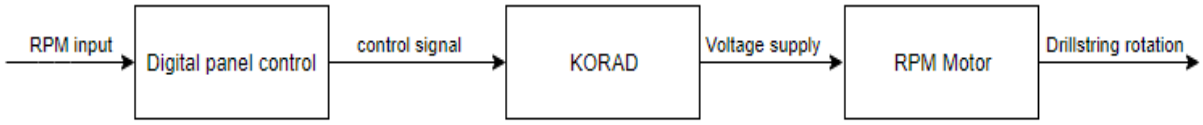

Figure 41. Open-loop control for RPM control

3.2.4.2 Closed-loop control

A Closed-loop Control System, also known as a feedback control system is a control system which uses the concept of an open-loop system as its forward path but has one or more feedback loops (hence its name) or paths between its output and its input. The reference to “feedback”, simply means that some portion of the output is returned “back” to the input to form part of the system’s excitation.

Closed-loop systems are designed to automatically achieve and maintain the desired output condition by comparing it with the actual condition. It does this by generating an error signal which is the difference between the output and the reference input. In other words, a “closed-loop system” is a fully automatic control system in which its control action being dependent on the output in some way. The feedback signal is proportional to the error i.e. the difference between the actual and desired output value.

In this experimental setup, WOB is controlled through closed-loop control. There is also an option to control WOB through open-loop control in manual control mode whereas closed-loop is under auto mode. In auto mode, the desired WOB is given as input and top drive hoists in the vertical direction to achieve that WOB (as shown in Figure 42).

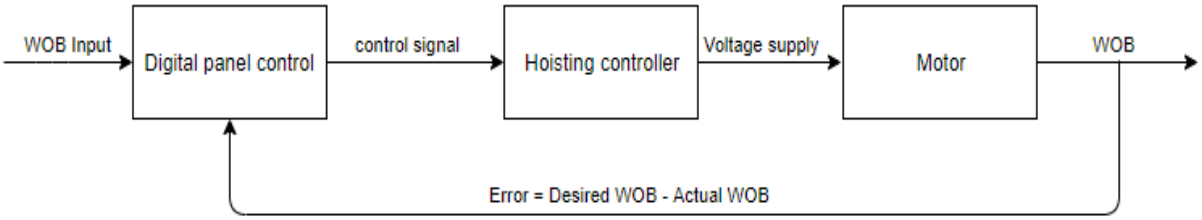

Figure 42. Closed-loop control for WOB control

3.2.5 Digital control panel and its operation

Typical hardware drilling control panel is shown in Figure 43, as hardware control. The gauges on the panel display values for different parameters such as pressure, flowrate, depth and other through physical gauges and meters, whereas, the controllers are in the form of buttons and jockey.

Figure 43: Typical hardware drilling rig control panel [40].

A simulator is a device that replicates some physical operation virtually with some level of fidelity. Shown in Figure 44, modern-day drilling simulator. This simulator has digital screens showing various control parameters and sensor inputs. The virtual rig is shown on the screen that extends into 3-D space to give a feeling of real drilling rig environment. In a typical drilling simulator, the physical controls and display panels are replaced by virtual controllers and virtual display on the computer screen that can be operated via mouse click. The virtual drilling rig setup can replicate

all the drilling operation steps with the control of buttons on the screen. Drilling is an expensive and complex operation to execute in an oil and gas exploration environment [30]. Necessary training is needed for drilling engineers to operate the drilling rig with deft and accuracy, at the same time, it is risky to train an individual on a real drilling rig. Drilling simulator, like the one shown in Figure 44, can be used for such purposes, preparing an individual for uncertain situations.

An attempt has been made to replicate the display panel of drilling simulator in the display panel as shown in Figure 45. This does not have all the extensive controls and data display as the scope of this research is limited to automation of the hoisting system, for which the display panel has been developed. This display panel includes controls and sensor input data that a hoisting system relates.

Figure 44: Simulator systems of Drilling Systems used by Pan American Energy [39].

The Block Diagram as shown in Figure 45 runs in the background, which is where the actual programming (using G-code) is done.

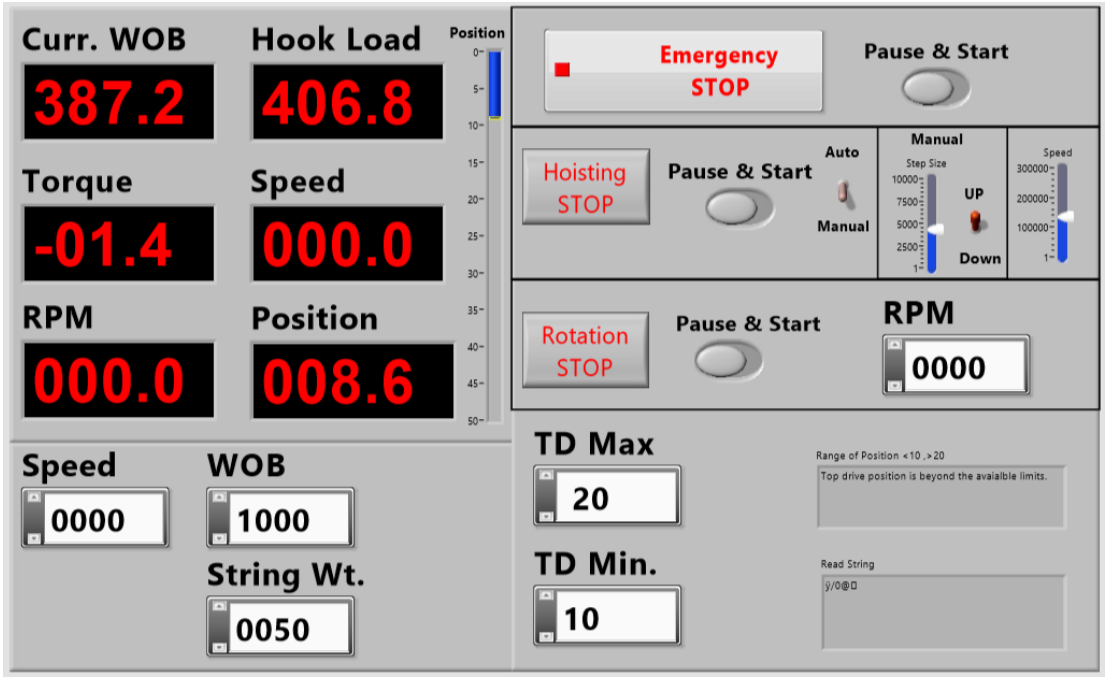

Figure 45. Digital display panel control

The digital control panel is a user interface for controlling the drilling process. The digital control panel is designed such that it is simple and user-friendly to operate.

Control panel is divided into four parts, namely:

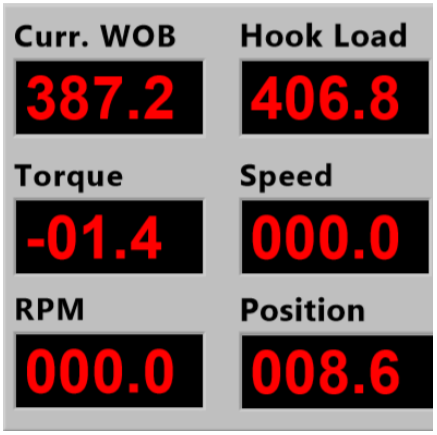

Figure 46: Display parameters on the panel.

1. The value display panel on the left top: Six values are displayed on this section of the panel, shown in Figure 46.

   i. Current weight on bit (Curr. WOB): this tells the present value of weight on bit value while the drilling is operational.

ii. Hook Load: it is the difference between the drillstring weight and weight on bit, acting on the hook at the top of drillstring.
iii. Torque: the torque acting at the top of the drillstring.
iv. Speed: it is the distance traveled by top drive per unit time. It only shows the absolute value.
v. RPM: rotation per minute is the rotation speed of the drill string
vi. Position: it gives the TVD position of the bit with reference to the surface

2. Button control panel on the right top. This section is divided into three sub-sections.
    a. As shown in Figure 47, the emergency stop, Pause & Start button are used for the safety of the complete system. This button control ensures the safety of the drilling, once this button is selected the operation needs to be started again from the beginning after necessary safety measure has been taken or correction action has been done. Pause/Start button allows intercepting the drilling operation, giving the user an added layer of safety measure where the operator can pause inspect and resume the operation.

Figure 47: System safety buttons.

    b. Hoisting section is furthermore divided into three sub-sections, as shown in Figure 48:

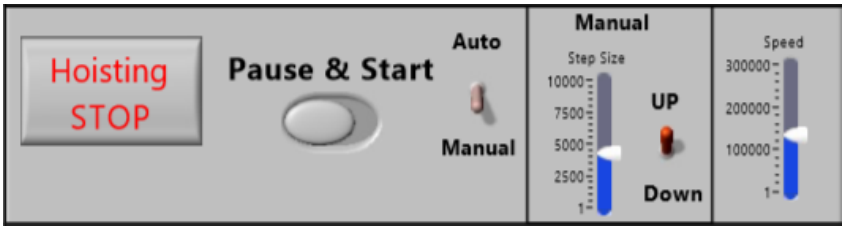

Figure 48: Hoisting control switches, buttons, and sliders controllers.

        i. The first section, Hoisting Stop button which allows stopping the vertical motion of the top drive, all the pause/start button works in a similar fashion except this one only controls the movement in the vertical direction. Auto/Manual switch allows switching between manual and automatic hoisting of the drill string.
        ii. This section is operative when manual mode is selected through the switch from the first sub-section. It has a Step size incrementor and an Up/down switch. As the name suggested Step size is the distance traveled by the top drive in a single command and Up/down switched the direction of emotion.

iii. Speed is the rate at which the top drive moves in the vertical direction. It is operative in manual mode.

c. This section has a Rotation motion stop button, as shown in Figure 49, stops rotational motion, followed by Pause/Start and RMP value controller which allow changing the rotational speed by changing the value.

Figure 49: Rotary (RPM) controllers.

3. Shown in Figure 50, value type control on the left bottom
   a. Weight on bit (WOB): to set the desired weight on the bit in grams.
   b. String weight: to set the appropriate string weight value in grams.

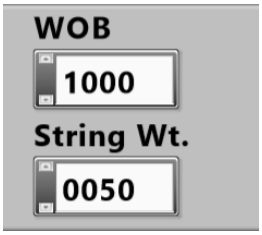

Figure 50: User input value control.

4. As shown in Figure 51, the two controllers 'TD Max' and 'TD Min.' stands for top-drive maximum and minimum hoisting limits. The hoisting of top-drive is not supposed to go beyond these limits. If the limits set under these two boxes is reached, immediately error message display on the right top box and the motion of the top-drive stops.

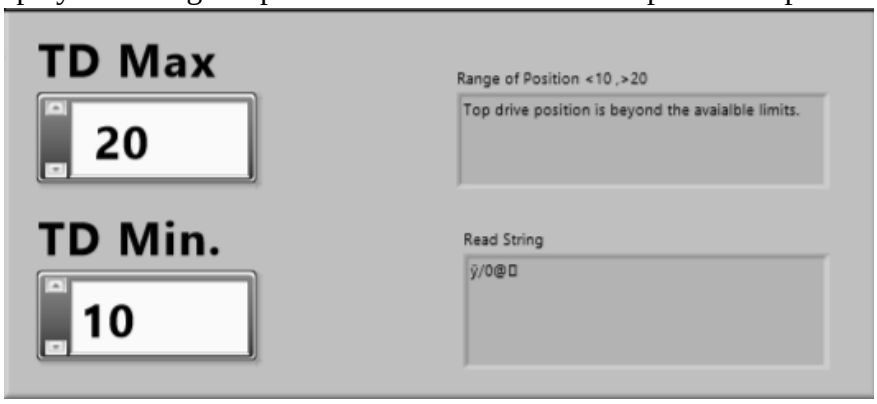

Figure 51: Hoisting limit control and error message display.

3.2.6 Structure of the program

The complete hoisting system is programmed using LabVIEW software. Programming hoisting system can be divided into two main parts i.e. vertical movement control and rotational control. Vertical movement allows up and down motion of the top drive, and rotational control allows rpm control.

3.2.6.1 Connecting to DAQ

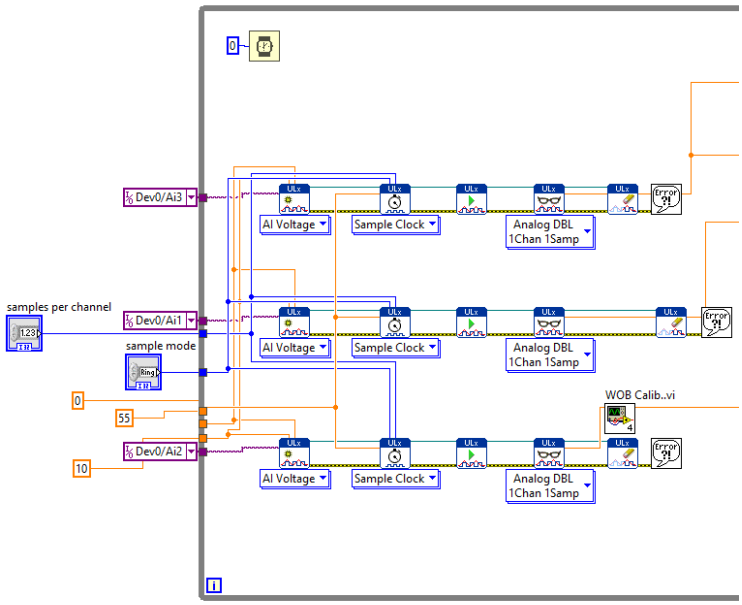

Figure 52. Sensor input to LabVIEW

DAQ card is connected to three sensor inputs torque sensor sensing torque acting on the drill string, potentiometer scale for position tracking and Load cell for sensing weight-on-bit is received through channels I/O Dev0/Ai3, I/O Dev0/Ai1, and I/O Dev0/Ai2 respectively. In the above figure three channels are connected to the respective sensors with minimum (0) and maximum (10) voltage signal limit as input to the series of sub-VI's (Al Voltage, Sample Clock, Ulx read, Analog DBL 1Chan 1Samp, Ulx write) and a sampling frequency of 55 Hz, as input to the Sample clock VI.

3.2.6.2 Hoisting control logic

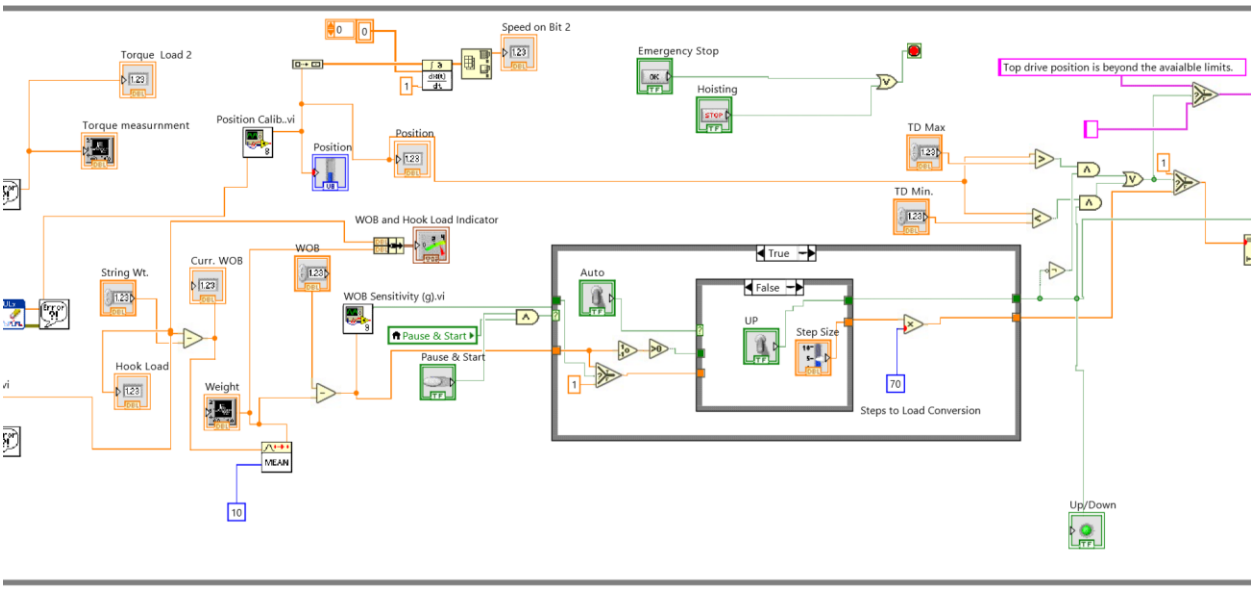

Figure 53. Block diagram of hoisting control panel

Shown in Figure 53, is more importantly, the closed-loop control logic behind automatic WOB control using the position sensor input and the WOB sensor input. The Block diagram is divided into smaller blocks to better understand the function of each VI and the logic behind using them. The flow of logic is from left to right, hence, the flow of explanation follows the same order.

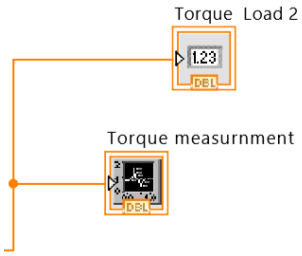

Figure 54: Torque sensor input VIs

Shown in Figure 54, 'Torque Load 2' VI display the exact amount of torque experienced by the drillstring at that instant in Nm and 'Torque measurement' VI displays the torque value over a period in graphical format.

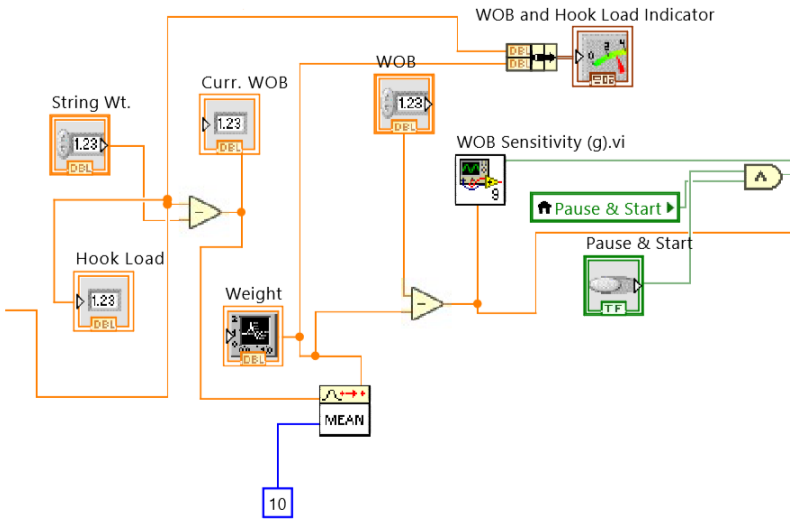

Figure 55: VIs for weight-on-bit algorithm

As shown in Figure 55, 'String Wt.' VI receives user input for the weight of the drillstring in grams, 'Hook Load' is received from the sensor input, where, 'Curr. WOB' VI calculates the current WOB using, $Current\ WOB = Drillstring\ weight - Hook\ load$. After which the 'MEAN' VI average out the value of WOB for the last 10 samples, to lower the variance in the received input signal. This average value is further used in the indicator 'WOB and Hook Load indicator' VI and in finding the difference from the desired WOB. The 'WOB' VI is the user input for the desired WOB. The 'WOB Sensitivity (g)' VI receives calculated input ($desired\ WOB - Current\ WOB$), this difference is further used to adjust the vertical position of the drillstring to achieve current WOB near to the desired WOB. The 'WOB Sensitivity (g)' VI has a sensitivity factor of ±30 grams i.e. only if the difference fluctuates by more than 30 grams the top drive will trip in or out the drillstring to compensate for it.

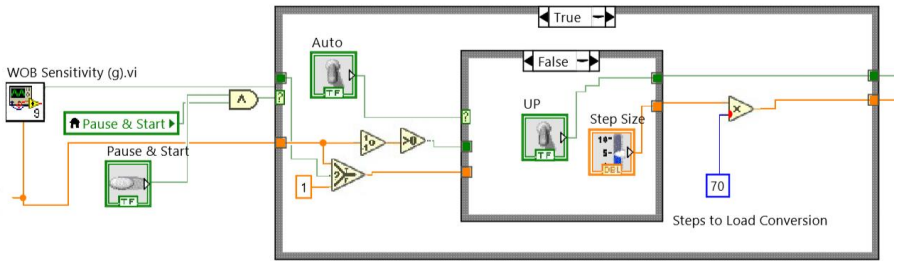

Figure 56: WOB automatic adjustment algorithm

The block diagram, shown in Figure 56, is the heart of the closed-loop control of WOB. The concept implemented in the block diagram is explained in the process flowchart is shown in Figure 57. The binary operations are depicted with rhombus, input/output values and actions are shown with box. The WOB is adjusted by movement of the drillstring tripping in/out is proportional to the difference between desired and current WOB, when in automatic mode, a conversion factor of x70 converts to the necessary step size. For example, the difference is 50 grams, steps traveled by the motor will be 50x70 = 3500 steps, where, 1 step = 6.17×10^{-5} mm. As

shown in the flowchart Figure 57, a closed loop control is implemented for automatic WOB adjustment.

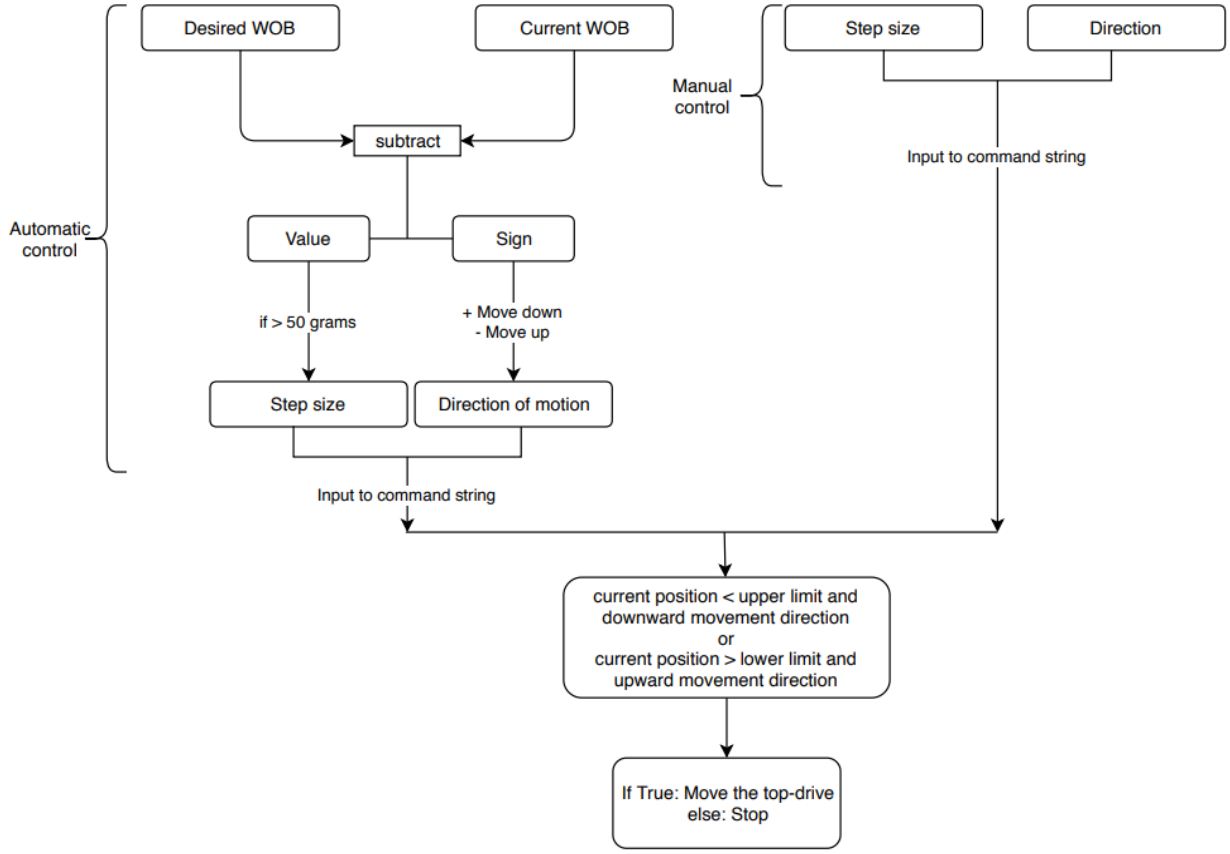

Figure 57: Flowchart showing the working logic for WOB adjustment

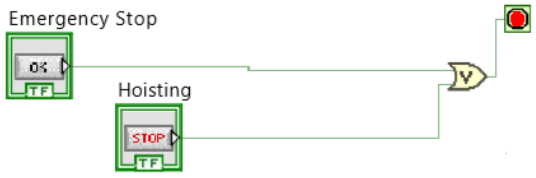

Figure 58: Stop button VIs

As shown in Figure 58, the hoisting movement can be completely stopped by two buttons, 'Emergency Stop' VI which stops the whole system and 'Hoisting' VI to stop the tripping motion. Once any of this button is pressed, the system will need to be restarted to control hoisting motion.

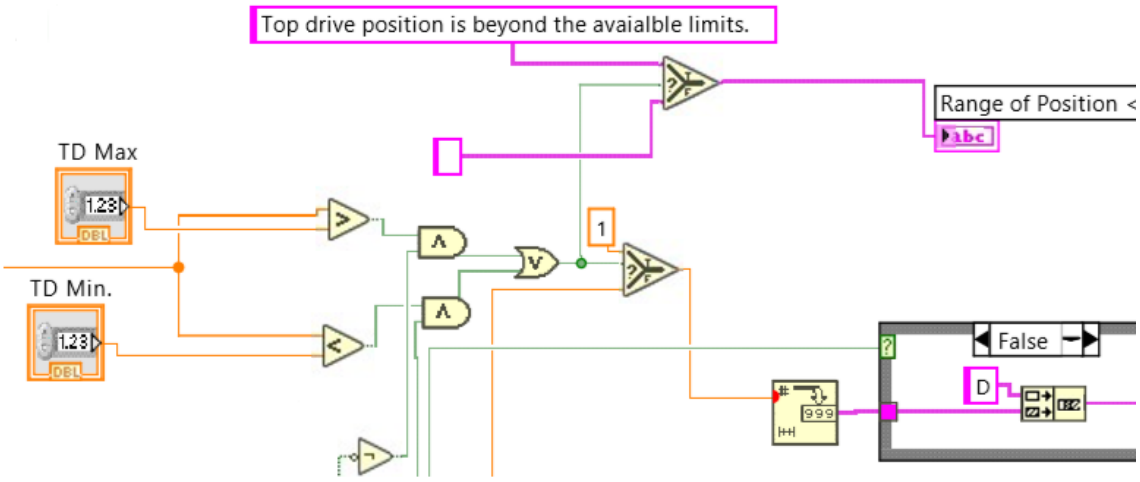

Figure 59: The block diagram sets boundary limits on the tripping motion of top-drive

In Figure 59, The 'TD Max' and 'TD Min.' VI is user input for the upper and lower boundary limits respectively for the tripping motion of the top-drive when top-drive hits these limits an error message is generated and the motion stops in that direction. When the direction of motion is reversed top-drive continues to move. The concept of this motion is explained in the flowchart Figure 60.

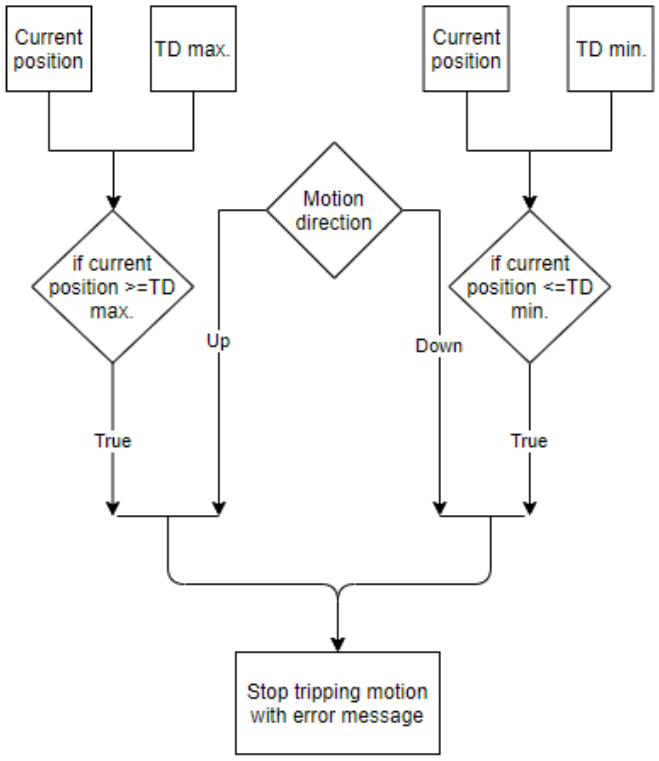

Figure 60: Flowchart showing the concept of boundary limit implementation on the tripping motion of the top drive

3.2.6.3 Sending string to r256 controller

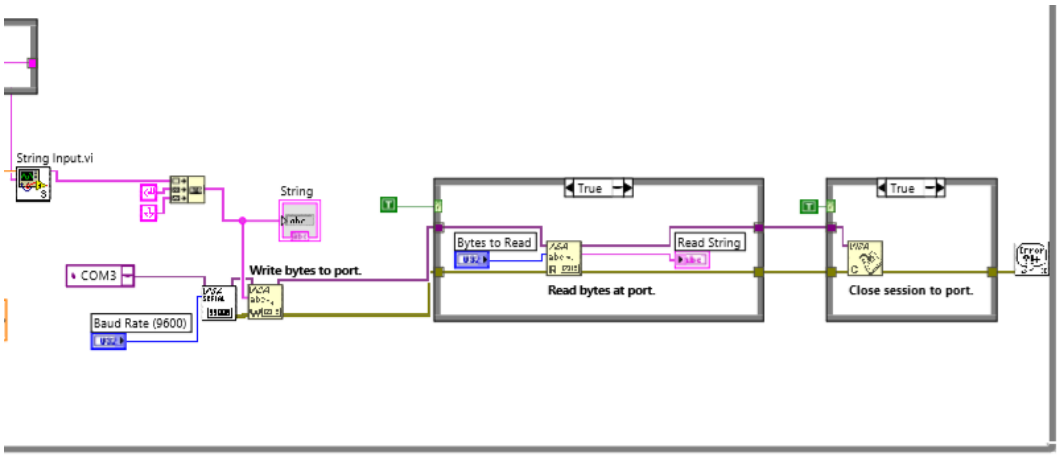

Figure 61. Block diagram for writing final command string to hoist actuator

All the signals from VIs such as the direction of movement, step size, speed, acceleration, holding current and running current after being processed are combined into one 'String' command and are sent to the port where it is written and read to the actuator port of connection (as shown in Figure 61). Based on the value of thee input the stepper motor responsible for controlling hoisting (tripping) motion actuates.

3.2.6.4 Rotational controller logic

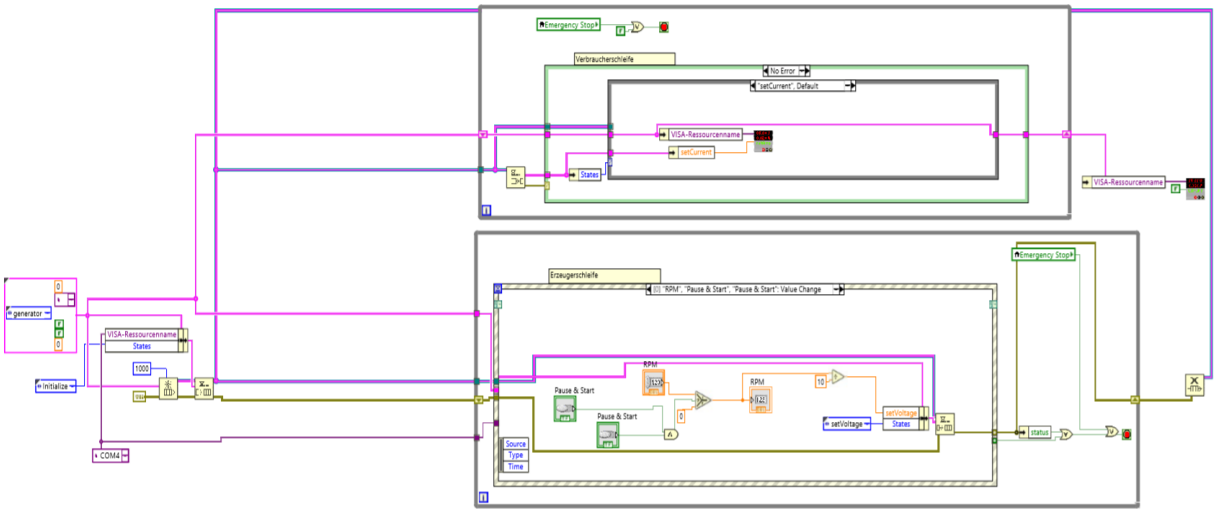

Figure 62. Block diagram for RPM actuator control

Figure 62 shows the block diagram for RPM actuator control. The signal is queued to an actuator. The upper part of the diagram sends the signal to the actuator and the lower part processes the control input.

This block diagram is broken down into smaller blocks and discussed through the section of the block diagram and flowcharts explaining the concept from left to right.

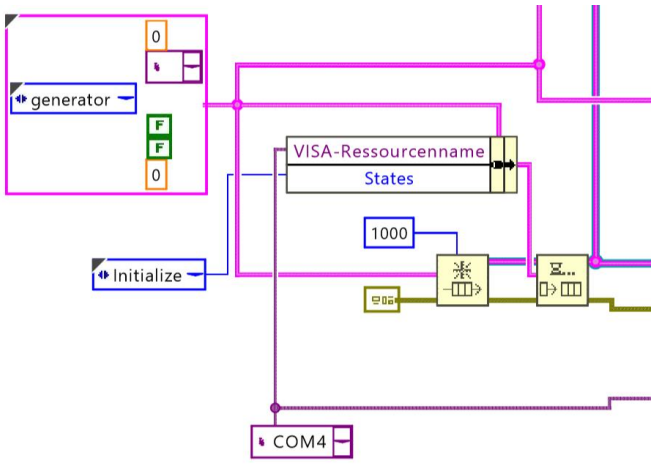

Figure 63: Block diagram showing connecting VIs to the RPM controller.

In Figure 63, the Visa resource name VI is connected to DAQ through COM4 USB port. The queue elements as shown in Figure 64 has max queue size of 1000, data type as defined by the box having a generator.

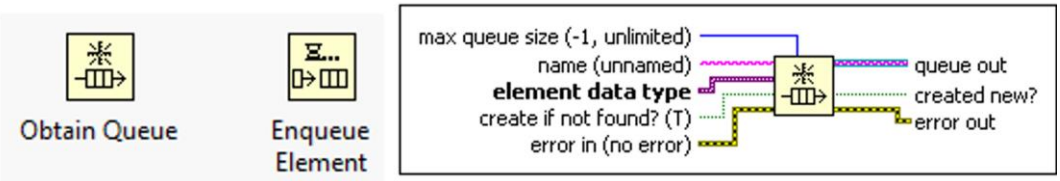

Figure 64: Queue elements and their inputs/outputs.

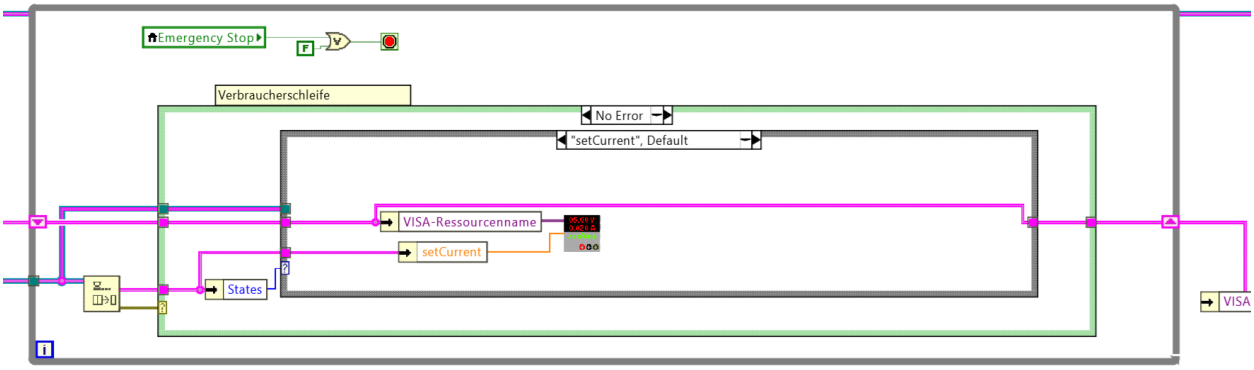

Figure 65: Block diagram showing current input to the KORAD.

As shown in Figure 65, if the set current value is changed, as per the case structure, the value I written to the KORAD VI. This block diagram is responsible for controlling the current input supplied to the RPM motor through KORAD. KORAD works as the power supply required for RPM motor. KORAD VI is shown with half black and gray color receiving input from VISA and set current value. The current value is set in the KORAD same as the input.

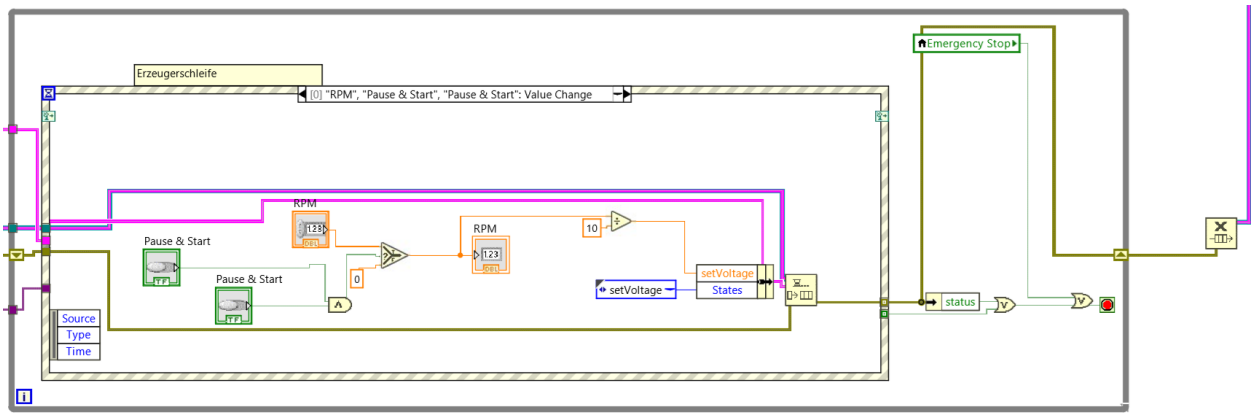

Figure 66: Block diagram for controlling RPM by changing voltage.

As shown in Figure 66, the block diagram is the implementation of RPM control by changing the voltage output sent to KORAD. The voltage control is encased in a for loop structure and further into an event case structure. The case event works on the case when the Pause & Start buttons (for RPM and complete system) is changed in value or RPM input is changed. Thus, the RPM motor continues to receive the same input unless the system is paused, restarted or voltage value controlling the RPM is varied.

3.2.7 Benefits of Automation

3.2.7.1 Safety

Safety is the top priority in the field of oil and gas, as it always mentioned: “Safety first”. The top assembly has three layers of safety installed in its control algorithm. The first level of safety is the emergency stop button. The emergency button is used when the drilling operation needs to be halted completed, any sudden abnormal behavior should stop all the drilling operations immediately. The second layer of safety is the individual hoisting and rotation stop buttons. Purpose of the hoisting is to stop the hoisting motion of the top drive, similarly, the rotation stop button only stops the rotational motion of the rotary drive. If any of the systems needs to be restarted if first or second layer stop buttons are used for stopping the drilling operation, after which the system needs to be restarted to resume the activity. The third layer of safety offers ‘Pause & Start’ button. The digital panel control has three ‘Pause & Start’ button one for the overall system and one each for hoisting and the rotational system as shown in Figure 26. All the three ‘Pause & Start’ button has the same purpose i.e. the overall or individual hoisting or rotational operation can be stopped and resumed, as required. The third layer of safety ‘Pause & Start’ button allows intercepting the drilling operation, thus, the operator can pause inspect and resume the operation.

3.2.7.2 Ease of user interface

As shown in Figure 45, the panel display is a virtual control connected to the hardware such as DAQ, through DAQ to the sensors and controllers, and others. This virtual panel is like an actual drilling simulator panel, which does not require hardware knobs or switches but instead a screen

display of these components. This display panel allows the user to view all the output parameters such as WOB, RPM, Torque, depth, and other parameters varying with time, as well as, absolute values, it lets user manage all the operations through this panel such as ROM control, tripping speed, direction, distance and step size. It is a compact display of all the information and control system.

3.2.7.3 Automatic WOB adjustment

WOB is an important parameter in adjusting the ROP [23]. Once, WOB is set to a certain value it is likely to fluctuate while drilling in progress, it is also necessary to adjust WOB when drilling through different formation to achieve optimum MSE.

Manual adjustment of WOB will require adjusting parameters such as tripping speed, step size, direction, and the tripping distance to set the right WOB. These parameters are difficult to control manually and simultaneously as the drilling is in progress to adjust to the desired WOB. Automatic movement of the hoisting system allows to adjustment of the WOB automatically, once the desired WOB is given as an input to the system. The automatic WOB adjustment algorithm allows the tripping in and out of the drillstring automatically such that the WOB is kept constant as per the given user input.

To adjust the WOB automatically inputs used are current WOB and desired WOB (input by the user). Hoisting of top-drive is done such that current WOB gets closer to the desired WOB. For example, if current WOB is 500 lbf and desired is 600 units (lbf or grams) the algorithm will more the top-drive downwards pressing the drillstring more on the formation, thus, increasing the WOB and vice versa. This tripping motion of the top-drive is proportional to the difference between the magnitude of the two WOB (current and desired) i.e. if instead of 100 units (500-600 = -100) the difference is 200 units the top-drive will take twice as larger steps then before to adjust to the WOB. This allows quick movement of top-drive as after each continuous step the hoisting motion deaccelerate and then accelerates. The constant of proportionality is adjustable and yet to be decided once complete setup is ready to be tested. Currently the constant of proportionality is 70 i.e. if the WOB difference is 200 lbf, step size will be 200 x 70 = 14000 steps, which is equal to 14000 x $6x10^{-5}$ mm/step = $8.4x10^{-1}$ mm, so top-drive will continue to hoist $8.4x10^{-1}$ mm until the two WOBs are near equal (within tolerance range). The value of this constant (70 in this case) shall be determined based on the tolerance limit of the two WOBs, as the step size should not be more than the tolerance limit otherwise the top drive will keep on oscillating in the tripping motion, assuming the top-drive is hoisting at a constant speed. For example, if the tolerance limit is ‘x’ unit (lbf or grams), and ‘y’ unit (mm) of tripping distance is required to change WOB by ‘x’ units (lbf or grams), then, constant of proportionality, say C, will be $y/6x10^{-6}$ steps.

Chapter 4: Results

4.1 Sensor Calibration

Sensor calibration is a method of improving sensor performance by removing structural errors in the sensor outputs. Structural errors are differences between a sensor expected output and its measured output, which show up consistently every time a new measurement is taken. Each sensor is calibrated to the desired output behavior. The behavior is expected to be linear between the measured signal and the interpreted output.

4.1.1 Calibration of the position sensor

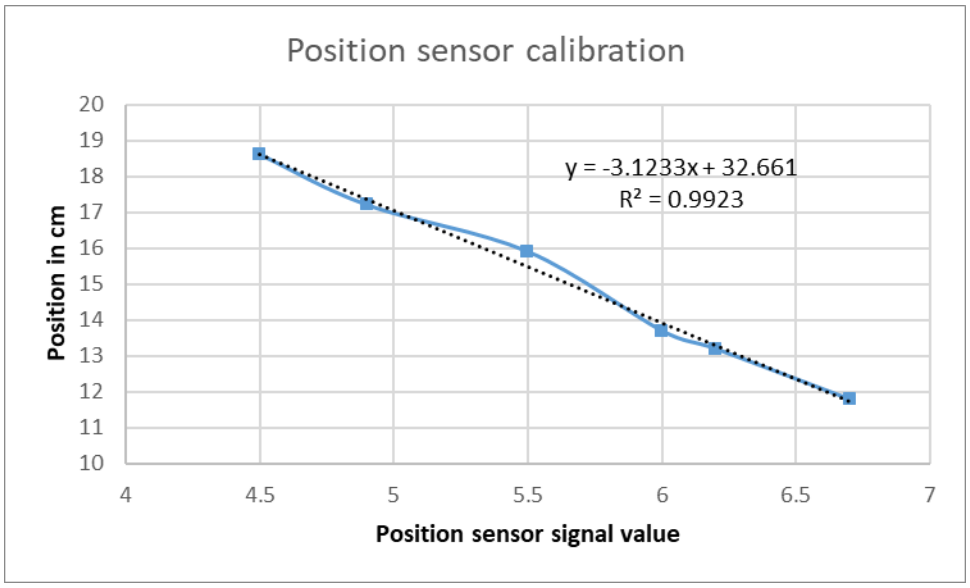

Figure 67. The graph for Position sensor calibration

In the above graph (as shown in Figure 67), position sensor correlation with the position scale is linear with an R^2 value of 0.992. On the X-axis is the sensor output and on the Y-axis is the position of the top drive. This is a potentiometer type sensor in which the output signal varies linearly with change in resistance. Resistance changes with change in position of the top-drive.

4.1.2 Calibration of Load Cell

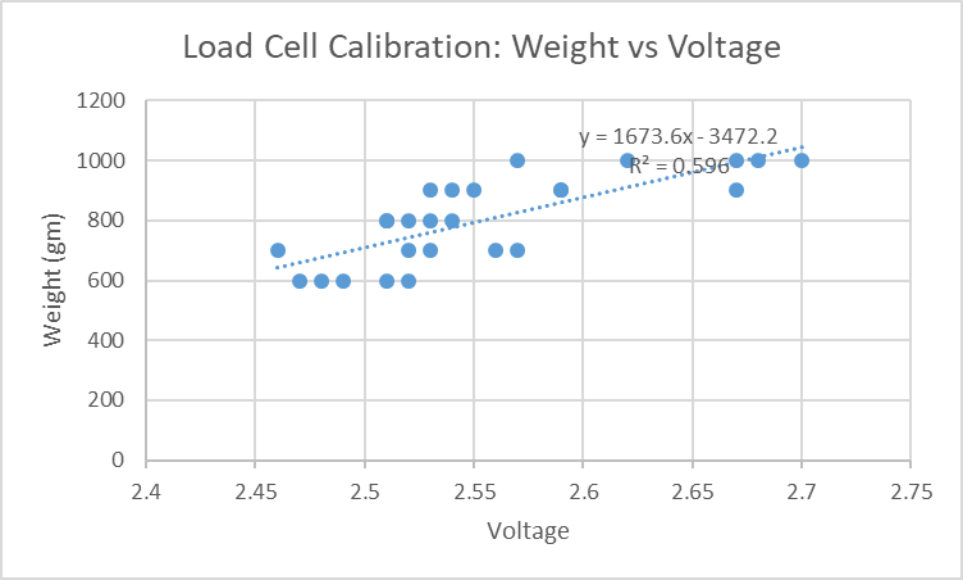

Figure 68. The graph for Load cell sensor calibration

Load cell sensor is calibrated against the tension at the hook based on the hook load. In the above graph (as shown in Figure 68), X-axis is the output voltage by sensor and Y-axis is the weight applied. The weight (hook load) shows a linear correlation with the voltage signal received with a relatively low R^2 value of 0.596. There can be observed a linear relationship of sensor input vs change in voltage but there is a lot of noise in the sensor signal due to which the accuracy is low. The sensor is very sensitive to the change in weight of the drillstring, due to motion there are inertial forces causing the WOB to fluctuate significantly. Hence, either signal needs to be processed, change the position of WOB sensor, change the WOB sensor and other to mitigate this issue. The suggestions are further discussed in the future work.

4.1.3 Calibration of Torque Sensor

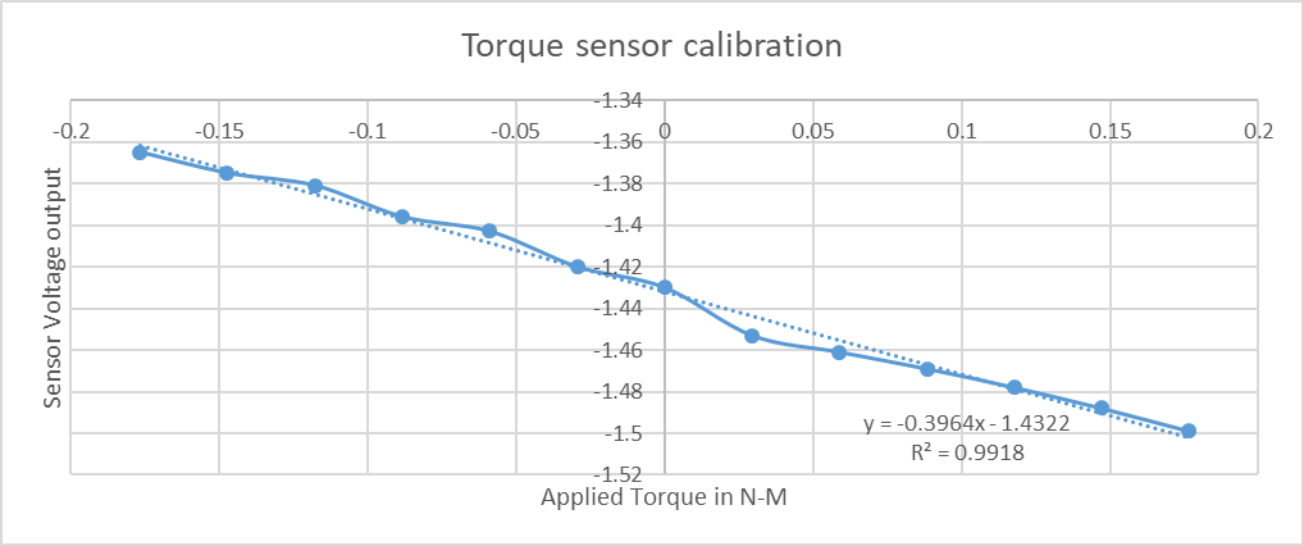

Figure 69: The graph for torque sensor calibration

In the above Figure 69, the torque sensor shows a strong linear relationship for Torque applied (in Nm) vs voltage generated by the sensor with an R^2 value of 0.991.

4.2 Actuator calibration

4.2.1 Calibration of RPM controller

RPM controller functions to increase and decrease the motor speed that rotates the drillstring. It is important that the motor RPM is the same as the given input. Thus, a strong linear relationship between the input signal and output RPM is required with a tolerance of ±0.05 rpm.

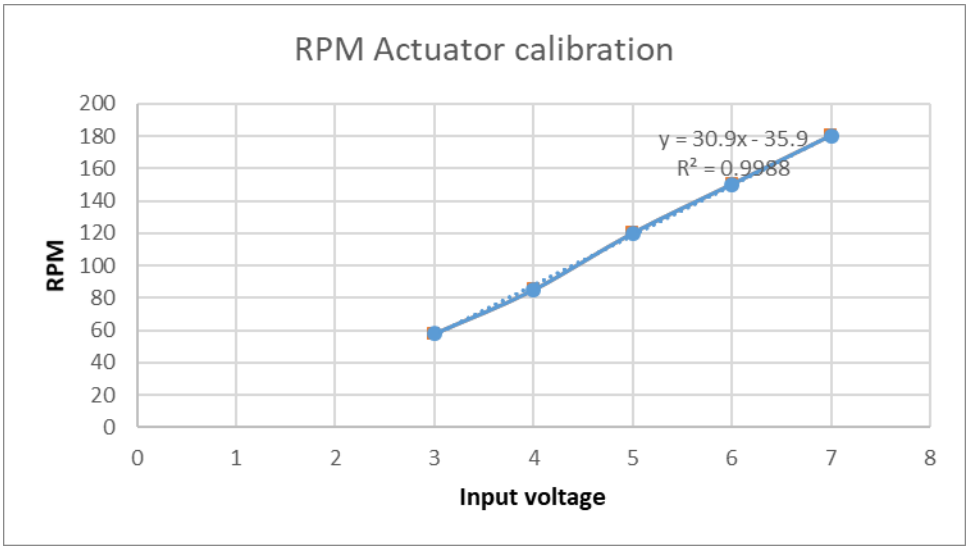

Figure 70. The graph for RPM actuator calibration

Above graph display (as shown in Figure 70), the correlation between supplied input voltage to the motor on x-axis and output RPM measured from tachometer on y-axis. R^2 value of 0.998 shows strong correlation between the two compared parameters with strong linear relationship, as required behavior.

4.2.2 Calibration of stepper motor

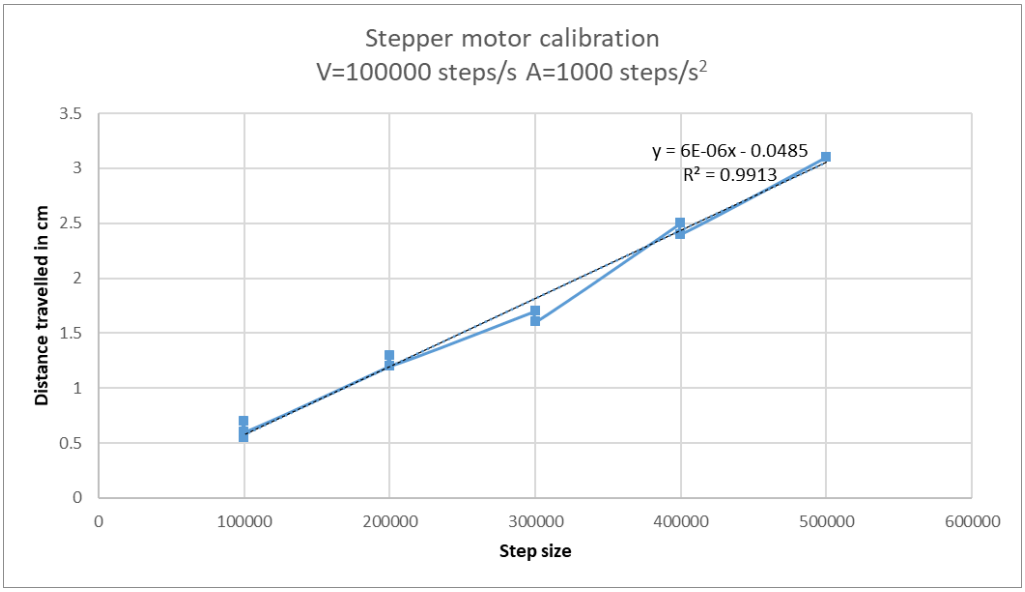

Figure 71. The graph for Stepper motor actuator calibration

Above graph display (as shown in Figure 71), the correlation between the input step size vs the distance traveled by the top-drive in mm, where, on the X-axis is the step size and on the Y-axis is the distance traveled in mm. The R^2 value of 0.9913 shows a strong correlation between the two compared parameters with a strong linear relationship, which is the required behavior. Constant of proportionality is $6x10^{-6}$ mm/step i.e. for every step motor turns top drive moves by $6x10^{-5}$ mm/step or $6x10^{-5}$ mm/step, where, a motor rotated by 1.8 degrees in each step.

4.3 Behavior analysis of hoisting system

The terminology used in the below explanations

Step size of stepper motor: A stepper motor is the DC electric motor that divides a full rotation into several equal steps. Each step size of a stepper motor is the smallest step towards completing a rotation.

Holding current: The holding current (hypostatic) for electrical, electromagnetic and electronic devices is the minimum current which must pass through a circuit for it to remain in the 'ON' state.

Running current: It is the current required to drive 100% of load at full voltage and frequency.

Stepper motor speed: Number of steps per second moved by the motor.

Hoisting Speed: Hoisting speed is the vertical distance traveled by the top-drive in mm/s.

4.3.1 Hoisting speed behavior with changing motor speed

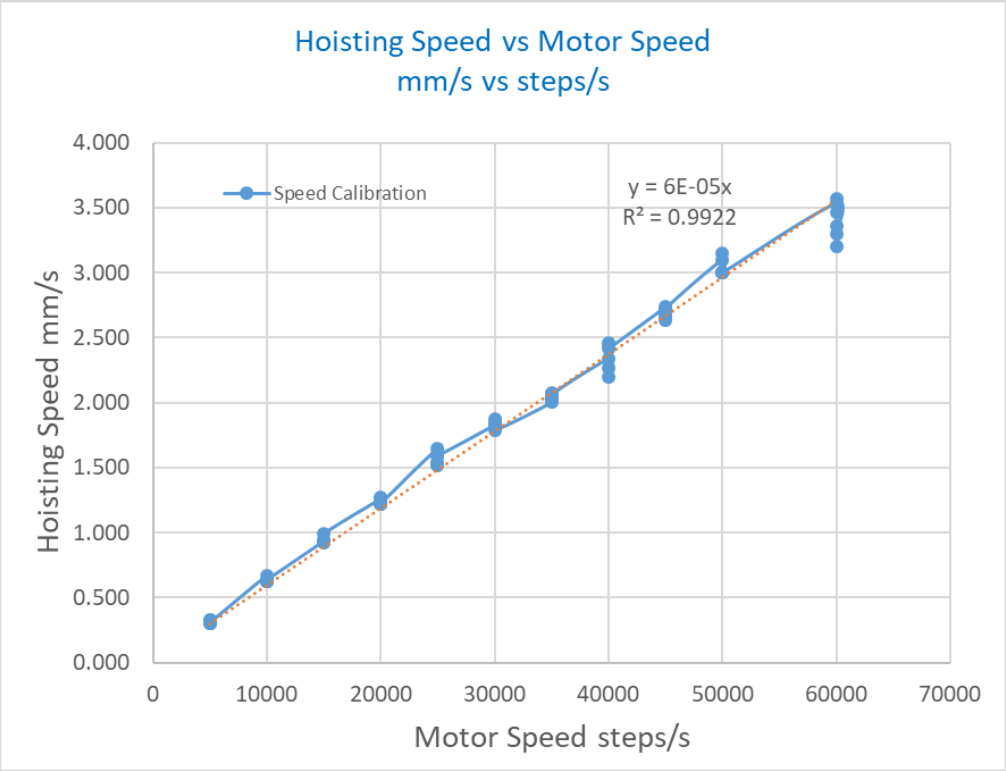

Figure 72. Graph showing the correlation between input speed to the stepper motor in step/s vs output hoisting speed in mm/s.

As shown in Figure 72, the relation between stepper motor speed vs hoisting speed. On the x-axis is the motor speed in steps/s and on the y-axis is the hoisting speed in mm/s. The correlation between the two speeds is linear, shown in the graph, is a good straight line fit with R^2 value 0.9922. Thus, it can be safely assumed that the motor speed is accurately tuned with the hoisting speed and that there is no slipping.

4.4 Determining maximum step size for stepper motor

In Figure 73, Figure 74 and Figure 75, the behavior of the user input of speed in step/s vs the actual output speed of the stepper motor, also in steps/s, is shown for different step sizes. In this analysis step size is the number of steps a stepper motor will run (continuous rotation) before executing the next command in the queue. The purpose of this analysis is to identify the range of maximum step size for which there exists a precise linear relationship between input and output speeds with R^2 value higher than 0.9990.

The output speed is first measured in mm/s with a linear mm scale and a timer and then it is converted to steps/s using constant of proportionality $6x10^{-5}$ mm/step, calculated in section 4.2.2 Calibration of stepper motor. These graphs were plotted for data from different scenarios such as top drive moving up or down, different weight loading, different step size, keeping holding and running current constant (50% and 20% respectively). It is desired to operate the stepper motor

within the step size range within which it has linear behavior between input and output speed so that the behavior of the motor is accurate. The graphs show this behavior for three different step sizes.

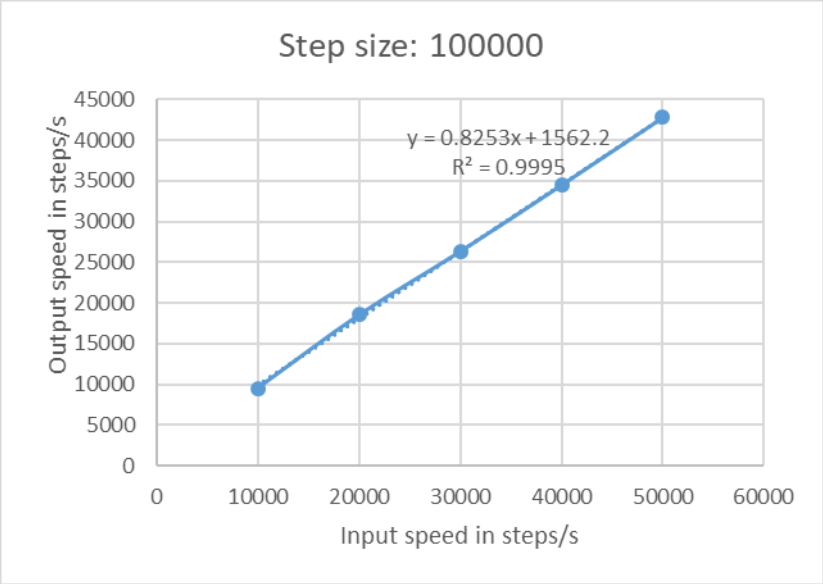

Figure 73. Input vs output speed in steps/s for step size = 100000

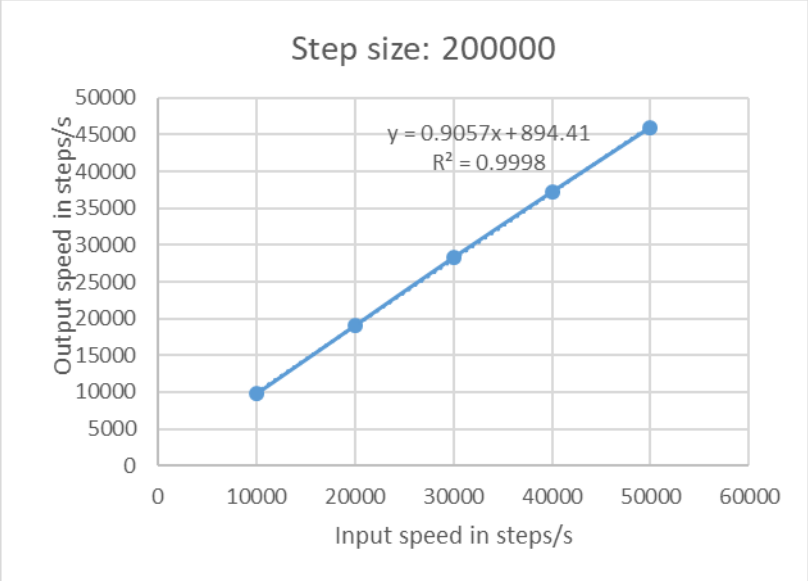

Figure 74. Input vs output speed in steps/s for step size = 200000

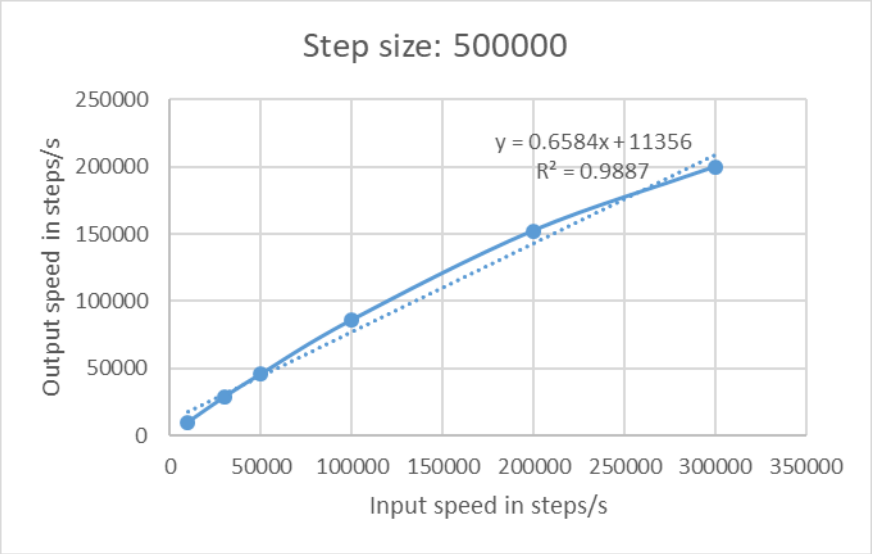

Figure 75. Input vs output speed in steps/s for step size = 500000

Linear behavior is observed up to step size 200000 with R^2 value > 0.990, for step size greater than 200000, non-linear behavior when step size is increased to 500000. Thus, the operating range of step size should be below 200000.

Another behavior observed is the slope of the linear relationship between the input and output speed changes with step size as shown in Figure 73, Figure 74, i.e. the slope of the linear relationship changes with change in step size. Thus, to have a consistent behavior a constant operating step size should be fixed.

The hoisting system has a tripping range of 150 mm between the minimum and maximum limit of 50 mm and 200 mm respectively (as per the scale of installation on the setup). The maximum allowable step size of 200000 is equivalent to $200000 \times 6 \times 10^{-5}$ mm/step = 12 mm. In this setup we do not need to compare the tripping length with that of a full scale drilling rig which typically has tripping range of 100 ft, due the fact that, in actual drilling rig as the drilling progress new pipe stand need to be added or disconnected from the drillstring which is typically 30 ft long requiring 100 feet of tripping capability, whereas, in the downscaled experimental setup one single continuous drillstring of constant length is used. This purpose of tripping the drillstring in and out in the experimental setup is only to change WOB and compensating for buckling of the drillstring.

4.4.1 Holding current limits

After identifying the step size limits, speed limits and keeping maximum acceleration and running current, the range of minimum holding current is analyzed in Table 6. Shown in Table 6, the values of all the constants are included in the first two rows. Holding current is measure for upward and downward directional movement of the top-drive varying the hook load. This is done for two different value of speeds. Table 6 shows that the range of holding current at which the top drive starts and stops to move in the vertical direction. Using this table, we get an idea of a lower limit for holding current. Holding current is the current is essential to hold the top drive in place in its vertical position, not allowing any slipping due to its own weight. It is necessary to keep holding

current value above the minimum limit to assure the top-drive motion is free from slipping or stops in between so that the system behavior is independent of holding current.

Table 6: Result shown is finding the minimum limit for the holding current required for top-drive to move continuously.

Weight	Step size	Speed	Acc.	Runn. Curr.	Step size	Speed	Acc.	Runn. Curr.
	100000	10000	1000	20%	100000	80000	1000	20%
	Range of Hold Current				Range of Hold Current			
	Downward		Upward		Downward		Upward	
	Stops at	Starts at	Stops at	Starts at	Stops at	Starts at	Stops at	Starts at
450	0.05%	0.09%	0.12%	0.13%	0.07%	0.09%	0.13%	0.14%
400	0.06%	0.09%	0.11%	0.12%	0.07%	0.09%	0.13%	0.14%
350	0.05%	0.06%	0.10%	0.11%	0.07%	0.09%	0.12%	0.14%
300	0.05%	0.08%	0.11%	0.12%	0.07%	0.09%	0.13%	0.14%
250	0.06%	0.07%	0.11%	0.12%	0.08%	0.09%	0.12%	0.13%
200	0.06%	0.07%	0.09%	0.10%	0.07%	0.08%	0.12%	0.14%
150	0.05%	0.06%	0.11%	0.12%	0.08%	0.09%	0.11%	0.13%
100	0.05%	0.07%	0.11%	0.12%	0.07%	0.08%	0.12%	0.13%
50	0.05%	0.06%	0.10%	0.11%	0.06%	0.08%	0.11%	0.12%

As shown in Table 6, the holding current required for starting and stopping the tripping motion is higher when moving the top-drive upwards (0.10%-0.13%), this is because the upward top drive motion is against gravity and higher holing current compensates for it. Keeping the holding current above 0.13% the system will be free from slipping of intermediate topping. The holding current is set to its maximum value of 60% for running experimental tests.

Chapter 5: Discussion

In this chapter, the test results are discussed in detail. This chapter analyzes and discusses the test results performed on the downscaled experimental drilling rig setup and their applicability on the actual drilling rig by comparing their behaviors.

5.1 Sensors

The sensors used in the setup are potentiometer scale for displacement measurement, load cell for WOB measurement, and torque measurement sensor.

5.1.1 Displacement sensor

The least count of the displacement scale is 1mm. The R^2 value of the displacement sensor is 0.992. Thus, the accuracy of the least count value for the displacement sensor will be 1±0.008 mm. Upscaling the least count and tolerance limit by a factor of 40 (from Table 4) for actual drilling rig in feet, the factor would be 0.131±0.001 feet. Thus, the accuracy of the upscaled factor of the displacement is ±0.001 feet, this an acceptable accuracy for any drilling rig in the world.

The displacement range of the top-drive is 150 mm i.e. the top drive can travel a total tripping distance of 150 mm in the downscaled experimental setup. Upscaling it by the factor of 40, this tripping range for actual drilling rig would be 19.7 feet. Normally, the tripping range in an actual drilling rig is 50 to 120 feet. In an actual drilling rig such high tripping range is required to pull in or push in the pipe stand which is typically 30 to 90 feet long. In the downscaled experimental setup, the drillstring will be of constant length i.e. tripping motion would be necessary only to change the WOB. The reason behind maintaining constant drillstring length is the experimental setup is that it is built with the ability to reproduce different forms of vibrations and drillstring behavior using downhole equipment setup (refer section 1.9.1, Figure 25). In an actual drilling rig operation typically 10-15 feet of tripping is enough to adjust the WOB. Thus, the experimental setup (having 19.7 feet upscaled tripping range) would successfully replicate the tripping motion of an actual drilling rig.

5.1.2 WOB sensor

The WOB sensor has the R^2 value of 0.596, with least count of 50 grams. Thus, the accuracy will be 50 grams ± 20.2 grams. Upscaling this limit by a factor of 40 (from Table 4), the range for an actual drilling rig will be 0.110 ± 0.044 lbs. There is no standard range of weight that should be applied to the bit, it can be anywhere between 1,000 lbs. to 100,000 lbs. Although, the least count of the sensor is enough to account for the required accuracy in measurement of WOB of an actual drilling rig, the tolerance limit of the sensor is very high. Thus, the solution to this issue is further discussed in the future discussion section.

5.1.3 Torque sensor

The torque sensor has R^2 value of 0.991, with a least count of 0.003 in-lbs and maximum range of 12.5 in-lbs. The accuracy of the sensor is 0.003 ± 0.00027 in-lbs. Upscaling this limit by a factor of 40 (from Table 4) and converting the units to ft-lbs, the range for an actual drilling rig will be 0

to 41.67 in-lbs. Typically the torque range in an actual drilling rig range from 0 to 200,000 ft-lbs. The torque sensor used for this setup has upscaled torque range of 0 to 41.67 ft-lbs (1.04 ft-lbs x 40). Thus, the sensor limit is in order of magnitude 10^3 less than the torque value typically observed on a drilling rig. For this range (0 to 200,000 ft-lbs) a sensor should have a range of 0-5000 ft-lbs in the downscaled experimental setup.

5.2 Controllers

5.2.1 RPM controller

A DC powered motor is used as RPM motor in the downscaled experimental setup. A typical rotary table in an actual drilling rig has max. RPM of 300 [31,32]. Applying the downscaling factor used in this experimental setup (1:40 from Table 4), thus, the required maximum RPM in the experimental setup is 300/40 = 7.5 rpm, whereas, the experimental setup has an RPM range of 0-180. As shown in Figure 70, the R^2 value for the RPM controller is 0.998, with an accuracy of 1±0.002 RPM. Thus, this setup exceeds the requirement of RPM control behavior and operation range as compared to an actual drilling rig.

5.2.2 Stepper motor for displacement, WOB control and tripping speed

The stepper motor generates linear motion by rotating the screw on which the top-drive is mounted through a slider. This slider allows a stable motion of top-drive. The stepper motor is actuated by the signal received from the computer through the DAQ card.

The purpose of the controller is to move the top-drive linearly in the vertical direction accurately. The least count of the stepper motor is 1 step equivalent to $6.0x10^{-5}$ mm, where, a motor rotated by 1.8 degrees in each step. The controller receives input for step size, speed, acceleration, holding current, and running current (for their definition refer to section 4.2). Using test result the values and range of these parameters are identified such that the controller acts linearly.

Typically, the tripping (hoisting) speed in a drilling rig operation ranges from 0 to 230 feet/min [33], which is equal to 0 to 120 mm/s. Applying the downscaling factor of 40 (from Table 4) to calculate speed range for the experimental setup, it should be able to hoist with speed 0 to 3 mm/s. Therefore, all the test performed were in this speed range or equivalent of 0 – 50000 steps/s (3 mm/s ÷ $6.0x10^{-5}$ mm/steps).

5.2.2.1 Speed of stepper motor

The input speed (steps/s) vs output speed of top-drive on linear scale plotted in Figure 72 for a constant step size of 100000 (6 mm), acceleration at 1000 steps/s^2 (or $6x10^{-2}$ mm/s^2), holding current at 60% and running current at 20%, show a linear correlation with R^2 value of 0.9922 for speed range of 0 – 60000 steps/s or 0 – 3.6 mm/s. Thus, for a fixed step size the top-drive linear motion is proportional to the input speed. Next step is to verify the linear behavior at different step sizes.

5.2.2.2 Step size

The test was performed for different step size plotting the correlation between input step size vs output step size (as shown in Figure 76) with constant acceleration at 1000 steps/s^2 (or 6x10^{-2} mm/s^2), holding current at 60% and running current at 20%. The purpose is to identify the maximum limit of the step size at which the system is linearly correlated for input (in mm/s) and output step size (in mm/s). Input speed is the user controlled and output speed is the speed at which the top-drive moves.

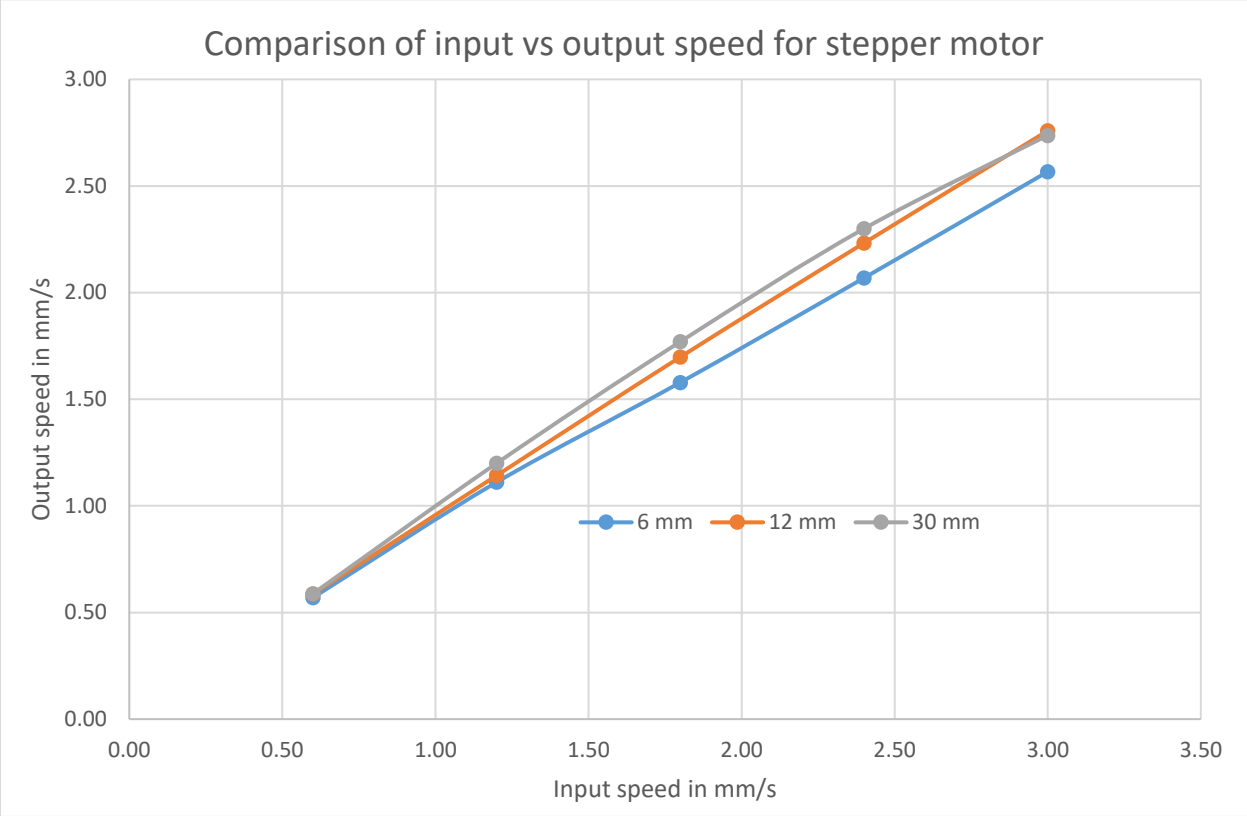

Figure 76: Showing the correlation between input and output speed for stepper motor at different step size.

In the shown Figure 76, the input vs output speed of the stepper motor is plotted for different step size. There can be observed a linear correlation for 6 mm and 12 mm step size, whereas, a visible non-linear correlation for 30 mm step size with R^2 values 0.9995, 0.9998, and 0.9887 respectively.

Two important observation from the Figure 76 is that the slope of the correlation between the two speeds changes with step size and for step size more than 12 mm i.e. at 30 mm there is a non-linear behavior is observed. It is necessary that the input vs output has a constant slope and linear behavior, otherwise, the speed of top-drive cannot be gauged correctly without a sensor, also, the speed will not be under user control when top-drive motion is controlled manually.

5.2.2.3 Acceleration

The stepper motor has a maximum acceleration limit of 1000 steps/s^2 (or $6x10^{-2}$ mm/s^2). Stepper motor comes to halt after completing motion for input step size and restarts the motion for the next step size input in the queue. During this transition, the motor accelerates and deaccelerates. It is best to keep the acceleration maximum for smoother top-drive tripping motion.

5.2.2.4 Holding current and running current

From the test result shown in Table 6 for two different stepper motor speed, it is observed the min. max. range of holding current required to at which top-drive stops to move 0.05% to 0.13%. Keeping the holding current above these this range will allow the motor to rotate continuously. It is not important to analyze the behavior of the motion at different holding or running current, as the parameters such as speed, distance and acceleration can be controlled separately. Thus, holding current and running current should be kept to their maximum limit i.e. 60% and 20% respectively for best performance.

Table 7: Summarized value range for experimental setup vs an actual drilling rig.

Parameter	**Experimental setup**	**Actual drilling rig**	**Required after downscaling**	**Criteria met?**
RPM	0-180 rpm with accuracy of ±0.002	0-300 rpm	They are dynamic parameters, hence, cannot be downscaled using geometrical downscaling factor.	
Tripping speed	0-18 mm/s	0-1170 mm/s		
Torque sensor	0-1.04 ft-lbs	0-200,000 ft-lbs		
Tripping range	0-150 mm	0-36576 mm, required 0-6096 mm (for WOB adjustment)	0-150 mm	Yes

Comparing the column 2 and column 4 for deciding if the criteria is met. The two columns compare the size of experimental vs downscaled actual drilling rig.

Chapter 6: Conclusions and recommendations for future

6.1 Concluding remarks

- WOB, RPM, and TORQUE are the major factors, that are under human control, that play a strong role in controlling the drilling performance. Varying the range of these parameters better drilling efficiency can be achieved at a lower cost. These parameters can be controlled through the top assembly.
- Safety is the first and foremost requirement in the oil and gas sector. Three layers of safety are added in designing the control system of the experimental setup, out of which two layers have ability to completely halt overall or individual drilling operations in the situation of undesired process outcome, and one layer to pause and resume the operation to allow investigation of the drilling operation. The error message box displays the most likely cause of operation abnormality. Another safety aspect is setting limits on the hoisting motion of the top-drive so that it does not hit the top or bottom boundaries.
- WOB adjustment can be operated manually or automatically. Closed-loop control allows automatic adjustment of WOB as per the given user input.
- Virtual display panel, designed like a drilling simulator panel, lets the user control and visualize different parameters through virtual gauges, meters, sliders, switched, buttons and other. The panel is designed to provide a user-friendly and interactive interface to the user.
- Except for WOB sensor, all other sensors such as torque, displacement, and others are precisely calibrated to respond linearly to the measurement property. Controllers are linearly calibrated; the accuracy or RPM is high enough that no RPM sensor is needed. The linear correlation value (R^2) show a strong correlation between the input and output signals for sensor and controllers.
- WOB sensor has low precision due to its high sensitivity to the noise (inertial effects). Further investigation needs to be done to resolve the issue.
- Top assembly should be operated within the operating range of the parameters that are identified with experimental results. The hoisting motor step size should be less than 200000 steps (12 mm) and should be kept constant throughout the drilling operation when under manual control. Holding current should be greater than 0.13%, suggest operating at the maximum holding current of 60%. Acceleration should be kept maximum at 1000 steps/s^2 (or $6x10^{-2}$ mm/s^2) allowing quick adjustments in WOB. Running current should be kept to the maximum value of at 20%.
- The tripping range of the experimental setup is 150 mm, equivalent to 19.7 feet on an upscaled drilling rig. Tripping motion is required in the experimental setup only to control the WOB and counter buckling of the drillstring, since, not actual drilling will be performed by the setup, instead, downhole conditions will be recreated. Hence, the available tripping range in the experimental setup is sufficing.
- The experimental setup has an RPM range of 0- 180 with an accuracy of ±0.002 RPM.
- Automation is improved by using data gathered from sensors to make better decisions. Greater number of sensors provide more data to make better decisions, monitor and

automate the controller. Data results in drilling optimization and result in less personnel, ensuring higher safety standards.

- A three-phase process – 'Design, Simulate & Test' can be adapted to carry out any drilling automation research project. This framework is used in this work and all the three phases were covered.

6.2 Future work

6.2.1 WOB measuring load cell sensor

The WOB measured by the load cell has an R^2 accuracy of 0.596, which is very low for linear scale correlation. This sensor is sensitive to inertial effects due to which noise is introduced in the measurement signal. The sensor can be mounted above the rotary motor to eliminate some inertial effect, replaced by a new less sensitive sensor, installing multiple load cells or noise filtering system can be used.

6.2.2 Torque sensor

The current torque sensor has a measurement range of 0 to 12.5 in-lbs as compared to the required range of 0 to 5000 in-lbs. This sensor needs to be replaced by a new sensor for the required range of operational torque.

6.2.3 Integration with real drilling rig

The important addition to be seen in this new experimental setup is the integration of Hardware-In-the-Loop (HIL). This addition allows the connection of the setup to any drilling simulator that supports such an option. This innovative feature permits the collection of data directly from the model and simulate the behavior of the string in real time and have the simulator adjust the drilling parameters to mitigate the vibrations to a safe range. The interface used to communicate with any drilling simulator is using standard drilling rigs protocols and accept worldwide web access if necessary. A schematic of the concept implementation is shown in Figure 77. The experimental drilling vibration setup does not require full access to the drilling simulator, hence it only provides new data through the standard I/O interface, that some simulators have recently introduced.

6.2.4 Installing more sensors

More sensors such as vibration sensors, buckling measurement sensor can be installed into the experimental setup. Using a greater number of sensors provide more data about different aspects of drilling and helps make a robust decision. It is also important the sensors provide precise data allowing accurate judgment.

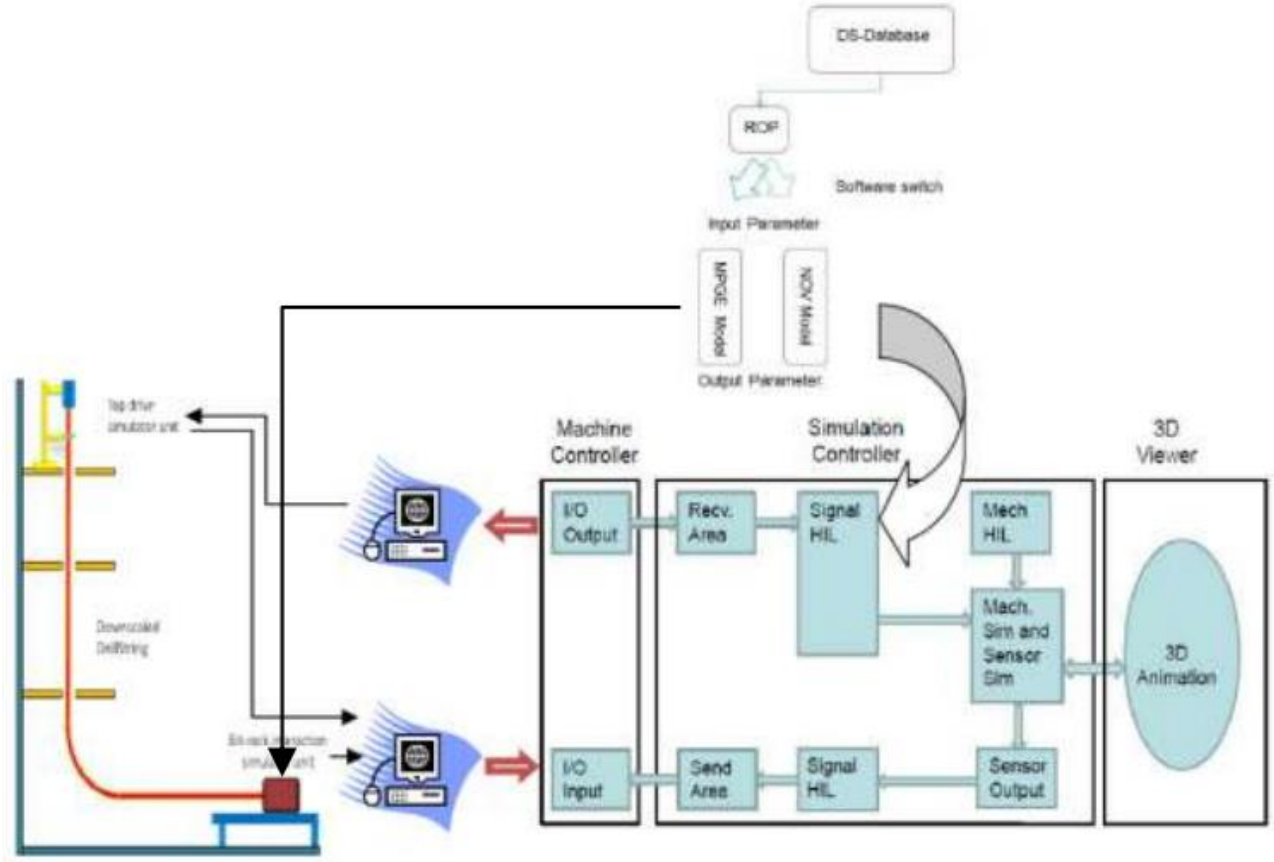

Figure 77. Proposed schematic of the concept implementation [6]

6.2.5 Remote access

The display panel controls the drilling experimental setup through input signals received from sensors and output signals generated for controllers. This experimental setup can be completely remote controlled with the help of two implementations. Firstly, connecting remotely to the computer that is directly connected to the hardware (such as controllers, DAQ and other) through a VPN, this would require having internet access on both the computers. Secondly, installing cameras to view all the motions in the experimental drilling rig setup such as tripping in and out, rotation of drillstring through top drive through a camera. Together these two implementations will allow view, control and even analyze the operations.

Chapter 7: References

[1] Ahmad Ghasemloonia, D. Geoff Rideout, Stephen D. Butt in June2014, A review of drillstring vibration modeling and suppression methods.

[2] Soendervik, K. 2013. Autonomous Robotic Drilling Systems. Presented at the SPE/IADC Drilling Conference, Amsterdam, 5-7 March. SPE-163466-MS

[3] Shusheng Bi & Jie Liang, 2011. Robotic drilling system for titanium structures.

[4] Olsson T, Robertsson A, Johansson R, 2007. Flexible force control for accurate low-cost robot drilling. In: IEEE International Conference on Robotics and Automation, Roma, Italy. 4770–4775

[5] Jardine, S., Malone, D., Sheppard, M., 1994. Putting dampers on drilling's bad vibrations. Oil field Rev.6 (1), 15–20.

[6] Antonio Rafael Marquez Chacin, 2017. Thesis on Investigation of drill-string vibrations using finite element method simulations and design and implementation of experimental setup

[7] Kapitaniak, M.; Hamaneh, V. V.; Chávez, J. P.; Nandakumar, K.; Wiercigroch, M. (2015): Unveiling complexity of drill–string vibrations: Experiments and modelling. International Journal of Mechanical Sciences, 101, 324-337.

[8] Kovalyshen, Y., 2014. Experiments on sitck-slip vibrations in drilling with drag bits. Presented at the US Rock Mechanics / Geomechanics Symposium, Minneapolis, Minnesota, 1—4 June. ARMA 14-7108.

[9] Esmaeili, A.; Elahifar, B.; Fruhwirth, R.K; Thonhauser, G., 2012. Laboratory Scale Control of Drilling Parameters to Enhance Rate of Penetration and Reduce Drill String Vibration. Presented at the SPE Saudi Arabia Section Technical Symposium and Exhibition, Al-Khobar, Saudi Arabia, 8—11 April. SPE-160872MS.

[10] Foster, I.; Water, A.H.; and Dinnie, R, 2010. Asymmetric Vibration Damping Tool-Small Scale Rig Testing and Full Scale Field Testing. Presented at the IADC/SPE Drilling Conference and Exhibition, New Orleans, Louisiana, 2—4 February. SPE-128458-MS.

[11] Foster, I. (2011): Axial Excitation as a Means of Stick Slip Mitigation - Small Scale Rig Testing and Full-Scale Field Testing. Presented at the SPE/IADC Drilling Conference and Exhibition, Amsterdam, Netherlands, 1—3 March. SPE-139830-MS.

[13] Patil, P.A. and Teodoriu, C., 2012. Model Development of Torsional Drillstring and Investigating Parametrically the Stick-Slips Influencing Factors. Journal of Energy Resources Technology 135 (1). JERT-12-1158.

[14] Patil, P.A., 2013. Investigation of Torsional Vibrations in a Drillstring Using Modeling and Laboratory Experimentation. Papierflieger-Verlag.

[15] Stephen Rassenfoss, 2011. JPT, Drilling Automation: A catalyst for change.

[16] Fred E Dupriest, William L Koederitz, 2005. Maximizing drill rates with real-time surveillance of mechanical specific energy. In SPE/IADC Drilling Conference. Society of Petroleum Engineers.

[17] Franca, A.F.P., 2010. Drilling action of roller cone bits: modeling and experimental validation. J. Energy Resour. Technol. 132, 0431011–0431019.

[18] Eric Cayeux, IRIS; Dan Sui, Olaleke Akisanmi, and Omar Alani, Unversity of Stavanger, 2017. Challenges in Automation of a Laboratory-Sale Drilling Rig and Comparison with the Requirements for full Scale Drilling Automation.

[19] FushenRen, BaojinWang, LeiZhao, and AnheZhu, 2017. Experimental Investigation and Analysis of Dynamic Buckling of Drill String in Horizontal Well.

[20] N. Mihajlovic, A.A van Veggel, N. van de Wouw, H. Nijmeijer, 2006. Analysis of Friction-Induced Limit Cycling in an Experimental Drill-Sting System.

[21] Alfred W. Eutes III, Colorado School of Mines, 2007. The Evolution of Automation in Drilling.

[22] J. Dunlop, R. Isangulov, W.D Aldred, SPE, H. Arismedi Sanchez, J. L. Sanchez Flores, SPE, J. Alarcon Herdoiza, SPE, J. Belaskie, SPE, J.C. Luppens, SPE, Schlumberger, 2011. Increased Rate of Penetration Through Automation.

[23] Vimlesh A. Bavadiya, University of Oklahoma; Zeenab lsaihati, Saudi Aramco; Ramadan Ahmed, Univerity of Oklahoma; Kyle Gustafson, Kimray Inc, 2017. Experimental Investigation of the Effects of Rotational speed and Weight on Bit on Drillstring Vibrations, Torque and Rate of Penetration.

[24] Walt Aldred Cambridge, England, Jacques Bourque Mike Mannering Gatwick, England, Clinton Chapman Bertrand du Castel Randy Hansen Sugar Land, Texas, USA, Geoff Downton Richard Harmer Stonehouse, England, Ian Falconer Houston, Texas, Fred Florence National Oilwell Varco Cedar Park, Texas, Elizabeth Godinez Zurita Villahermosa, Mexico, Claudio Nieto Petróleos Mexicanos (PEMEX) Villahermosa, Mexico, Rob Stauder Helmerich & Payne, Inc. Tulsa, Oklahoma, USA, Mario Zamora M-I SWACO Houston, Texas (2012) Schlumberger. Drilling Automation.

[25] Leon H. Robinson, Ph.D., International Drilling Consultants; Mark S. Ramsey, PE, SPE, Texas Drilling Associate (2001). Are You Drilling Optimized or Spinning Your Wheels?

[26] Henry Le, Stephen Christy, Mohammad Aljubran, Vimlesh Bavadiya, John Kibe, Ramadan Ahmed, 2015, University of Oklahoma, Mewbourne School of Petroleum and Geological Engineering. Drilling Systems Automation Technical Section (DSATS) Drillbotics design report.

[27] Zach Cox, Tawfik Elshehabi, Cody Smith, Rachel Richard, Dr. H. Ilkin Bilgesu, 2016, West Virginia University. Drilling Systems Automation Technical Section (DSATS) Drillbotics design report.

[28] Enrique Z. Losoya, Ibrahim El-sayed, Tyrell Cunningham, 2017, Texas A&M University. Drilling Systems Automation Technical Section (DSATS) Drillbotics design report.

[29] Alexander Saersten andeland, Andreas Thuve, Mikkel Arno, Per Oystein Turoy and Sebastian Knoop, Norwegian University of Science and Technology, 2018. Drilling Systems Automation Technical Section (DSATS) Drillbotics design report.

[30] K.K. Millheim (Amoco Production Co.), 1986. The Role of the Simulator in Drilling Operations.

[31] Technical specification for ZJ40BD modular drilling rig, www.rbauction.com, May 2018.

[32] Predator oil and gas drilling system, www.epiroc.com, May 2018.

[33] Khulief, Y.A., Al-Sulaiman, F.A., 2009. Laboratory investigation of drillstring vibrations. J. Mech. Eng. Sci. 233 (Part C), 2249–2262.

[34] Lu, H., Dumon, J., Canudas-de-Wit, C., 2009. Experimental study of the D-OSKILL mechanism for controlling the stick–slip oscillations in a drilling laboratory testbed. In: proceedings of the IEEE Multi-Conference on Systems and Control. IEEE. Saint Petersburg, Russia, pp. 1551–1556.

[35] www.eia.gov, May 2018.

[36] Reference: http://www.utdallas.edu/~pujana/latin/PDFS/Lecture%2011-%20Oilbasics.pdf

[37] www.ni.com, May 2018.

[38] www.omega.com, May 2018.

[39] www.oilandgasmiddleeast.com, May 2018.

[40] www.csincusa.com, May 2018.

[41] www.mccdaq.com, May 2018.